Energy Storage Solutions for Wind Generator Connected Distribution Systems in Rural Ontario

by

Mohammed Nahid Rahman

A thesis

presented to the University of Waterloo

in fulfilment of the

thesis requirement for the degree of

Master of Applied Science

in

Electrical and Computer Engineering

Waterloo, Ontario, Canada, 2009

Author’s Declaration

I hereby declare that I am the sole author of this thesis. This is a true copy of the thesis, including any required final revisions, as accepted by my examiners.

I understand that my thesis may be made electronically available to the public.

Abstract

Environmental awareness and uncertainty about continued supply of fossil fuel has given rise to the renewable energy movement. Wind based power generation has been at the forefront of the motion to integrate distributed energy sources in the traditional power system. Due to various technical restrictions, wide scale penetration of wind generated power has been held back by most utilities. One such restriction is the variability of generation due to the technology's dependence on Mother Nature. Energy storage devices can complement the wind generators by reducing this variability. These devices can store excess generation for supply during low generation periods.

There are several promising technologies for both energy storage and power storage applications. Power storage devices provide short term fluctuation dampening capability while energy storage devices allow longer term storage. Pumped hydro, Vanadium Redox battery and Sodium-Sulphur battery are some of the viable energy storage technologies.

This project provides a set of algorithms and guidelines to obtain the optimal configuration parameters of an energy storage device. To verify the efficiency of the algorithms, a model system has been obtained from a local utility. This system represents a typical radial distribution system in rural Ontario. The load demand, wind speed and energy prices for a period of one year have been obtained from utilities and Environment Canada.

The main goal in determining the location of the storage device within a distribution system is to minimize the total cost of energy and the total energy loss during the period of analysis. Locating the storage device near the wind turbines or near the largest loads lead to the optimum results. Buses that are located near those elements can be considered as suitable locations for the storage device.

The energy storage capacity and charge-discharge rate of the storage device are selected based on four criteria: maximize wind turbines' load following capability, maximize capacity factors of the wind turbines, minimize system energy losses and minimize system energy costs. A weight based multi-objective optimization algorithm has been proposed to assign various priorities to these criteria and obtain a single solution. The larger the energy storage capacity of the storage device, the better the improvement in system performance. Lower charge-discharge ramp rates provide superior results.

The parameters for storage device operating schedule, i.e. charge-discharge trigger levels, have been selected using similar criteria and weighted objective approach as for the capacity selection process. Higher charge trigger levels and moderate discharge trigger levels provide the optimum system performance.

Once a set of parameters for the storage device has been selected, bus voltages over the period of study are analyzed. Voltage variations outside certain limits have been identified. Finally, a Monte Carlo based simulation approach is presented to obtain output parameter (system performance) variation ranges for pseudo random changes in input parameters.

Acknowledgements

First and foremost, I would like to express my sincere gratitude to my co-supervisors Dr. Magdy Salama and Dr. Ramadan El-Shatshat for their kind advice, insight and direction for the duration of this project. Without their help and guidance, undertaking this project would not have been possible. I would also like to thank Dr. Kankar Bhattacharya for his encouragements and advice at various stages of my graduate studies. I appreciate the kind suggestions and insights of Dr. Abdel-Galil in preparing this thesis. I am indebted to all the professors with whom I had the opportunity to take various courses during my undergraduate and graduate degrees at University of Waterloo.

This research work has been funded under the sponsorship of Natural Sciences and Engineering Research Council (NSERC) of Canada and Hydro One Network Inc. I would like to thank Mr. Ravi Seethapathy and Mr. Bob Singh for their guidance and mentorship during the time spent at Hydro One facility in Toronto.

I also want to acknowledge the support of my friends and colleagues during my study at the University of Waterloo. Amit Singh, Mohit Bhatnagar, Kaushik Sarkar, Atul Kachru, Shaguna Khazanchi and others have provided me with precious advice and motivated me to pursue graduate studies.

Last, but by no means least, I would like to thank my parents, my brother Shazid Rahman and my fiancé Sharah Taasnuva for all their help and support during the length of this project. Their love, devotion and sacrifices have made it possible for me to complete my Master of Applied Science degree.

Dedication

To my parents, my brother Shazid Rahman and my fiancé Sharah Taasnuva...

Table of Contents

List of Tables

List of Figures

Chapter 1: Introduction

1.1. Background

With the rising environmental awareness, increasing fossil fuel prices and international treaties to curb greenhouse gases, wind energy has been gaining increasing importance around the world. Germany, USA, Denmark, India and Spain are the top five producers of wind power – accounting for about 83% of worldwide production [1]. According to a study performed by Gas Research Institute of the USA, distributed energy sources are expected to capture about 30% of the energy market by 2030 [2]. Of the available renewable energy sources, wind power generation is considered one of the most promising technologies. The worldwide rated capacity of installed wind power was 46,000 MW during 2004 and is expected to quadruple to about 175,000 MW by 2012 according to Electric Power Research Institute, USA [3].

1.2. Wind Power Generation and Energy Storage Devices

Wind-based power generators capture the kinetic energy from air currents flowing close to earth's surface and convert that energy to electricity. The 'fuel' for this technology is the wind and output of wind generators vary based on availability of wind. Since load demand follows hourly, weekly and seasonal patterns independent of wind speed, power generated from wind sources may not always be available when it is most needed. As a result, during excess generation periods, energy is "spilled" or discarded while, during high demand periods, other sources of energy may be needed to supply the unmet demand.

Energy storage devices transform electrical energy to another energy form to reserve excess or cheap energy for subsequent usage. When demand is higher than the available generation, this stored energy is converted back to electrical form and supplied to the grid. Depending on the type of the storage technology, the energy can be stored in thermal, mechanical, chemical, electromagnetic or electrostatic form within the device. Storage devices allow renewable energy sources, such as wind power, to provide a constant energy supply. Predictable power supply is one of the major difficulties in wide scale integration of wind based power sources into

the electricity grid. Using storage devices as buffers, the predictability can be increased to the level where wind generators can be assumed to be dispatchable.

1.3. Research Motivation

The wide–scale implementation of wind technology has long been undermined due to the uncertainty and intermittency resulting from its dependence on wind speed. Use of storage devices is one method of mitigating these drawbacks. To achieve the best performance from the wind turbine – storage device combination, the storage device should offer the following characteristics:

a. Location of the storage device or facility should be optimized to provide best system performance including minimum overall cost of energy and minimum system losses
b. Energy storage capacity of the device should be optimized to ensure sufficient supply during low wind periods
c. Energy storage and discharge rates should be optimized to provide flexibility in charging and discharging of the storage device
d. Storage device operation settings/triggers should be optimized to intelligently determine when to store and discharge the device
e. Impact on existing level/quality of service in the system should be minimized
f. The results expected from the wind turbine – storage device combination should be predictable within a certain range

1.4. Research Objectives

This research aims to develop a set of algorithms and guidelines to properly determine the parameters of a storage device for use in the distribution level. The parameters to be determined include location within the system, energy storage capacity, energy charge-discharge rates and storage device triggering sensor levels. To achieve the aforementioned goal, the following steps need to be undertaken:

a. Develop a custom power flow calculation program in Matlab environment. This program should be optimized for radial distribution systems with distributed generation and energy storage devices.

b. Develop a guideline to locate the storage device that minimizes cost of energy and/or system losses.
c. Develop a tool to identify energy capacity and energy charge-discharge rates of the storage device
d. Develop a tool to identify storage device operation mode triggering sensitivity levels
e. Analyze system performance when a storage device with chosen parameters are installed
f. Provide a confidence level for the proposed solution for varying input parameters

1.5. Thesis Layout

The remainder of this thesis has been divided into 10 chapters to facilitate proper flow of the discussion and analysis.

Chapter 2 provides a brief discussion of the theoretical background on power generation from energy stored in wind currents.

Chapter 3 provides a brief discussion on storage device functionality. This chapter also includes a critical literature survey and state–of–the–art on various storage technologies and their respective advantages and disadvantages.

Chapter 4 illustrates various components of the Matlab tool developed for this project. This chapter also provides a validation test to compare results of the Matlab tool with a commercially available software package.

Chapter 5 presents the model system used for validating the algorithms proposed in this project. Various input data sets are also discussed and analyzed in this chapter.

Chapter 6 discusses methods to obtain the optimal location of the storage device in the distribution system. Two optimization problems have been proposed and results using the model system have been analyzed.

Chapter 7 discusses methods to obtain the optimal capacity parameters of the storage device. This chapter presents various objectives that can be used in obtaining the capacity parameters and proposes a method to prioritize these objectives.

Chapter 8 discusses methods to obtain the optimal charge-discharge triggering level parameters of the storage device. Like the previous chapter, this chapter also provides various

objectives for obtaining the optimal value and then proposes a multi-objective approach to obtain a single solution.

Chapter 9 analyzes the impact on bus voltages due to the recommended storage device parameters from the previous three chapters.

Chapter 10 provides a statistical analysis of the results obtained by illustrating the probability distribution of variations in different output parameters.

Chapter 11 presents the thesis summary and directions for future work.

Chapter 2: Basics of Wind Generation

Wind energy is a clean source of electricity that does not pollute the air or emit greenhouse gasses. As of September 2009, Canada had an installed capacity of 2,854 MW of wind energy. Figure 1 shows the wind energy capacities of various provinces and territories in Canada [4].

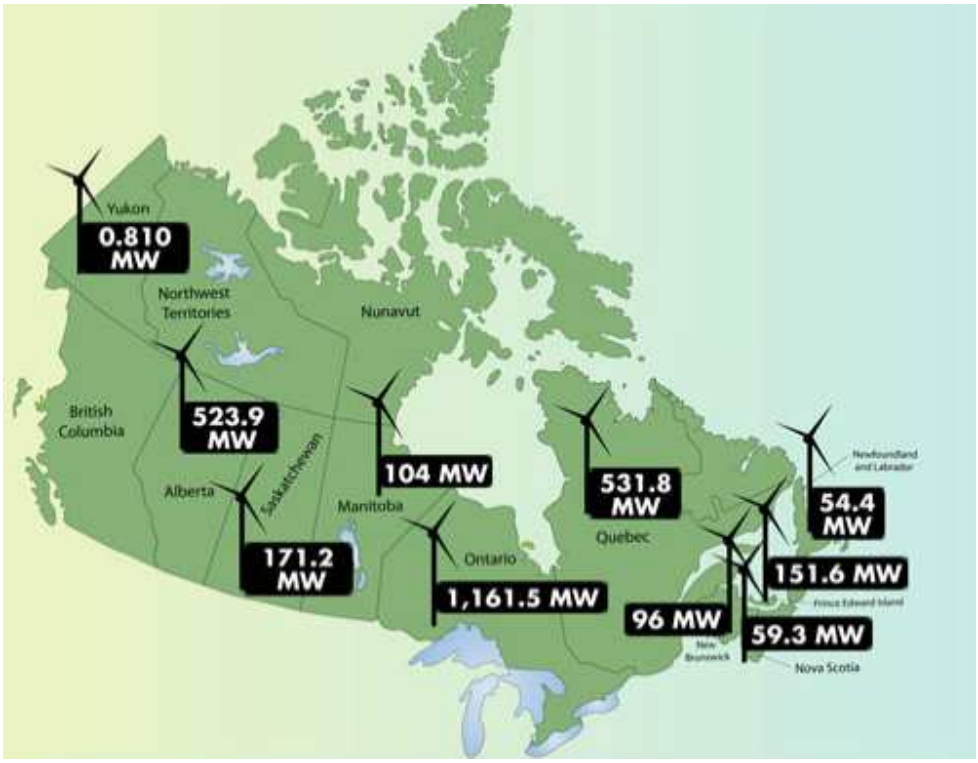

Figure 1 – Wind Generation Capacities of Canadian Provinces and Territories, 2009

Irregular distributions of solar energy create wind patterns across the globe. Wind turbines utilize the energy stored in air currents flowing close to earth's surface. The air currents create a torque on the rotor blades of the wind turbine and transfers wind's kinetic energy. The blades convert this energy into mechanical (rotational) form. A generator takes this mechanical energy as input and outputs electrical energy. Figure 2 shows an overview of the energy conversion process of a typical wind turbine. Each of these steps has its own efficiency factor. The efficiency of the overall process is the efficiency of the wind turbine. In the figure, larger arrows show higher energy content.

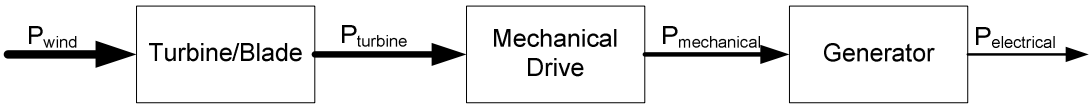

Figure 2 – Energy Conversion Process of a Wind Turbine

2.1. Harvesting Energy from Wind

The energy content of wind depends on its density, intercepting area and speed of impact on that area. For a wind turbine, the intercepting area is the area of the circle created by the rotation of the rotors. The following formula can be used to calculate the energy stored in wind.

$$P_{wind} = \frac{1}{2}\rho A v^3 \quad (1)$$

where,

P_{wind} power stored in wind [W]

ρ air density [kg/m^3]

A intercepting area (area of the wind rotor) [m^2]

v wind speed [m/s]

A wind turbine cannot extract all the power stored in the wind. If all the kinetic energy were transferred to the rotor blades, the air mass would stop completely near the wind turbine and any future energy conversion would be impossible. According to Betz' theorem, the theoretical maximum for energy conversion using wind turbines is limited to 59% of energy stored in the wind flowing through the turbine.

Generally, the density and the energy content of the wind increase with heavier wind. Under normal atmospheric pressure and 15 ^{o}C temperature, air density is 1.225 kg/m^3 [5]. Higher altitude, humidity and temperature reduce wind density. The area covered by the rotor blades depend on the length of the rotor blades. Wind turbines with higher rated output will have a taller rotor structure. The taller structure allows longer blade length which, in turn, facilitates higher intercepting area. The higher the intercepting area, the greater the wind mass harnessed by the blade. Figure 3 summarizes the relationship between rotor diameters and rated output of

wind turbines [5]. In practice, the rotor diameters are often varied to achieve maximum output depending on local wind characteristics.

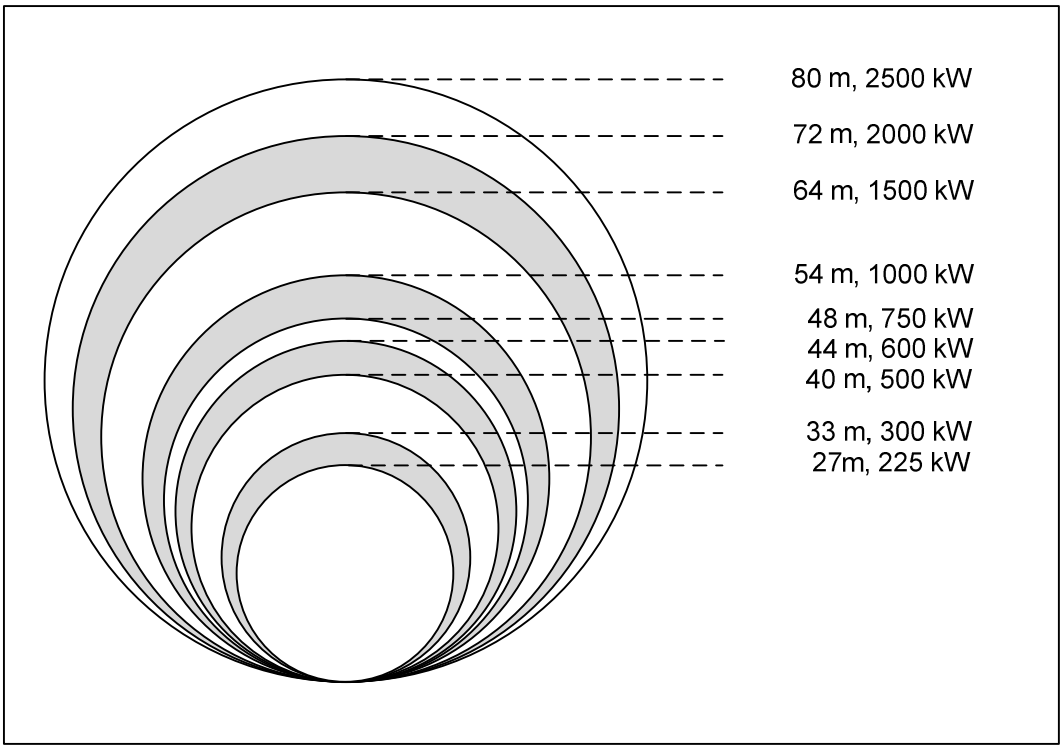

Figure 3 – Relationship between Rotor Diameters and Rated Output of Wind Turbines

Wind turbine output is more directly influenced by the speed of wind. The relationship between wind speed and energy stored in wind is cubic. Wind turbines are usually configured to operate within a certain range of wind speeds. The curve that represents the turbine output for various wind speeds is known as a power curve. Wind turbines start producing electricity at a cut–in speed of around 3 to 5 m/s [6]. At speeds higher than the cut-in speed, the power output of the turbine increases as a cubic function of the wind speed until the output is equal to the rated capacity. After this point, the turbine output remains constant with increases in wind speed until the speed exceeds a certain cut–off speed. Typical cut–off speeds are around 20 to 25 m/s [6]. When wind speeds are higher than the cut–off speed, the turbine is shut off. Figure 4 shows the power–curves (power output vs. wind speed) for two General Electric 1.5 MW wind turbines [7]. Both models have a cut-in speed of 3.5 m/s. The rated output level is achieved at 11 m/s for the XLE model and at 14 m/s for the SLE model. The cut-off wind speeds are 20 m/s and 25 m/s respectively.

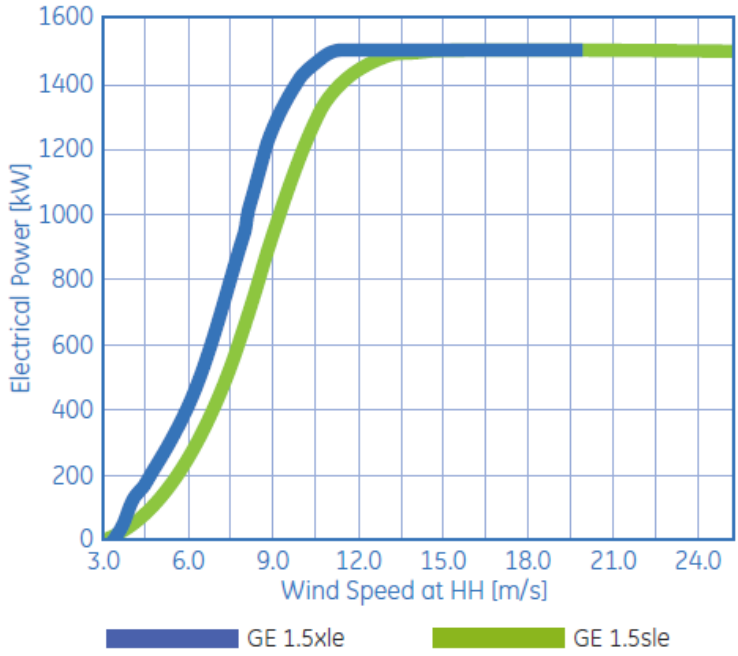

Figure 4 – Power Curve of General Electric Wind Turbines

2.2. Variances in Wind Speed

One of the major challenges in adopting wind power generation on a large scale is its dependability on Mother Nature. The fuel used for this generation technology is wind. Although it is freely available, wind's availability and speed do not necessarily coincide with the customer demand [8]. As wind speed changes, the output power of a wind generator changes as well.

Wind speeds vary continuously as a function of time and height. At very high altitudes, wind speed is not affected by the characteristics of earth's surface. But at lower heights, roughness due to urbanization and farming plays a major role in determining the speed at which the wind impacts the turbine rotors. In the wind industry, a roughness factor is used to indicate the terrain condition of the surrounding area.

Table 1 summarizes applicable roughness factors for various types of terrain [9]. Roughness factors range between 0.10 for smooth surfaces and 0.30 forests and small towns. As rule of thumb, 0.14 is used as the roughness factors for wind generation analysis [9].

Table 1 – Roughness Factors for Various Terrain Types

Terrain Type	Roughness Factor
Smooth Surface, Ocean, Sand	0.10
Low Grass or Fallow Ground	0.15
High Grass or Low Row Crops	0.18
Tall Row Crops or Low Woods	0.20
High Woods with Many Trees, Suburbs, Small Town	0.30
General Rule of Thumb	0.14

The higher the height of the turbine, the lower is the impact of the roughness factor. In general, wind speed measurements are available from weather stations. The measuring height of these weather stations is rarely as high as the wind turbine. The following formula can be used to determine the effective wind speed at the turbine height when the roughness factor and wind speed at another height is known.

$$v = v_{ref}\left(\ln\frac{z}{z_0}\Big/\ln\frac{z_{ref}}{z_0}\right) \tag{2}$$

where,

v_{ref} reference wind speed recorded at known height [m/s]

z_{ref} height at which reference wind speed is measured [m]

z_0 roughness factor of the area

z turbine height [m]

v wind speed at turbine height [m/s]

Wind speed profiles usually demonstrate geographical and seasonal trends. Within these trends, wind speed may vary significantly. Figure 5 shows the hourly average wind speeds for January 2006 measured at a height of 80 m above ground in a rural Southern Ontario location. For the 30 day period shown, the hourly average wind speeds vary from 0 m/s to about 18 m/s.

As the resolution of sampling is increased, from hourly average to minute average for example, the variances in wind speed are more apparent.

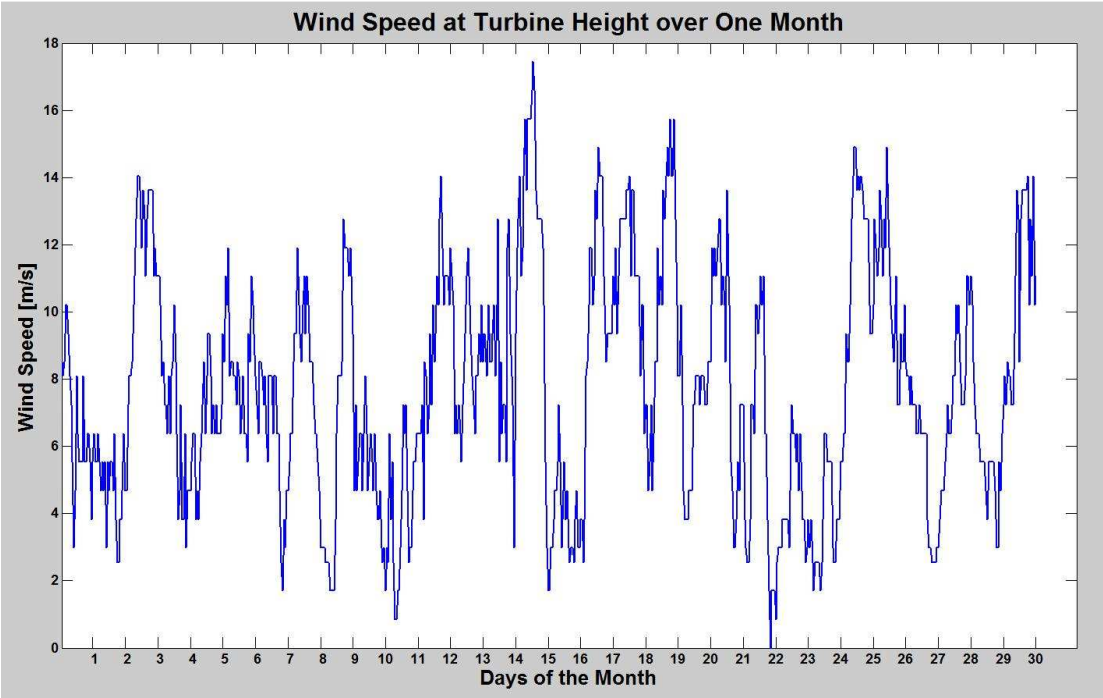

Figure 5 – Wind Speed Variation over One Month

As seen from the plot above, the wind speeds are not in the turbine's rated speed range for most of the hours. The output of the wind turbine will be limited depending on the availability of wind.

Various published works have suggested the two parameter Weibull Distribution model to best describe the wind speed probability distribution [[10] – [15]]. The two parameters of this model are the shape parameter *k* and the scale parameter *c*. The probability of a wind speed *v* is given by the Weibull Distribution as:

$$f(v) = \frac{k}{c}\left(\frac{v}{c}\right)^{k-1} \exp\left[-\left(\frac{v}{c}\right)^{k}\right] \tag{3}$$

There are various methods of determining the values for the shape factor and the scale factor. As a rule of thumb, the shape parameter is set to 2 and the scale factor is defined as a function of average wind speed, $\bar{v}$.

$$c = \frac{2}{\sqrt{\pi}}\bar{v} \tag{4}$$

With the above values, probability distribution of wind speed can be expressed by a simplified equation as shown below. This distribution is known as the Raleigh Distribution.

$$f(v) = \frac{\pi v}{2\bar{v}^2}\exp\left[-\frac{\pi}{4}\left(\frac{v}{\bar{v}}\right)^2\right] \tag{5}$$

Figure 6 shows the probability distribution of various wind speeds for an area with average wind speed of 10 m/s.

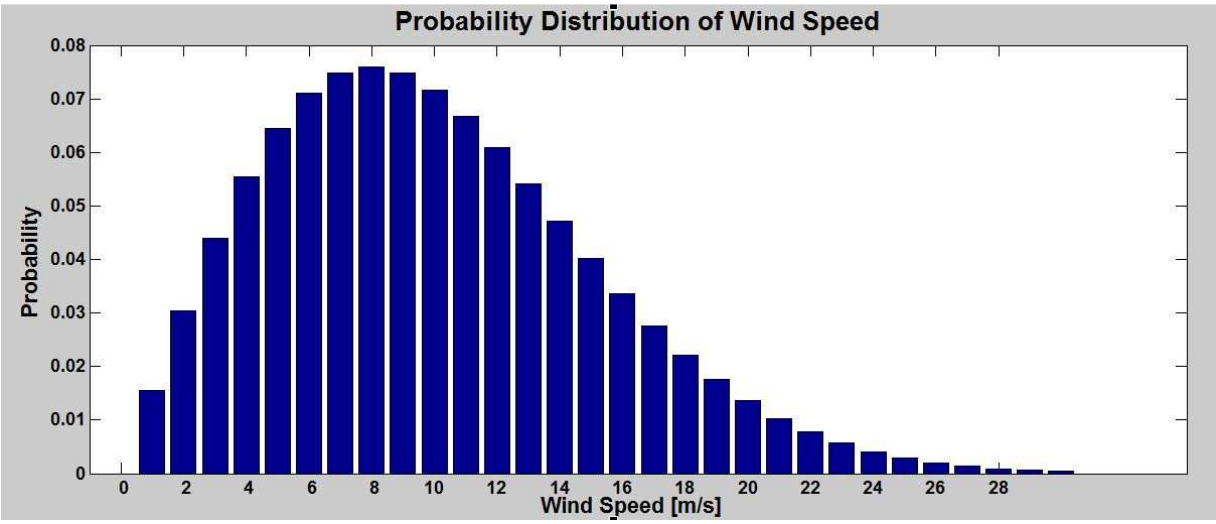

Figure 6 – Probability Distribution of Wind Speed (Avg. Speed 10 m/s)

2.3. Capacity Factor

Typically utilization of a wind turbine is expressed in terms of its capacity factor. Capacity factor is the ratio of average power output during a set of hours (usually a year) and the rated power output over the specified period of time. Capacity factor can be expressed by the following equation:

$$CF = \frac{\sum_{h=1}^{H} P_{out,h}}{H \times P_{rated}} \tag{6}$$

where,

CF	capacity factor
$P_{out,h}$	power output during hour h [kWh]
P_{rated}	rated output for the wind turbine [kWh]
H	number of hours under study

A low capacity factor indicates that the available wind generation capacity is not being utilized at its fullest. From a system planning point of view, wind power generation is considered a non–firm source as the amount of generated power cannot be controlled from a centralized control location. In Germany, wind power generators are given a capacity credit of only 7.4%. This implies that for every 100 MW of wind generation capacity, only 7.4 MW of traditional power generation capacity can safely be replaced [16]. Utilities from different parts of the world assign varying capacity credits to their wind resources based on historical wind data of the region.

2.4. Wind Power in Ontario

Ontario has an installed wind generation capacity of 1168 MW [17]. Bulk of the wind energy is obtained from seven large scale and three smaller wind farms located across Ontario. Figure 7 shows the wind farms located in Southern Ontario.

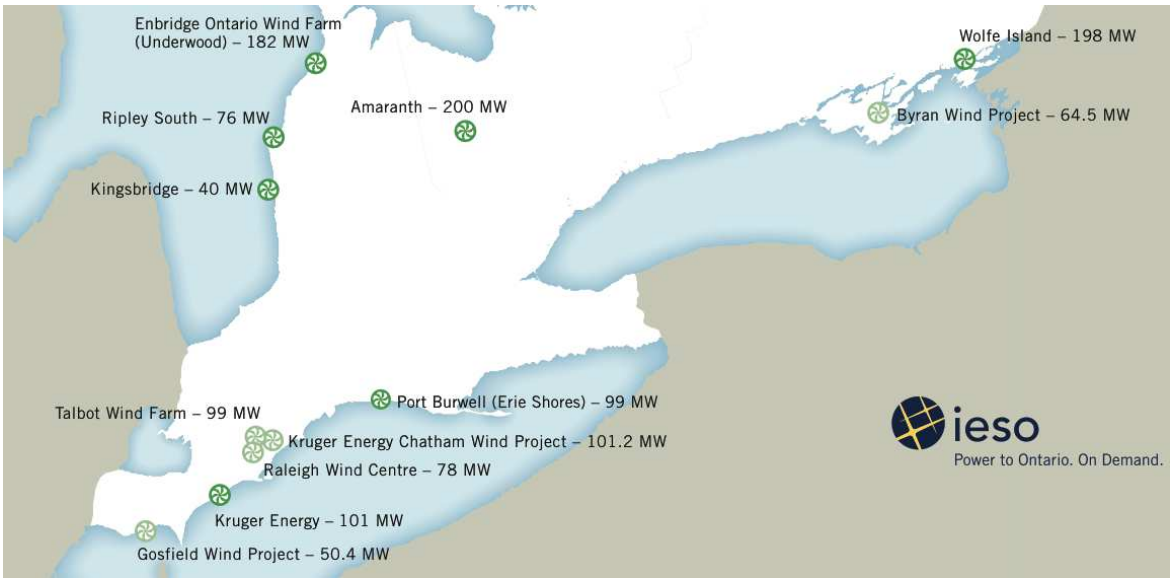

Figure 7 – Wind Farms in Southern Ontario

The wind farms in Ontario have a combined capacity of 1100 MW. The remaining 68 MW wind energy is obtained from distribution level wind generators under Ontario Power Authority

contracts. The largest wind farm in Ontario is rated at 197.8 MW located in the Township of Frontenac Islands. This farm was brought into service in June 2009. Melancthon I and II (Amarnath) located in the Township of Melancthon also rated to produce 200 MW of wind power.

Table 2 provides details about the wind farms in Ontario [18]. Four manufacturers of wind turbines have been used in these ten farms. Among them, GE 1.5sle model has been used at five locations while Siemens and Vestas turbines have in operation in two locations each. The remaining wind farm uses Enercon wind turbines.

Table 2 – Wind Farms in Ontario

Name	Location	Capacity (MW)	Operational	# of Turbines	Type of Turbines
Amaranth I	Township of Melancthon	67.5	Mar. 06	45	GE 1.5sle
Kingsbridge I	Huron County	39.6	Mar. 06	22	Vestas V80
Erie Shores (Port Burwell)	Norfolk and Elgin Counties	99.0	May 06	66	GE 1.5sle
Prince I	Sault Ste. Marie District	99.0	Sep. 06	66	GE 1.5sle
Prince II	Sault Ste. Marie District	90.0	Nov. 06	60	GE 1.5sle
Ripley	Township of Huron-Kinloss	76.0	Dec. 07	38	Enercon E82
Kruger (Port Alma)	Port Alma	101.2	Oct. 08	44	Siemens Mark II
Amaranth II	Township of Melancthon	132.0	Nov. 08	88	GE 1.5sle
Enbridge (Underwood)	Bruce County	181.5	Feb. 09	110	Vestas V82
Wolfe Island	Township of Frontenac Islands	197.8	Jun. 09	86	Siemens 2.3 MW

Chapter 3: Basics of Energy Storage

Energy storage devices enhance predictability of renewable energy sources by smoothing out fluctuations in the difference between load and generation. Thus, systems with high penetration of renewable energy can benefit from storage devices. These devices can store energy during low demand periods and whenever excess energy is available. The electrical energy is usually stored in another form of energy such as thermal, chemical, mechanical, electromagnetic or electrostatic. When demand is high or load is greater than the generation, the stored energy is converted back to electrical form and fed back into the system. Thus, storage devices can provide peak shaving of the load demand and lead to stability in market prices. Storage devices can also provide a pseudo demand-side management by acting as a load during low demand periods and as a source during high demand periods.

In addition to supporting high penetration of renewable energy sources, storage solutions open many other possibilities in the traditional power system. Storage allows loads to be supplied during power outages – thereby reducing downtime and improving system reliability. System stability and power quality can be improved by dampening power and frequency oscillations in the power system. Storage facilities can also provide ancillary services such as spinning reserve and reactive power compensation. Load following and levelling as well as energy management capabilities are also enhanced in the presence of energy storage devices. Storage devices along with installation of renewable energy sources can help defer expensive transmission and generation capacity expansion.

3.1. Configuration of a Storage Device

A typical storage device can be divided into three major components: central storage (CS), power transformation system (PTS) and charge-discharge control system (CDCS) [19]. The CS is the medium in which energy is stored. The size of the CS directly influences the energy storage capacity of the device. The PTS includes the power conditioning system and the power electronic converters used in energy conversion. The throughput capability of the PTS system dictates the rate at which energy can be stored and discharged from the storage device. This rate is often referred to as the ramp rate of the device. The CDCS can be considered the brain of the storage device. This control unit determines when to start the charging phase, how long

to store energy and when to discharge the energy into the system. The CDCS senses internal parameters such as trigger level configuration, present charge levels etc. It also collects external information such as present demand levels from relays in the power system. Figure 8 below shows a schematic diagram of the typical organization of these three modules [19].

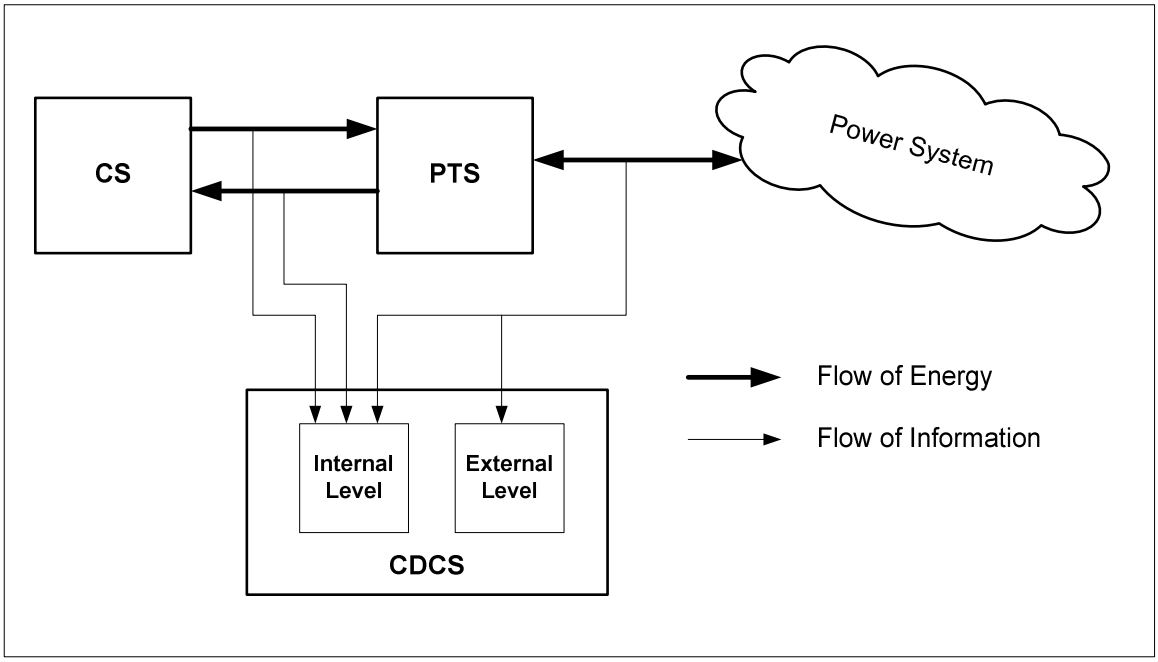

Figure 8 – Schematic Diagram of Structure of a Typical Storage Device

3.2. Charge-Discharge Algorithm

The algorithm for the charge-discharge control system (CDCS) can be divided into two categories: fixed period and variable period. For fixed period charge-discharge routine, the storage device starts charging and discharging at a pre-set time of the day for a pre-set duration. This pre-set time is usually selected based on the historical characteristics of load demand in the area. The duration is usually selected based on the size of the storage device as well as historical load and generation characteristics. The variable period control system uses relays and sensors to measure the load demand at a certain point in the power system [20]. If the load demand is below certain trigger level, the storage device starts the charging phase and continues in that phase until the device is fully charged. The charging phase can also terminate if the load demand becomes higher than the configured trigger level. Similarly, if the load demand is above certain other trigger level, the storage device starts discharging energy and

continues in that phase until all the stored energy has been discharged. The discharging phase can also terminate if the load demand falls below the trigger level.

3.3. Grid Connection of Storage Device

Storage devices can be connected in both parallel and serial configurations with respect to the the rest of the power system. When connected in series, the storage device is located in between the source and the load. In effect, the PTS unit work as part of the transmission line. For this configuration, a larger PTS unit is often required as the PTS unit must be able to accommodate the power flowing through the transmission line. Figure 9 shows the schematic of a storage device connected in serial [19].

Figure 9 – Schematic of Series Connection of Storage Device

In parallel configuration, only the energy exchange from the CS unit passes through the PTS module. As such the PTS module defines the energy charge-discharge rates of the storage device. Figure 10 shows the schematic of a storage device connected in parallel [19].

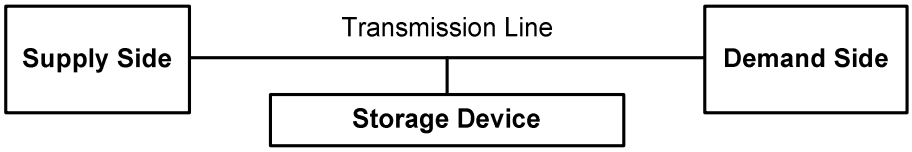

Figure 10 – Schematic of Parallel Connection of Storage Device

3.4. Cycle Efficiency

Cycle efficiency of the storage device refers to the ratio between the energy supplied from the device during discharge phase and the energy consumed by the device during charging phase. During both charge and discharge phases, some energy is lost in the energy conversion process. Energy conversion related losses are significant for thermal storage devices due to restrictions imposed by the Carnot process. Another major source of energy loss in the storage

device is energy leakage within the central storage. For example, pumped hydro storage devices suffer from lower cycle efficiency levels due to evaporation and leakage through the turbines.

3.5. Literature Review of Current Storage Technologies

An extensive literature review has been performed to obtain information about the state-of-the-art in storage device technologies. Nine storage technologies have been analyzed and evaluated in various publications and journals. These nine technologies are: pumped hydro, flywheel, super-magnetic energy storage (SMES), compressed air energy storage (CAES), lead acid battery (LAB), vanadium redox battery (VRB), sodium-sulphur battery (NaS), lithium ion battery (Li-ion), and zinc-bromide (ZnBr) battery. Table 3 provides a high level overview of the main characteristics of the nine technologies.

Table 3 – High Level Comparison of Energy Storage Technologies

Energy Storage Technology	Power Capacity	Energy Capacity	Life Cycle Duration	Efficiency	Other Comments
Pumped Hydro	Very high	Very high	Long	Moderate	Special Siting Requirement
Flywheel	High	Low	Long	High	Short Term Storage
Super-magnetic Energy Storage (SMES)	High	Low	Long	High	Short Term Storage
Compressed Air Energy Storage (CAES)	High	High	Long	Low	Special Siting Requirement; Adverse Environmental Impact
Lead Acid Battery (LAB)	High	High	Long	Low	High Cost; Adverse Environmental Impact
Vanadium Battery (VRB)	High	High	Long	High	Emerging Technology
Sodium-Sulphur (NaS) Battery	High	High	Long	High	High Production Costs
Li-ion Battery	N/A	High	N/A	High	Not feasible for large scale implementation
Zinc Bromide (Zn-Br) Battery	Moderate	Moderate	Long	High	Emerging Technology

In comparing and contrasting different storage technologies, various sets of evaluation criteria have been proposed in the literature [[21], [19]]. The key parameters include:

- Energy Density
- Ramp Rate
- Cycle Efficiency
- Life Time
- Response Time
- Cost
- Environmental Impact
- Siting Requirements
- Maturity of Technology

Subsequent parts of this report discuss the above mentioned characteristics of the selected storage technologies in further details.

3.5.1. Pumped Hydro Energy Storage

Pumped hydro energy storage is the most developed and most widely used energy storage technology. According to a study done by Electricity Storage Association, there are about 90 GW of electric energy storage worldwide, almost all of which is pumped hydro storage. There are approximately 280 pumped hydro energy storage facilities worldwide [22].

Traditional hydro generating stations are not storage facilities in the strictest sense but their output can be controlled to provide regulation support. Unlike a hydro generating station, a pumped hydro storage system allows two–way water flow. During off–peak hours, the generator acts as a motor to store water in an elevated reservoir. During peak hours, the water is released to produce electricity.

Although large hydro stations have high generation efficiency, losses due to evaporation and leakage water reduces the overall efficiency for pumped hydro storage units. The overall efficiency of this technology is roughly 75% [[23], [24]]. Very high energy and power capacities are two main features of pumped hydro storage. Large pumped hydro storage units can hold up to 1000s of MWh energy. For example, a recently constructed unit in the Alps can store up to 8.5 GWh of energy and supply 1.06 GW of power [25]. Pumped hydro plants are capable of providing maximum ramp rate, approximately equivalent to their rated capacity, in less than 1

minute response time [21]. Life time of pumped hydro storages is very long – some have been in operation for over 50 years [24].

Of the major difficulties with pumped hydro storage is its low energy density. Siting of these storage facilities require large areas preferably with different elevation levels. If geographical restrictions do not allow upper and lower reservoirs, underground reservoirs can be used as well. This option leads to higher cost of construction and longer lead time. Lack of suitable locations and impact on the environment are major drawbacks of pumped hydro storage.

3.5.2. Fly-wheel Energy Storage

Fly-wheel storage devices store energy in the rotating mass of a rotor. Although conventional steel and titanium blades have proven to be viable options for grid integration, newer glass and carbon fibre reinforced plastics allow substantially higher rotating speeds. The amount of energy stored in a flywheel is a function of the rotating speed. As such, the newer materials have increased the energy capacity as well.

Fly-wheels are established modular storage devices. Unlike batteries, fly wheels are not sensitive to depth of charge. The energy density of a fly-wheel is 1000 kWh/m^3. A typical fly-wheel has a life cycle of 20 years and 10s of million cycles [24]. A 100 kW, 25 kWh scale-power Smart Energy Matrix unit comprised of Beacon Power flywheels has been built, installed and is currently operating on the California Independent System Operator grid in San Ramon, California [27].

One of the major draw backs of fly-wheel storage devices is its high self discharge rates which can be between 1% and 10% per hour [24]. Fly-wheels are commercially used in the range of 1 kWh for 3 hours to 100 kWh for 30 seconds [26]. As such, fly-wheels are ideal for short term storage, including for the purpose of low-voltage ride through, but long term energy storage using fly-wheel storage devices is unlikely. Environmental impact of fly-wheel technology is similar to the impact of wind turbines. The rotation of the rotors creates high pitch noise and affects migration pattern of birds.

3.5.3. Super Magnetic Energy Storage (SMES)

SMES devices store energy in the magnetic field of a cryogenically cooled superconductive coil. The AC power is converted and stored as DC energy in the magnetic field. The central storage

system, i.e. the superconductive coil, is theoretically lossless – leading to a very high efficiency storage medium. Round trip efficiency of SMES devices are between 95% and 98% [26]. SMES devices are able to respond very quickly and can deliver large amounts of power for several seconds.

Energy storage capacity of SMES devices is very limited. As such, they are mainly suitable for power smoothing applications. Use of SMES in load-following or peak-shaving application alongside renewable energy sources is infeasible with the present technology. SMES devices have a life time of 20 years [24]. Due to the complexity of the technology, the production and installation of these devices is very expensive. SMES devices can be up to 1 MWh in energy storage capacity but the effect of magnetic field exposure on the surroundings is not completely known [21].

3.5.4. Compressed Air Energy Storage (CAES)

Compressed air energy storage devices store electrical energy by converting it into mechanical form. Air is compressed into a large container and, when energy needs to be discharged, the air is expanded to release the mechanical energy. Usually large salt caverns, abandoned mines and aquifers are used as the air container. CAES devices have been part of grid operation since 1970s [21].

The energy and power capacity of CAES devices depend primarily on the size of the container. Given a large mine can be located in the area, these devices can feature very high energy and power capacities. The compression process develops heat and, unless this heat is conserved, the cycle efficiency of CAES devices becomes low. In addition to the slow response rate due to dependence on a mechanical system, CAES devices' specific siting requirements make it an unviable option for most power systems. If aquifers are used as the air container, CAES systems may interfere with the eco-life near its vicinity. The cavern or mine based containers are susceptible to catastrophic raptures.

3.5.5. Lead Acid Battery (LAB) Energy Storage

Lead acid batteries have been used to store energy for many years. After pumped hydro storage, lead acid batteries are the most widely used storage devices. The modular and

minimum siting restrictions have made these batteries a popular choice. Lead acid batteries have relatively low capital cost. The response time for these batteries can be as low as 20 ms.

The life cycle of LAB devices are limited by the number of charge-discharge cycles. Typical cycle counts reached by lead acid batteries are around 1500. If depth of discharge is large, the life cycle of these batteries can be degraded. The use of lead has possible negative consequences to the nature. The efficiency of lead acid batteries is about 45%.

3.5.6. Vanadium Redox Battery (VRB) Energy Storage

Vanadium redox batteries are made up of two major sections: electrolyte tanks and charge/discharge stacks. Sulphuric acid solutions of vanadium are used for both cathodic and anodic electrolytes. These electrolytes are circulated in the stacks using a pump for charge and discharge operation. Figure 11 below shows a schematic view of the vanadium redox battery [28].

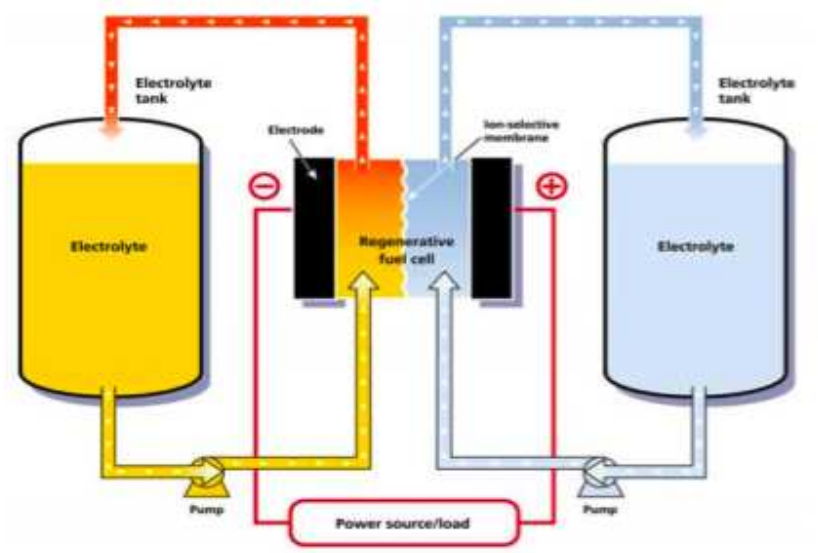

Figure 11 – Schematic of Vanadium Redox Battery

Anode: $V^{2+} \rightarrow V^{3+} + e^-$

Cathode: $V^{5+} + e^- \rightarrow V^{4+}$

VRB batteries feature low self–discharge, low construction costs along with high reliability and relatively high energy density [29]. Kashima–Kita, a private electric company in Japan, has implemented an 800 kWh rate battery in 1997. VRB batteries can reach an energy density of 1.5 kW/cm^2 and an overall efficiency of 80%. The Kashima–Kita implemented system has an expected lifetime of 1500 cycles.

VRB Power Systems Inc of USA has developed vanadium based battery systems that offer over 10,000 charge/discharge cycles between 20% and 80% state–of–charge. These batteries offer 65% – 75% efficiency and very low environmental effect [30]. Table 4 below summarizes the key advantages of Vanadium batteries over traditional lead–acid batteries [31].

Table 4 – Comparison of Lead Acid Battery and Vanadium Redox Battery

Property	Lead Acid Battery	Vanadium Redox Battery
Energy Density (Wh/litre)	12–18	15–25
Power Density (W/kg)	370	166
Temperature Range	-5^o – 40^o	0^o – 40^o
Efficiency	45%	65% – 75%
Depth of Discharge	25 to 30%	75%
Life Cycle	1500	100000
Cost ($/kWh)	$500 – $1550	$300 – $650

As seen from the table above, vanadium redox batteries offer higher efficiency, higher depth of charge and better life cycle. At the same time, VRB batteries have lower installation costs as well. In the United States, a 250 kW, 2 MWh VRB battery facility is in operation at Castle Valley, Utah. This unit is used as a load leveller. Another larger unit with 12 MWh is under construction in Sorne Hill, Ireland [30].

3.5.7. Sodium-Sulphur (NaS) Battery Energy Storage

First introduced in Japan in the 1980s, sodium–sulphur batteries are high temperature batteries. Vacuum thermal insulation is usually used to improve efficiency and energy density. The cells inside the battery module are anchored using sand and the cell temperature is controlled by electric heaters. The electrolytes used in sodium–sulphur battery is β–alumina with sodium and sulphur as –ve and +ve electrode active materials.

Recent improvements in sodium–sulphur battery technology have led to better performance and cost reduction. Sodium–sulphur batteries have a life cycle of 2250 cycles or more and efficiency of about 90%. Energy density of this battery technology is in the neighbourhood of 280 – 380 kWh/m^3 [32]. The energy density of sodium–sulphur batteries is almost three times the traditional lead–acid batteries. NaS batteries have a direct current efficiency of about 89%. This technology features no self discharge which contributes the high efficiency. The shelf life of these batteries can be as high as 15 years [21]. The maintenance cost of sodium–sulphur batteries is very low as well. The materials used in these batteries are abundant in nature and can be extracted at a very low–cost. Therefore, costs are expected to be significantly lower for mass production [25]. Modular nature of this technology enables short construction interval and flexibility in future expansion.

Tokyo Electric Power Company (TEPCO) has a 48MWh NaS battery in operation since 1995 in its Tsunashima substation. This specific system is primarily used for load levelling [32]. There have been more than 20 projects worldwide involving sodium–sulphur batteries as storage devices [25]. In North America, American Electric Power (AEP) has installed a 1.2 MW demonstration substation in Charleston, VA. This battery can supply power for up to 7 hour blocks for the overloaded substation. Another 6 MW substation is currently under construction [33].

3.5.8. Li-ion Battery Energy Storage

Lithium-ion battery storage devices are widely used in electronic devices to provide small amount of power at low voltages. The benefits of these devices include short access time, high energy density and high efficiency. But no large energy market is currently available for utility scale use due to technical and cost restrictions [21].

3.5.9. Zinc–Bromide Battery Energy Storage

Zinc–bromide batteries use a bipolar electrode design in which the current travels directly through the plastic battery stack. The two half cells, anode and cathode, are separated by a micro–porous separator. Zinc is electroplated in the anode and bromine is evolved at the cathode.

Overall reaction:	$ZnBr_2$	→	$Zn + Br_2$
Anode:	$Zn^{2+} + 2e^-$	→	Zn
Cathode:	$2Br^-$	→	$Br_2 + 2e^-$

A polybromide compound is usually used to minimize the self–discharge and improve system safety. Figure 12 shows a schematic of the zinc–bromide battery [34].

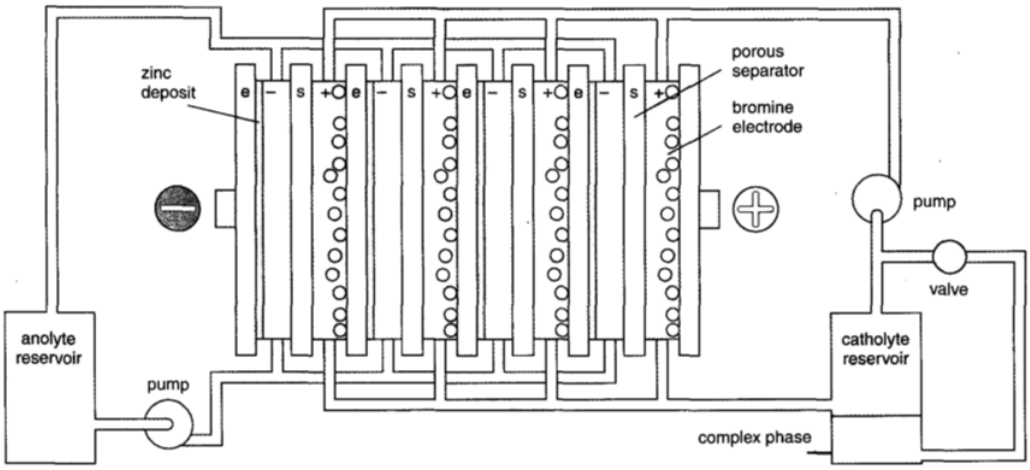

Figure 12 – Construction of a Zinc–Bromide Battery

In general, zinc–bromide batteries are suited for 50 kWh to 400 kWh applications. The lifetime of zinc–bromide batteries is roughly 2500 cycles which is approximately 10 years (one cycle for 5 days/wk). The efficiency of zinc–bromide batteries is in the range of 70% – 80% [34] .

Unlike lead acid batteries, zinc–bromide batteries can be fully discharged without adversely affecting the batteries life time. This deep discharge capability enables system designers to select batteries with lower rating and thus driving down the overall implementation costs.

Replacement costs are also significantly lower for zinc–bromide batteries since the stack and pumps account for roughly 20% of the overall storage system [35].

ZBB Energy Corporation is a major supplier of zinc–bromide batteries. Their batteries are based on 50 kWh modules that consists three 60–cell, 2500 cm^2 battery stacks connected in parallel. These modules are designed to supply 150A discharge while maintaining 96V at the output terminal for 4 hours. The pre–commercial units have an anticipated cost of $400/kWh [34].

Chapter 4: Implementation of Power Flow Algorithm

To achieve the research goals outlined in Section 1.4 a software tool has been developed in Matlab. The tool has the following features:

a. Fast, efficient algorithm for power flow calculations (optimized for balanced radial distribution systems)
b. Steady state considerations for wind turbines and storage devices
c. Customizable wind turbine specifications and ability to accept various wind profiles
d. Customizable storage device triggering (charging-discharging) sensitivity
e. Text based data–input method for evaluating set of options with efficiency

Four modules have been developed to use this tool to analyze various aspects of the storage device parameter selection. These four modules include:

a. Location Analysis Module: provides a comprehensive analysis of the effect of locating the storage device on various nodes of the system
b. Capacity Analysis Module: provides a weighted multi-objective analysis toolbox to investigate the effect of various combinations of energy storage capacity and charge-discharge capacity of the storage device
c. Triggering Level Analysis Module: provides a weighted multi-objective toolbox to investigate the effect of various combinations of storage device charge-discharge mode triggering levels
d. Variance Analysis Module: provides an insight about variances in system performance when selected input parameters are pseudo randomly varied

Various commercial and open source software packages, including Simulink SimPowerSys, PowerWorld, PowerSim, UWPlow and ETAP, have been evaluated. Even though these software packages perform their intended function with great efficiency, none of them included a comprehensive set of features required to conduct the intended analysis for this project.

Figure 13 below shows a schematic diagram for the various components of the tool built for this project. Some components of this tool have been obtained from the UWPSS project [39]. The UWPSS project provided a power flow calculation engine for a radial distribution system without regards to distributed generation sources and storage devices.

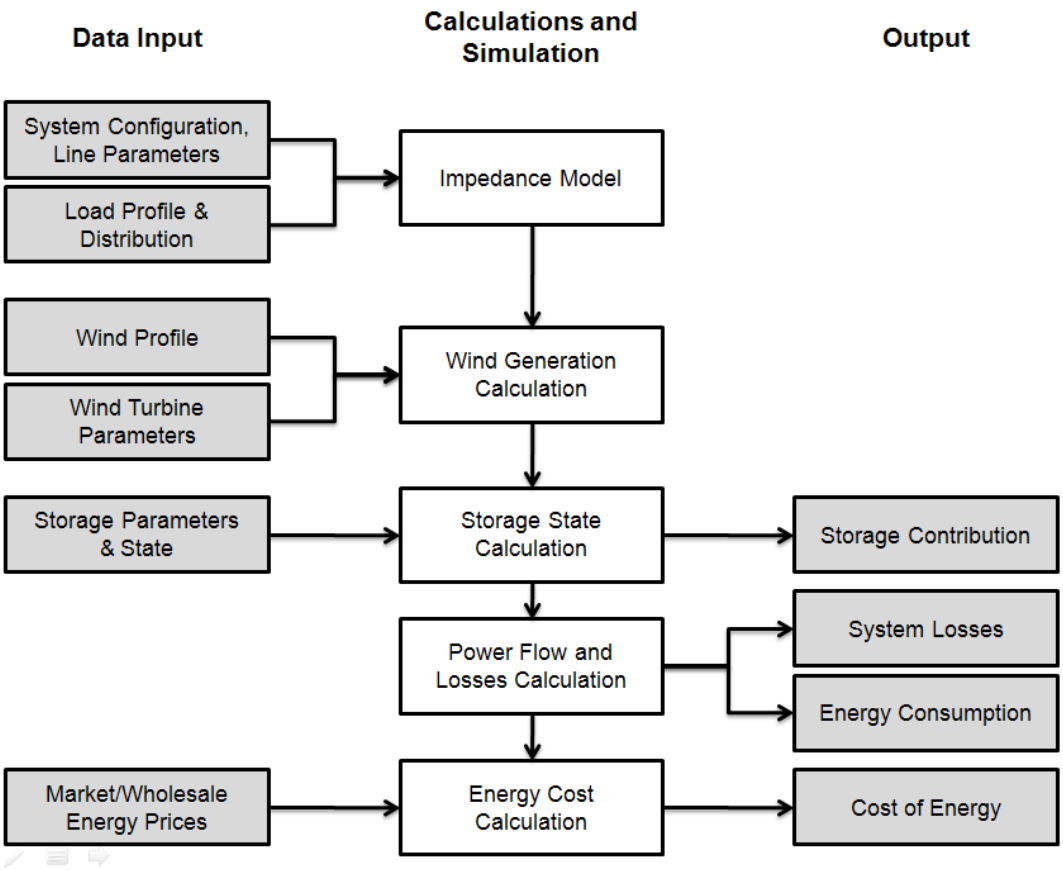

Figure 13 – Schematic Diagram of Matlab Tool

4.1. Data Input

The input to the system is provided via text files. There are six main component of the text input which can either be in one single file or in separate files. The main components are: a) system configuration, b) wind turbine data, c) storage device data, d) wind profile, e) load profile and f) energy price. The system configuration file includes substation/source parameters, nodal/feeder structure, feeder lengths and impedances, transformer data, load distribution and system rated (voltage and power) values for per unit analysis. The wind turbine data file contains information about the location, power factor and priority of wind turbines. It is assumed that backward flow of power out of the distribution system is not allowed. The storage device data file includes location, capacity, initial state and triggering parameters for storage devices. The remainder of the three input data sets include hourly data for wind speed, total load level and energy prices.

4.2. Impedance Model

The first step in the power flow algorithm is to build a representative model of the system under study. Using the feeder structure, a model of all the laterals and sub-laterals of the system is constructed. Then, the feeder lengths and impedances are used to develop a matrix of impedances between every two connected nodes. All values in this matrix are in per unit form. This tool uses polynomial load models to account for constant power, constant current, and constant voltage loads. The parameters of this polynomial load model are based on research done by Ontario Hydro [40].

$$P = P_0(a_0 + a_1 V + a_2 V^2 + a_3 V^{1.38}) \quad (7)$$

$$Q = Q_0(b_0 + b_1 V + b_2 V^2 + b_3 V^{3.22}) \quad (8)$$

$$a_0 + a_1 + a_2 + a_3 = b_0 + b_1 + b_2 + b_3 = 1 \quad (9)$$

where,

V	node voltage [volt or per unit]
P_0	real power consumed by load [watt or per unit]
Q_0	reactive power consumed by load [VAr or per unit]
a_0, b_0	coefficient for constant power (P,Q) load component
a_1, b_1	coefficient for constant current (I) load component
a_2, b_2	coefficient for constant impedance (Z) load component
a_3, b_3	coefficient for exponential load component

Using above equations allow a load to be defined as constant current, constant voltage, constant power, etc. by manipulating the a_i and b_i coefficients. For example, if a load is constant voltage, a_1 and b_1 coefficients should be non-zero and rest of the coefficients should be set to zero.

4.3. Wind Generation Calculation

This block computes the available wind energy for the specific hour based on wind turbine characteristics and wind speed data. Wind generator output is calculated based on power curves which can be obtained from the turbine manufacturers. The power curve is divided into various sections to obtain a mathematical relationship between the wind speed and the output

of the generator. By default, the GE 1.5SLE turbine power curve is used to calculate the output power. The configurable parameters of a wind turbine are shown in Table 5.

Table 5 – Wind Turbine Configuration Parameters

Parameter	Description
nodeLoc	Location of the wind turbine
Status	1 = operational 0 = out of service
SpeedDataSet	Wind speed data set applicable to the wind turbine (may vary for different turbines located across the study area)
PowerFactor	Power factor of the wind turbines at point of common coupling with the rest of the system

Wind speeds are typically available at a height different from the height of the turbine blades. Thus, the available wind values need to be conditioned for height adjustment using formula (1) as previously discussed. These wind speeds are used to obtain maximum available wind generation for the hour. Since back-feed beyond the source/substation is assumed to be restricted, excess energy, if available, is discarded. The usable wind power values for each turbine are added to the load distribution matrix as negative loads for power flow calculation.

4.4. Storage State Calculation

This block computes the behaviour of the storage device based on the device configuration and system state. Table 6 provides a list of configurable parameters for the storage device.

Table 6 – Storage Device Configuration Parameters

Parameter	Description
nodeLoc	Location of the storage device
stateVar	-1 = discharging 1 = charging 0 = out of service

maxCharge	Energy storage capacity of the device
pCharge	Present charge level
cRamp	Charging phase ramp rate
dRamp	Discharging phase ramp rate
cTrigger	Source current (per unit) limit below which charging starts
dTrigger	Source current (per unit) limit above which discharging starts
cTlevel	Percentile value used to determine cTrigger
dTlevel	Percentile value used to determine dTrigger
cycleCount	Number of cycles

The state of the storage device is calculated based on load demand and its initial conditions (i.e. state of the device from the previous hour). The two trigger levels – charging trigger and discharging trigger – determine whether to charge or discharge energy. If the source current is below the charging trigger, the device starts to charge itself. The rate at which the device can store energy is limited by the charging ramp rate. The charging phase continues until the source current is greater than the charging trigger or if the device's charge level reaches the maximum charge limit.

If the source current is above the discharging trigger, the device starts to discharge energy. The discharge rate is limited by another ramp rate. This phase continues until the source current dips below the discharging trigger or if the stored charge of the device is depleted.

The charging and discharging trigger values are adjusted based on recorded source current levels. The duration/size of the data set is a configurable variable. By default, source current levels over a week (i.e. 168 hours) are recorded. Storage device settings contain two values – charging trigger percentile ("*cTlevel*") and discharging trigger percentile ("*dTlevel*") – for calculating the new trigger limits. The recorded data set is sorted in ascending order and the percentile values are used to calculate the new triggering values. For example, if the *cTlevel* and *dTlevel* are set to 20 and 80 respectively, it implies that the charging phase starts when the substation supplied current is lower than 20% of the values recorded over the previous week and the discharging phase starts when the substation supplied current is higher than 80% of the values recorded during the same time period.

4.5. Power Flow and Losses Calculation

This block calculates the voltages and currents at each bus of the system under study. It receives the network structure, load distribution matrix and impedance model from the previous components. The calculation is optimized for balanced radial distribution systems. The network structure is divided into one main branch and many sub-branches. The power flow calculation starts from the lateral level farthest from the source/substation. For the first iteration, the voltage of the starting node of the lateral is assumed to be the same as the generator voltage. Node currents and voltages are calculated iteratively until a specified convergence/error limit is reached or until a specified maximum number of iterations are completed. This is regarded as "local" convergence. As voltage and current profile for higher laterals change, it is required to carry out local iterations again. Therefore, multiple iterations are carried out at global level – again with a specified convergence/error limit and maximum number of iterations limit.

For a lateral structure as shown in Figure 14, nodal voltage at any arbitrary node *n* is be calculated using the following formula [41]:

$$V_n = V_S - I_t\left(\sum_{i=1}^{n} Z_i\right) + \left(\sum_{i=1}^{n-1} I_i\right)\left(\sum_{j=i+1}^{n} Z_j\right) \tag{10}$$

where,

V_n voltage at node *n* [per unit]
V_S sending end voltage [per unit]
Z_i impedance of section *i* of the feeder [per unit]
I_t total sending end current [per unit]
I_i current flowing through node *i* [per unit]

Current at node *n* can be calculated using the following equation [41]:

$$I_n = \left(\frac{S_n}{V_n}\right)^* \tag{1}$$

where,

S_n Complex power consumed by loads at node *n* [per unit]

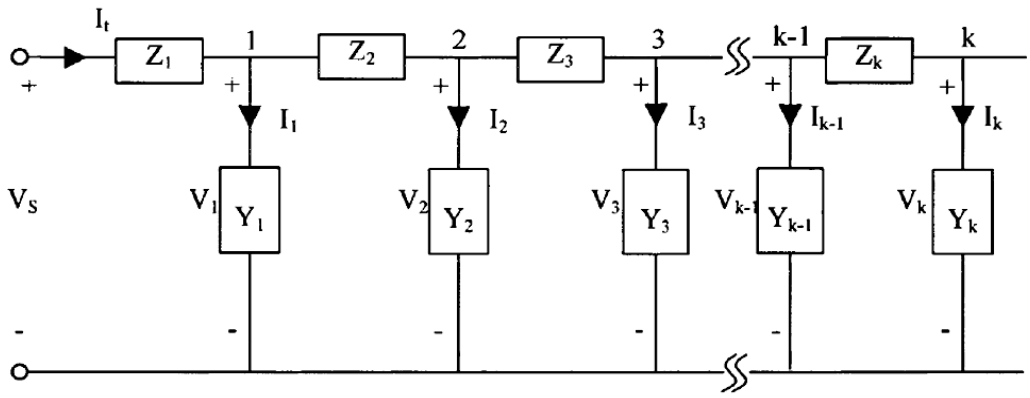

Figure 14 – Schematic of Sample Network

Equation (10) can be further reduced to the following set of equations. These equations simplify the calculations and thus improve system performance.

$$I_n^{\Re} = \frac{1}{\left(V_n^{\Re}\right)^2 + \left(V_n^{\Im}\right)^2}\left[V_n^{\Re}P_n + V_n^{\Im}Q_n\right] \tag{2}$$

$$I_n^{\Im} = \frac{1}{\left(V_n^{\Re}\right)^2 + \left(V_n^{\Im}\right)^2}\left[V_n^{\Im}P_n + V_n^{\Re}Q_n\right] \tag{3}$$

where,

I_n^R	real component of node current [per unit]
I_n^I	imaginary component of node current [per unit]
V_n^R	real component of node voltage [per unit]
V_n^I	imaginary component of node voltage [per unit]
P_n	real power component node *n* [per unit]
Q_n	reactive power component node *n* [per unit]
n	node number

The following formulas are used to calculate the real and reactive powers at each node:

$$P_n = V_n^{\Re}I_n^{\Re} + V_n^{\Im}I_n^{\Im} \tag{4}$$

$$Q_n = V_n^{\Im}I_n^{\Re} + V_n^{\Re}I_n^{\Im} \tag{5}$$

4.6. Validation of Matlab Tool

To validate the results of the Matlab tool, a small test system is constructed and the results are verified against results obtained from power flow algorithm in PowerWorld. For simplicity, a system without wind turbines and storage devices was chosen. This validation is meant to validate the results of the power flow calculation of the Matlab tool. Since, the Matlab tool models wind turbine outputs and storage devices as loads (positive or negative based on the state), a typical radial distribution system with sub–laterals will be sufficient for the validation. A schematic diagram of the test system is provided in Figure 15.

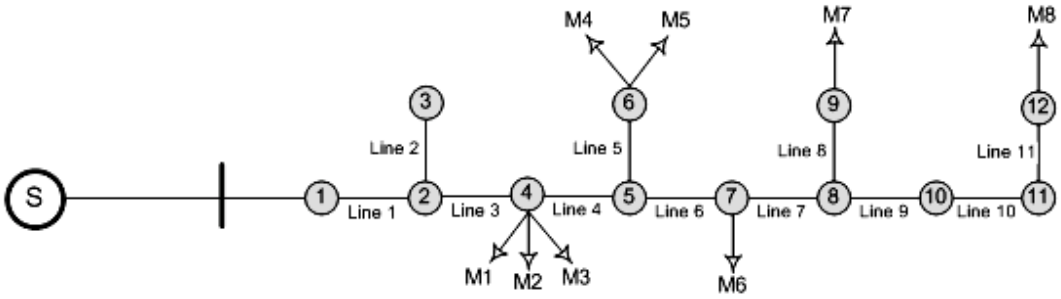

Figure 15 – Schematic Layout of Matlab Tool Test System

4.6.1. Matlab Tool Data

The system is first modeled in the Matlab tool developed for this project. The rated system voltage and power are chosen to match PowerWorld default values. The source is a 9 MVA substation operating at 16 kV. The structure of the feeder network is a radial with balanced loads. There are 8 constant–power loads in the system operating in various power factors. The input data to the Matlab tool is shown in Appendix 1.

4.6.2. Power World Test System

The test system is then modeled in PowerWorld Simulator v12.0. The schematic of the system in PowerWorld is shown in Figure 16. PowerWorld displays loads in MW units by default. As a result, some of the smaller loads are displayed as “0 MW” and “0 MVAr” in the figure. In fact, those are loads smaller than 0.5 MW and 0.5 MVAr respectively.

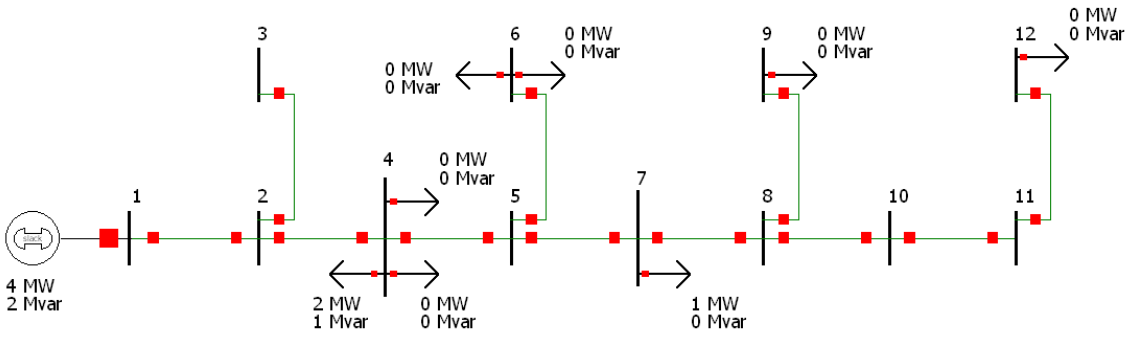

Figure 16 – Power World Layout for Matlab Tool Test System

4.6.3. Results Comparison

The power flow results from both the Matlab tool and PowerWorld Simulator are provided in Table 7. The tolerance of the Matlab tool is set at 0.001 – indicating that it assumes convergence when the error/improvement is less than 0.1%. As seen from the table below, the Matlab tool results and the Power World results match perfectly for the first three digits after the decimal point. Thus, it can be concluded that results obtained from the power flow calculation engine of the Matlab tool are accurate and comparable with commercially available software packages.

Table 7 – Power Flow Result Comparison: Power World vs. Matlab Tool

Bus	Matlab Tool [A] Voltage, pu	PowerWorld [B] Voltage, pu
1	1.0000	1.0000
2	0.9697	0.9699
3	0.9697	0.9699
4	0.9677	0.9679
5	0.9667	0.9669
6	0.9666	0.9668
7	0.9664	0.9666
8	0.9662	0.9664

9	0.9662	0.9664
10	0.9663	0.9664
11	0.9663	0.9664
12	0.9663	0.9664

Chapter 5: Description of Model System

To validate the algorithms proposed in this research, data for a practical rural distribution system has been obtained from a local utility. The schematic diagram of the system is shown in Figure 17 below. The area is connected to a substation/source at Bus 1. There are 26 customers connected to the system with an aggregated peak load demand of 13.28 MW.

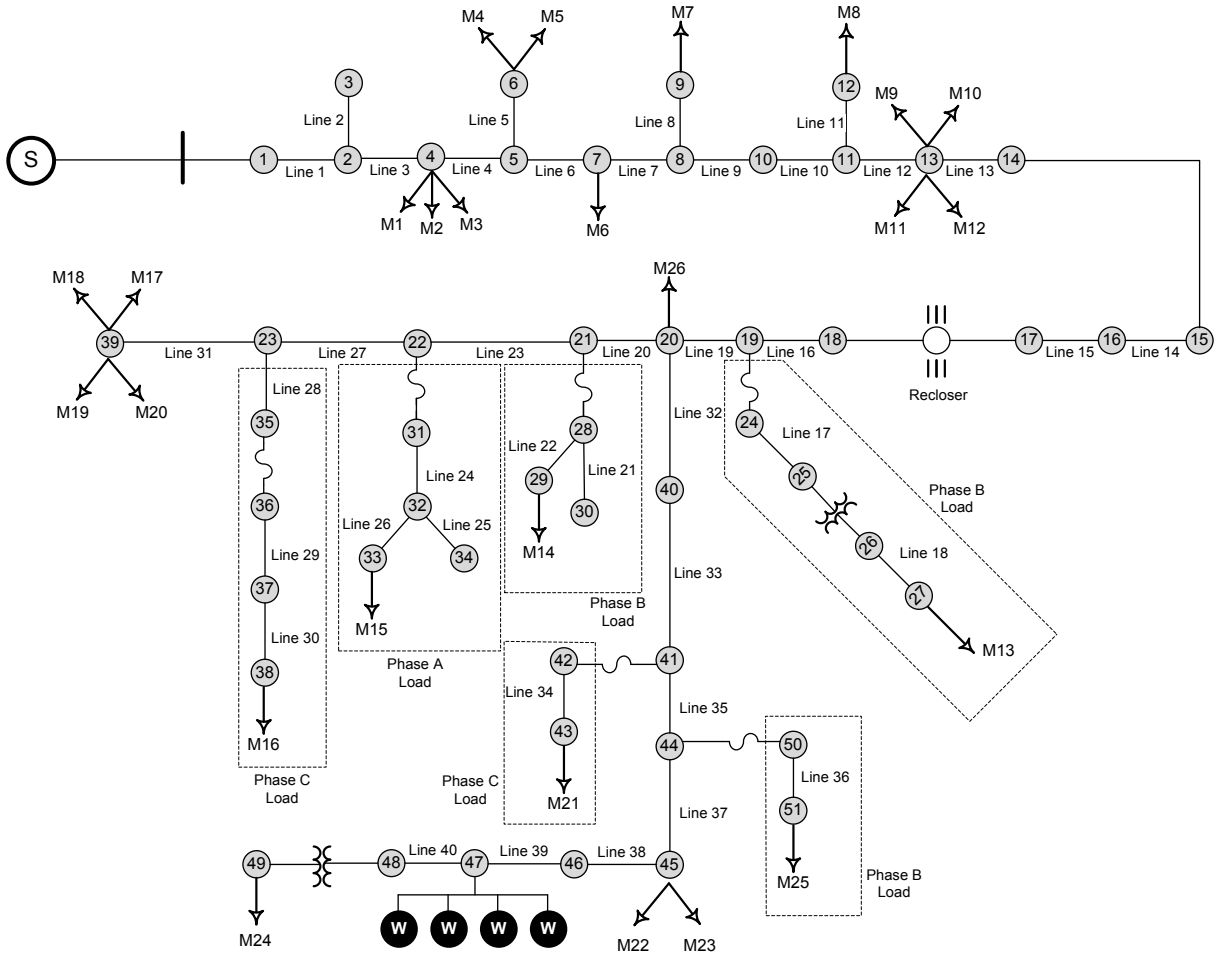

Figure 17 – Schematic of Model System

As proposed in [42], four wind turbines with rated output 1.5 MW each are located at Bus 47. Loads M13 through M16, M21 and M25 are single phase loads. Since the software tool assumes balanced loads, only the customers on Phase A will be considered for the analysis. Feeder lengths, impedances and load diversity for the test system are given in Appendix 2 and Appendix 3.

5.1. Hourly Load Demand Data

Hourly average load demand for the model system has been obtained from a local utility company. The data set includes hourly average demand for the period starting 1st January, 2006 and ending 31st December, 2006. It is assumed that the loads keep their proportionate values constant under various aggregated demand levels. As such, the individual load values can be scaled up/down based on the total demand for the area. An upper limit and a lower limit have been used to filter and eliminate outliers in the data set. The limits are set at three standard deviations around the mean load demand. Figure 18 below shows the monthly average load demand for the year under study. The demand pattern shows that the area is winter peaking. The load demand is highest during the month of February. Low load demand is observed for the spring period. Demand increases slightly over summer and fall.

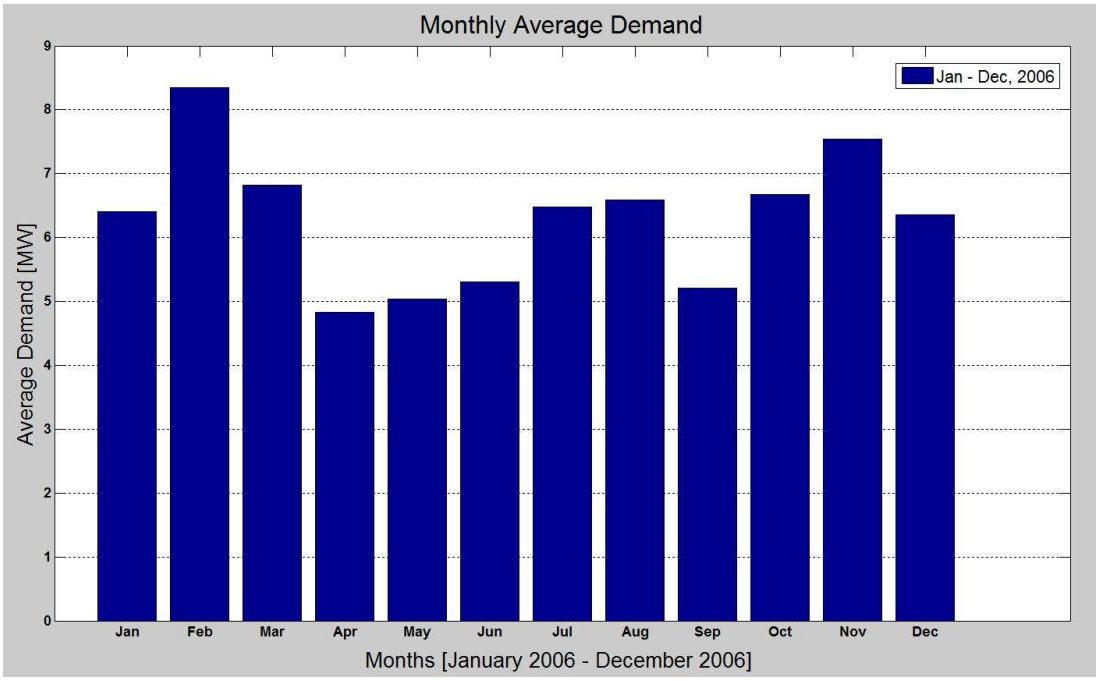

Figure 18 – Monthly Average Demand, 2006

Figure 19 shows the average hourly demand on the feeder for four different months – January, April, July and October. The hourly demands for all four months have a very similar pattern. The average demand for every hour shows two peak demand periods: morning (9 am – 11 am) and evening (6 pm – 9 pm). The day time (11 am – 5 pm) demand values are higher than the nightly demand but lower than the two peaks.

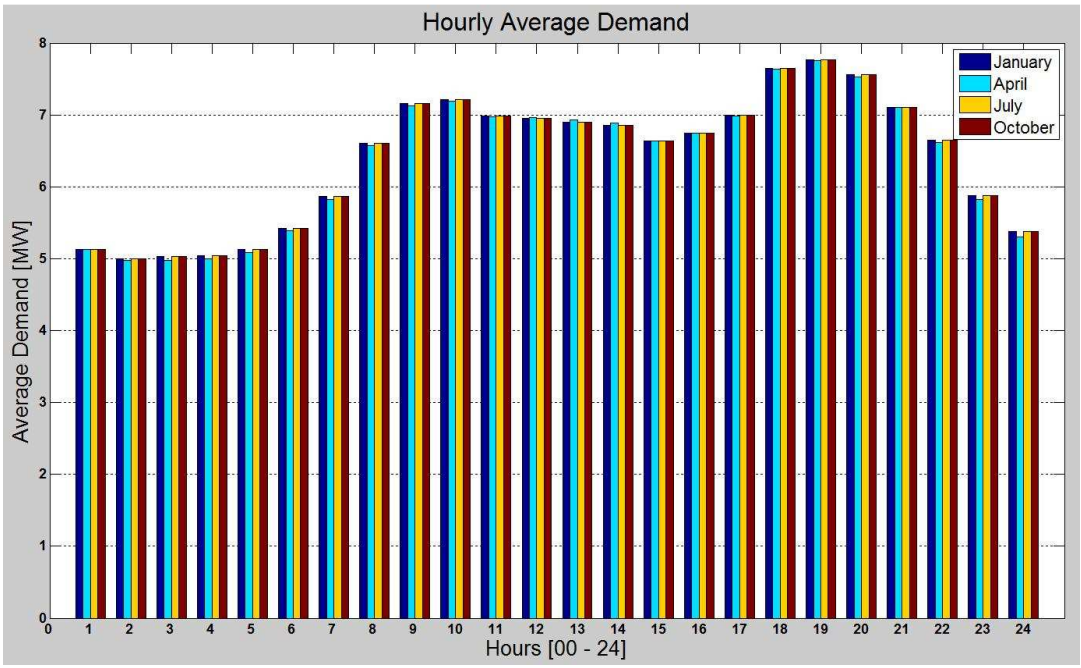

Figure 19 – Hourly Average Demand, 2006

5.2. Wind Turbine Parameters

Specifications of wind turbines have been chosen based on the GE 1.5 SLE turbines. As discussed before, GE 1.5 SLE turbines are most widely used turbines in Ontario. Table 8 outlines the parameters used for power output calculation [7]. The power curve for this specific turbine model has been presented previously in Figure 4.

Table 8 – Wind Turbine Parameters

Parameter	Setting
Rated Capacity	1500 kW
Cut–in Wind Speed	3.5 m/s
Rated Wind Speed	14 m/s
Cut–out Wind Speed	25 m/s
Tower Hub Height	80 m
Rotor Diameter	77 m

5.3. Wind Profile Data

Wind speed data for a weather station close the location of the model system has been obtained from National Climate Data and Information Archive [43]. This data represents the average wind speed for every hour in 2006. The date and hour stamps for the wind speed and load demand data sets have been matched to avoid any inconsistency.

Monthly average wind speeds have been plotted in Figure 20. Wind speed in this area is highest during the winter months. December, January and February are the months with the strongest wind. Wind speed starts to decrease over the spring and reaches a minimum in August.

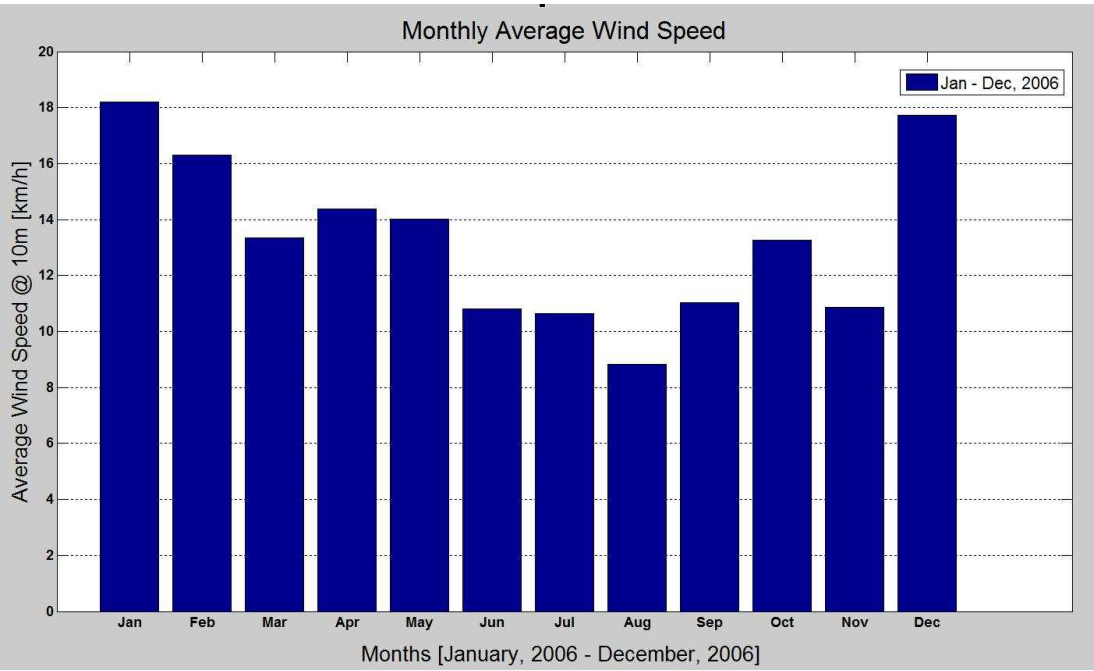

Figure 20 – Monthly Average Wind Speed, 2006

Figure 21 shows the average wind speeds for each of the 24 hours in a day for January, April, July and October. The hourly averages are consistent for all the four months under consideration. Average wind speeds for every hour has a somewhat bell-shaped pattern with a maximum between 1 pm and 2 pm. Wind speed is slower in the late evening and early morning time period.

Wind speed data theoretically follows the Weibull distribution. The wind speed distribution for the whole year has been plotted in Figure 22 below. Comparing with distribution provided in

Figure 6, it is noted that the wind speed data used in this analysis roughly follows the same shape as the theoretical expectation.

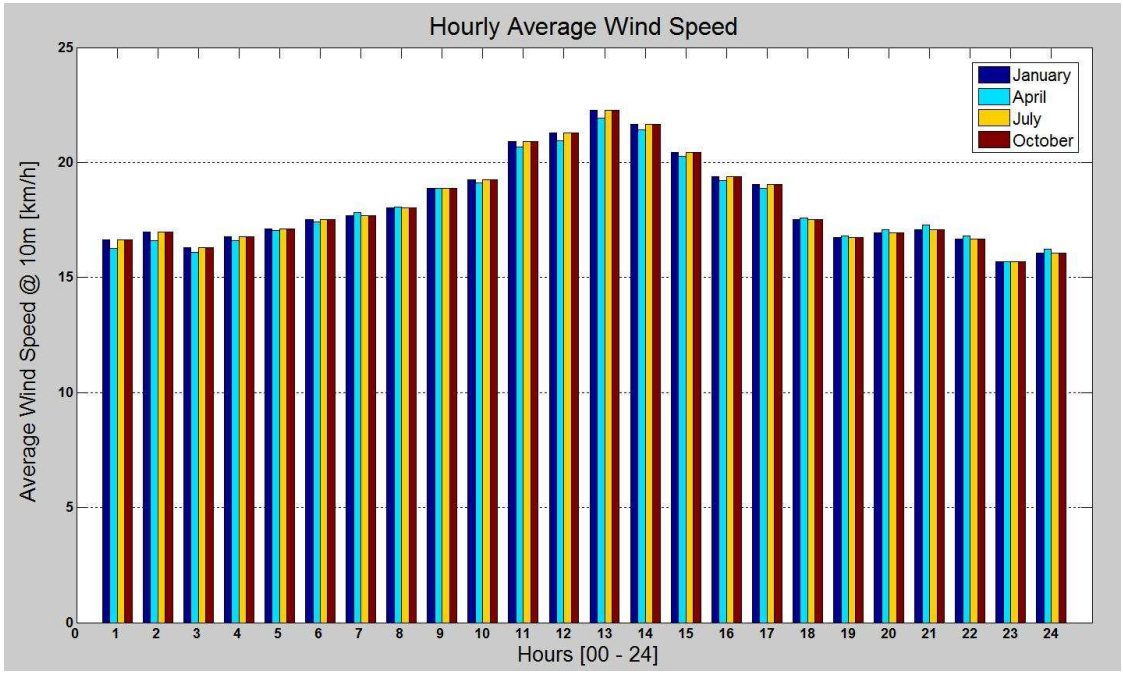

Figure 21 – Hourly Average Wind Speed, 2006

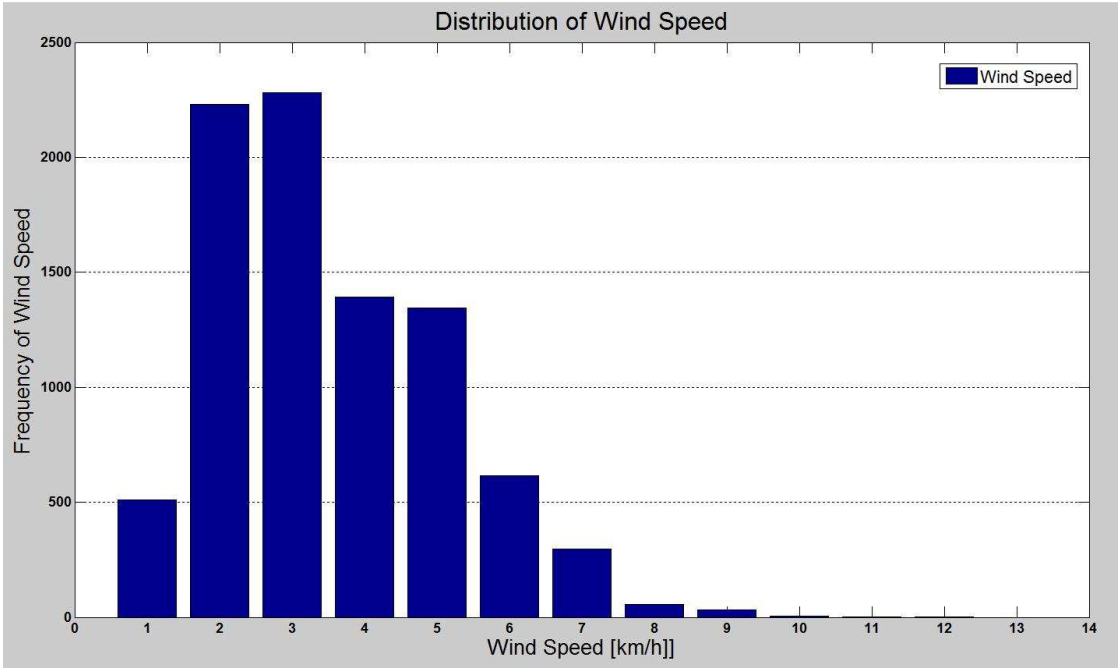

Figure 22 – Frequency Distribution of Wind Speed, 2006

5.4. Energy Price Data

Hourly Ontario Energy Price (HOEP) data obtained from Independent Electricity System Operator (IESO) [44]. Similar to load demand data and wind speed data, this data set includes the hourly energy prices for all the hours in the calendar year 2006. Figure 23 shows the monthly average energy prices for the year under consideration. Energy prices are highest during the winter months. The variation in prices between winter, spring and summer is not quite high. In fact, the three months with highest values of average monthly prices are during January, May and August. Energy prices are comparatively lower during fall with the lowest energy price during the month of September.

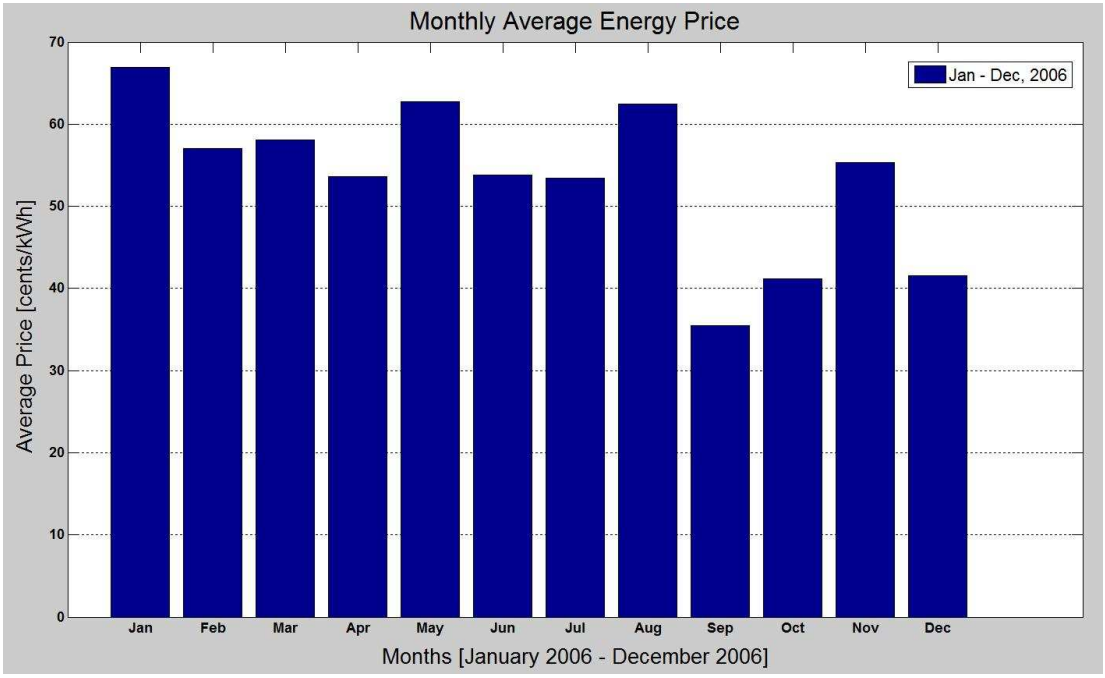

Figure 23 – Monthly Average Energy Price, 2006

Figure 24 illustrates the average energy prices for every hour during the months of January, April, July and October. Energy prices are highest during the late evening period and lowest during the early hours of the day. Two spikes in prices are observed in the hourly average price. The first sharp increase is during 8am – 9am and the second one lasts between 6pm – 8pm. A general decrease in prices is observed after 9pm. Overnight energy prices are considerably lower and more stable than the prices during the day.

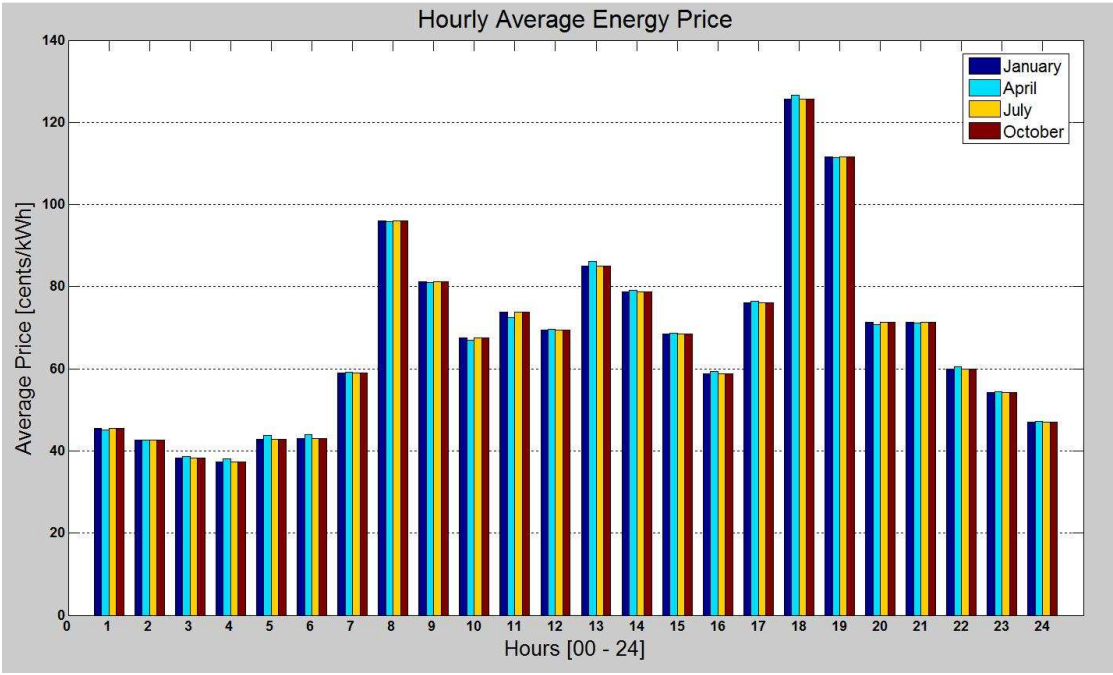

Figure 24 – Hourly Average Energy Price, 2006

5.5. Comparison of Wind Speed, Demand and Price Peaks

Load demand and energy prices are usually correlated for a large system. For smaller systems such as the model system used in this analysis, such correlation is slight since the typical distribution system plays very small role in determining the energy price. Wind speed is usually independent of the other two data sets. Figure 25 below shows the normalized hourly averages of wind speed, load demand and energy price.

The peak in wind speed is during the time period when the system experiences higher load demands. This indicates that the location is a suitable site for wind power generators. The wind power can help reduce the strain on the substation/source. The peak in the energy prices is during low wind periods. In fact, energy prices are low during high wind periods. This negative correlation between wind speed and energy prices indicates the need for a storage device. The cheaper energy during high wind periods can be stored for later usage when energy price is higher. This will help bring down the overall energy cost of the area.

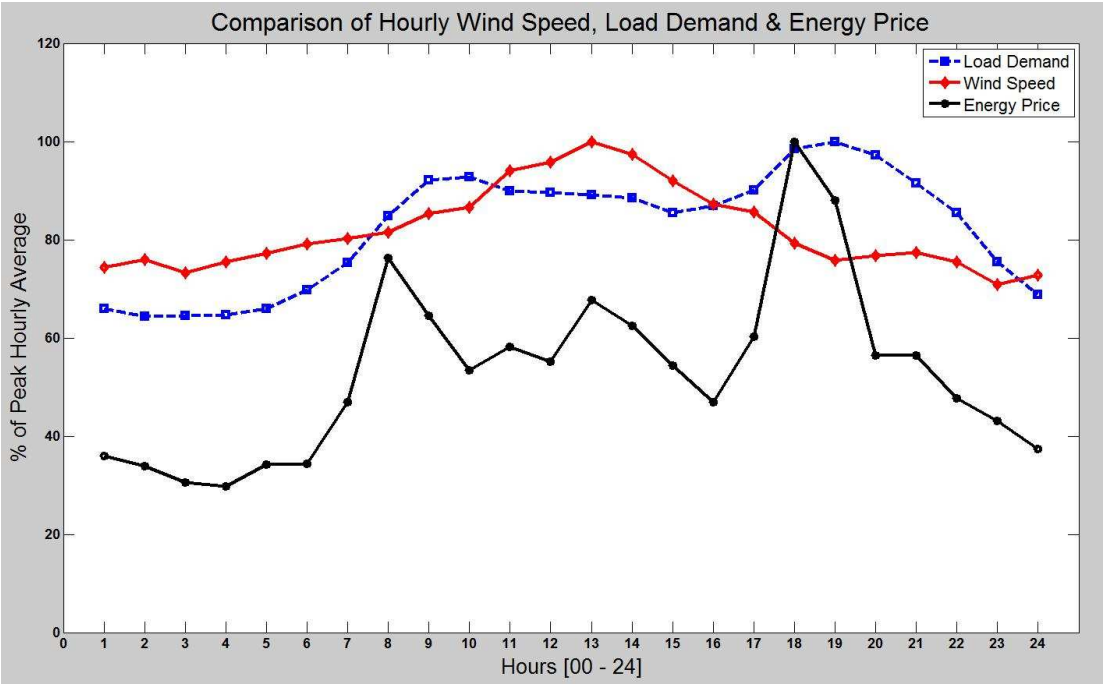

Figure 25 – Comparison of Wind Speed, Load Demand and Energy Price, 2006

Chapter 6: Selection of Storage Device Location

Location of the storage device is important in determining the technical and economic feasibility of the storage technology in the distribution system. Optimal location will ensure that the device is used most efficiently. Without any storage device installed, the losses in the system are mainly due to line losses between various buses. When a storage device is installed additional losses are incurred when power flows in or out of the storage device. These losses can be offset by reduction in line losses as well as by savings in energy cost due to demand shifting. The optimum location of the storage device will ensure lowest energy cost by lowering the system losses in the system. Capacity factor of wind turbines and energy supplied from the substation are generally not affected by the location of the storage device.

6.1. Location Optimization Problem

A mixed integer non-linear optimization technique has been proposed to obtain the optimum location of the storage device. The objective of this optimization problem is to minimize the annual cost of energy for the study area. Binary variables are used to determine whether a bus has a storage device attached to it. It is assumed that only one storage device will be placed in the system. If more than one storage device is required, location for each storage device can be optimized one-by-one. The annual cost of energy is calculated by summing hourly energy cost. The energy cost for an hour is obtained by multiplying the energy consumption for the hour and the hourly energy price. This formulation not only optimizes the system losses, it also ensures that the losses occur at a low energy cost period.

Objective:

$$\min \quad \sum_{h=1}^{H} E_{sub,h,b} * C_{energy,h}$$

Data from Power Flow:

$$E_{sub,h,b} = \mathrm{Re}\left(V_{sub,h,b} \times I^{*}_{sub,h,b} \times S_{rated}\right) \qquad \text{(i)}$$

$$[V_{sub,h,b} \quad I_{sub,h,b}] = \text{PowerFlowTool}\ (\ \mathrm{CONFIG_h},\ \ \mathrm{LOAD_{h,b}}) \qquad \text{(ii)}$$

$$\mathrm{LOAD_{h,b}} = E_{demand,h} + E_{storage,h,b} - E_{wind,h,b} \qquad \text{(iii)}$$

Wind Energy:

$$E_{wind,h}^{max} = \text{GE15SLE}\left(v_{wind,h}\right) \quad \text{(iv)}$$

$$E_{wind,h,b} \leq E_{wind,h}^{max} \quad \text{(v)}$$

Energy Storage:

$$\sum_{b=1}^{N} X_{storage,b} \leq 1 \quad \text{(vi)}$$

$$\text{abs}\left(E_{storage,h,b}\right) \leq MX_{storage,b} \quad \text{(vii)}$$

$$0 \leq E_{storage,h,b}^{T} \leq E_{storage}^{max} \quad \text{(viii)}$$

$$E_{storage,h,b}^{T} = E_{storage,h-1,b}^{T} + E_{storage,h,b} \quad \text{(ix)}$$

$$-E_{storage,h,b} \leq My_{CH,h,b} \quad \text{(x)}$$

$$I_{TRI,CH} - I_{sub,h} \leq M(1 - y_{CH,h,b}) \quad \text{(xi)}$$

$$E_{storage,h,b} \leq My_{DCH,h,b} \quad \text{(xii)}$$

$$I_{sub,h} - I_{TRI,DCH} \leq M(1 - y_{DCH,h,b}) \quad \text{(xiii)}$$

Binary Variables:

$$X_{storage,b} \in \{0,1\}$$

$$y_{CH,h,b} \in \{0,1\}$$

$$y_{DCH,h,b} \in \{0,1\}$$

Indexing Ranges:

$$h \in \{1, \ldots, H\}$$

$$b \in \{1, \ldots, N\}$$

where,

b	index for bus location of the storage device (integer)
$C_{energy,h}$	cost of energy during hour *h*

$\mathrm{CONFIG_h}$	system configuration parameters during hour *h*
$E_{demand,h}$	energy demand during hour *h*
$E_{sub,h,b}$	energy from substation during hour *h* for storage at bus *b*
$E_{storage,h,b}$	energy consumed by storage at bus *b* during hour *h*
$E^{T}_{storage,h,b}$	energy state (present charge) of storage at bus *b* during hour *h*
$E^{max}_{storage}$	energy capacity of storage device
$E_{wind,h,b}$	energy supplied by wind generators during hour *h* for storage at bus *b*
$E^{max}_{wind,h}$	energy generated by wind generators during hour *h*
GE15SLE( )	function to calculate wind generation using GE 1.5 MW SLE turbine power curve
h	index for hour (integer)
$I_{sub,h,b}$	current supplied from the substation during hour *h* for storage at bus *b*
$I_{TRI,CH}$	current level for charging phase trigger setting
$I_{TRI,DCH}$	current level for discharging phase trigger setting
$\mathrm{LOAD_{h,b}}$	load distribution and variation during hour *h* for storage at bus *b*
S_{rated}	rated power of the system
$V_{sub,h,b}$	voltage of the substation bus during hour *h* for storage at bus *b*
$v_{wind,h}$	velocity (average) of wind during hour *h*
$X_{storage,b}$	1 = storage device is located at bus *b* 0 = no storage device is located at bus *b*
$y_{CH,h,b}$	binary variable for charging trigger condition
$y_{DCH,h,b}$	binary variable for discharging trigger condition

In the above optimization problem, constraint (i) and (ii) calculates the energy supplied from the substation/source during any hour using the voltage and current information of the substation bus. Constraint (iii) calculates the net load demand by factoring in local generation from wind turbines and the effect of the storage device. Available and utilized wind energy values are obtained from constraints (iv) and (v). Constraint (vi) and (vii) ensures that only one storage device is located in the system and energy supply/consumption by a storage device is only possible if it exists. The charging and discharging triggering functionalities are maintained using constraints (viii) through (xiii). In this formulation, it is assumed that thermal capacities of the concerned feeders are high enough to sustain the increased power transmission resulting from the storage device installation. If a set of feeders have lower thermal capacities, buses on that feeder can be omitted from the set of feasible bus locations. Furthermore, if the storage device

technology has specific siting requirements, a reduced set of feasible buses can be included in the optimization process. Voltage drop due to excess load (storage device charging phase) and voltage increase due to excess generation (storage device discharging phase) are not included as part of the formulation. The voltage is relaxed under the assumption that voltage correcting devices, if required, can be installed as part of a moderately inexpensive system upgrade.

The solutions in this thesis is obtained by utilizing the Brute Force method of non-linear optimization. As such, the Matlab tool calculates the objective value for each combination of input data. For the location optimization problem, the input data include:

a) Location of the storage device
b) System load demand
c) Output of wind resources

The above optimization problem assumes priori information about the energy price. An alternate optimization problem is proposed in the scenario where energy prices are not known but a projected load demand is available. This problem minimizes the system energy losses to obtain the optimal location.

Objective:

$$\min \quad \sum_{h=1}^{H} E_{loss,h,b}$$

Data from Power Flow:

$$E_{sub,h,b} = \mathrm{Re}\left(V_{sub,h,b} \times I^{*}_{sub,h,b} \times S_{rated}\right) \quad \text{(i)}$$

$$[V_{sub,h,b} \quad I_{sub,h,b}] = \text{PowerFlowTool}\,(\,\mathrm{CONFIG_h},\ \mathrm{LOAD_{h,b}}) \quad \text{(ii)}$$

$$\mathrm{LOAD_{h,b}} = E_{demand,h} + E_{storage,h,b} - E_{wind,h,b} \quad \text{(iii)}$$

$$E_{loss,h,b} = E_{sub,h,b} - \mathrm{LOAD_{h,b}} \quad \text{(iv)}$$

Wind Energy:

$$E^{max}_{wind,h} = \mathrm{GE15SLE}\left(v_{wind,h}\right) \quad \text{(v)}$$

$$E_{wind,h,b} \leq E^{max}_{wind,h} \quad \text{(vi)}$$

Energy Storage:

$$\sum_{b=1}^{N} X_{storage,b} \leq 1 \quad \text{(vii)}$$

$$\text{abs}\,(E_{storage,h,b}) \leq M X_{storage,b} \quad \text{(viii)}$$

$$0 \leq E^{T}_{storage,h,b} \leq E^{max}_{storage} \quad \text{(ix)}$$

$$E^{T}_{storage,h,b} = E^{T}_{storage,h-1,b} + E_{storage,h,b} \quad \text{(x)}$$

$$-E_{storage,h,b} \leq M y_{CH,h,b} \quad \text{(xi)}$$

$$I_{TRI,CH} - I_{sub,h} \leq M(1 - y_{CH,h,b}) \quad \text{(xii)}$$

$$E_{storage,h,b} \leq M y_{DCH,h,b} \quad \text{(xiii)}$$

$$I_{sub,h} - I_{TRI,DCH} \leq M(1 - y_{DCH,h,b}) \quad \text{(xiv)}$$

Binary Variables:

$$X_{storage,b} \in \{0,1\}$$

$$y_{CH,h,b} \in \{0,1\}$$

$$y_{DCH,h,b} \in \{0,1\}$$

Indexing Ranges:

$$h \in \{1, \dots, H\}$$

$$b \in \{1, \dots, N\}$$

Both optimization problems discussed above should provide very similar results. The total energy cost can be divided into two parts – cost of energy consumed and cost of energy lost in the system. Cost of energy consumed is a function of hourly demand and energy price. Benefit of demand shifting is a direct function of the capacity of the storage device and is not directly influenced by the location of the device. Thus, if the location of the storage device is selected such that the system energy loss is minimized, the cost of energy for the system can also be minimized.

The two problems require *N* x *H* iterations of the power flow algorithm. As such, for a large system, it may be difficult for to simulate for every possible location of the storage device. In addition to the full optimization problem, the following locations have been identified as potential storage device locations:

- Close to the substation
- End of the longest lateral
- Near wind turbines
- Near largest load(s)

Impact of storing storage devices in these locations have been analyzed for the model system and will be discussed in the following subsections.

6.2. Test Cases

To avoid any influence of the energy capacity and charging/discharging ramp rates in determining the optimal location of the storage device, two cases have been proposed. For the first case, the size of the storage device is selected to be equal to the wind power capacity and the charging/discharging rate is kept at 25% of the storage capacity. In the second case, the storage device is sized at 25% wind generation capacity and the charging/discharging rate is kept at 100% of the storage capacity. The wind generation capacity of the area is 6 MW. Table 9 below summarizes the storage device parameters selected for the two cases. For both cases, the charging and discharging trigger levels are set at 20 and 80 respectively. For the potential storage device locations identified in the previous subsection, Table 10 provides the bus numbers specific to the model system.

Table 9 – Storage Device Parameters for Location Analysis Cases

Parameter	Case 1	Case 2
Location	Variable	Variable
Energy Capacity [MWh]	6	1.5
Initial Charge [kWh]	0	0
Charging Ramp Rate [kW/hr]	1500	1500
Discharging Ramp Rate [kW/hr]	1500	1500
Charging Trigger Level	20	20
Discharging Trigger level	80	80

Table 10 – Buses of Interest for Location Analysis

Location Description	Bus #
Close to the substation	Bus 1
End of the longest lateral	Bus 39
Near wind turbines	Bus 47
Near largest load(s)	Bus 4
	Bus 7
	Bus 49

6.3. Simulation and Results – Cost Minimization

The Location Analysis module of the Matlab tool has been used to obtain the most suitable location for the storage device. The 51 buses of the model system comprise the possible list of storage device locations. Annual cost of energy has been calculated using hourly load demand, wind speed and energy price data for 2006. Detailed results for the system annual cost of energy for each storage device location are available in Appendix 4.

Figure 26 shows the variations in annual cost of energy for a storage device with parameters outlined in Case 1. The x-axis shows the possible locations of the storage device while the annual system energy costs for locating the device at those buses are plotted on the y-axis. The system energy costs vary between $24.844 million and $24.900 million for various locations of the device. As such, the variation in the energy cost is rather low. The best result is obtained when the storage device is located at Bus 49 or Bus 48. The system energy cost is $24.844 million for both these locations.

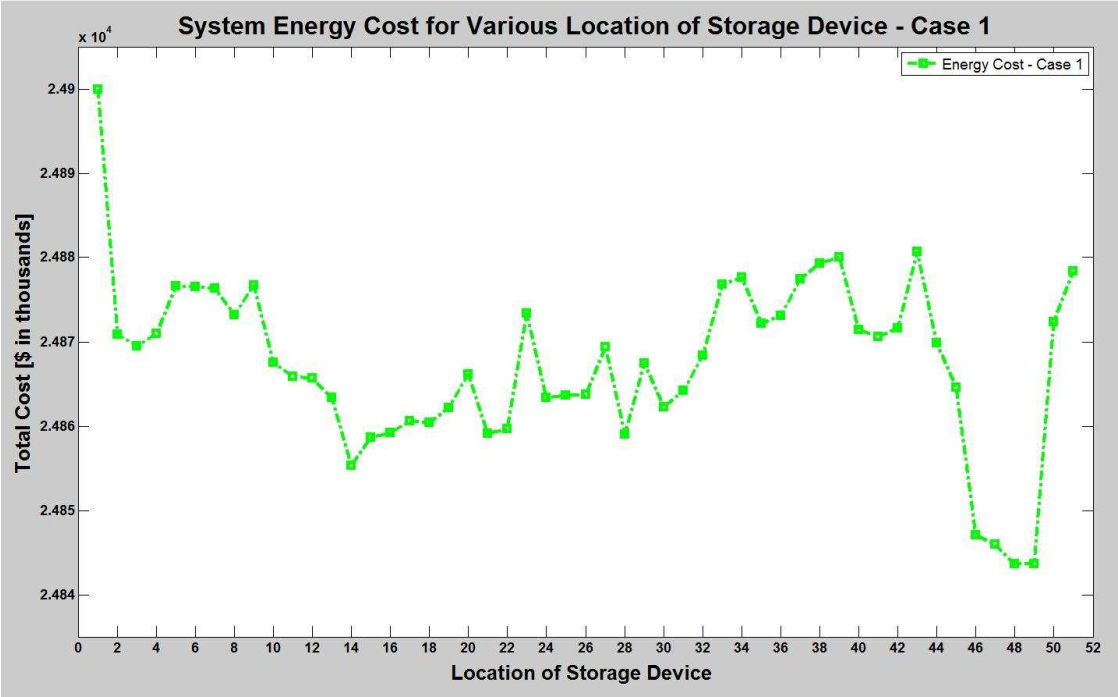

Figure 26 – System Energy Cost Comparison for Location Analysis (Case 1)

Locating the storage device close to the substation/source results in very high energy cost for the model system. This is primarily due to the long distance between Bus 1 and Bus 2. This long distance results in high impedances and power losses. Placing the storage device at the end of the longest lateral does not provide any significant improvements in costs. When the device is located near the wind turbines, the energy cost is very close to the lowest value. If the device is located near the larger loads, the energy cost is markedly lower than costs for the neighbouring buses. The proximity to the wind turbines and one of the larger loads ensure the lowest cost of energy for locating the device at Bus 48 or Bus 49. Table 11 summarizes the system energy costs for locating the storage device at each of the locations of interest.

Table 11 – System Energy Costs for Locations of Interest (Case 1)

Location Description	Bys #	System Energy Cost [Millions $]
Close to the substation	Bus 1	$24.900
End of the longest lateral	Bus 39	$24.880
Near wind turbines	Bus 47	$24.846
Near largest load(s)	Bus 4	$24.871

	Bus 7	$24.876
	Bus 49	$24.844

Figure 27 shows the system energy costs for various locations of the storage device when the parameters outlined in Case 2 are used. In this case, the best result is obtained when Bus 47 is selected as the location for the device. The energy cost for the other locations vary in a very narrow range of values – between $24.978 million and $24.990 million. The buses selected for the previous case – Bus 48 and Bus 49 – provide the second best results. The energy cost for both these buses is $24.979 million.

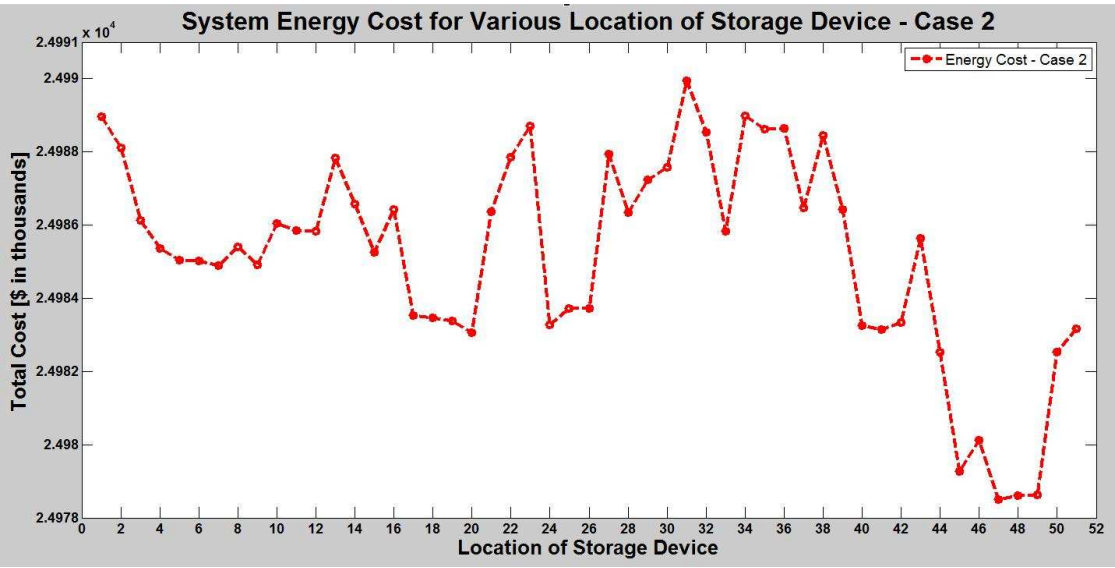

Figure 27 – System Energy Cost Comparison for Location Analysis (Case 2)

Similar to the previous case, the energy cost is very high when the device is located close to the substation/source. Placing the device near the end of the longest lateral does not provide any significant improvements in price. When the device is located near large loads, the energy costs are lowered. In this case, the best result is obtained when the storage device is located near the wind turbines. Table 12 summarizes the system energy costs for located the storage device at each of the locations of interest.

Table 12 – System Energy Costs for Locations of Interest (Case 2)

Location Description	Bus #	System Energy Cost [Millions $]
Close to the substation	Bus 1	$24.989

End of the longest lateral	Bus 39	$24.986
Near wind turbines	Bus 47	$24.978
Near largest load(s)	Bus 4	$24.985
	Bus 7	$24.985
	Bus 49	$24.979

6.4. Simulation and Results – Loss Minimization

Similar to the procedure for the cost minimization objective, the 51 buses of the model system are used as possible locations for the storage device. System energy loss is calculated using the same 2006 data set as in the previous objective. Figure 28 plots the system energy losses for the two sets of parameters (Case 1 and Case 2) of the storage device. For both cases, energy loss is minimized when Bus 47 is chosen as the storage device location. The system annual energy losses for each storage device location is available in Appendix 4.

For Case 1, system energy loss varies between 2.0513 GWh and 2.1008 GWh. With a system total energy demand of 55.094 GWh, these losses are between 3.72% and 3.81%. The lowest energy loss is incurred when the storage device is located near the wind turbines at Bus 47. Locating the device near the substation/source or at the remote branches of the system results in higher energy losses. Improvement in energy losses is observed when the device is located near large loads. Energy loss for locating the storage device at Bus 45 is almost as low as locating it at Bus 47. This is due to the proximity of Bus 45 to the main lateral to which many of the other large loads are connected.

Similar trends are observed for Case 2 where a smaller storage device is used. The range for system energy losses for Case 2 is between 2.0746 GWh and 2.0922 GWh. In this case, the system energy losses vary within a narrower range. The losses are also slightly higher than the previous case. Again, the best result is obtained for locating the device at Bus 47.

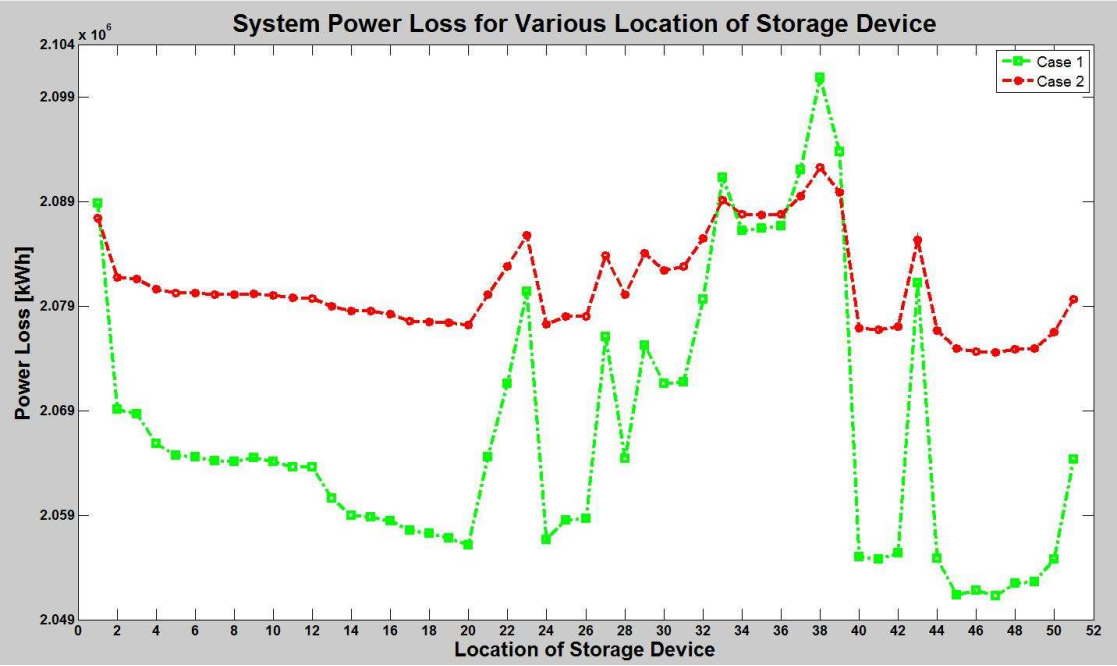

Figure 28 – System Energy Loss Comparison for Various Locations

Annual energy loss for the system for various locations of interest of the storage device has been summarized in Table 13. The pattern observed here is similar to the pattern observed for the cost minimization solution.

Table 13 – System Energy Losses for Locations of Interest

Location Description	Bus #	System Annual Energy Loss [GWh]	
		Case 1	Case 2
Close to the substation	Bus 1	2.0888	2.0874
End of the longest lateral	Bus 39	2.0937	2.0899
Near wind turbines	Bus 47	2.0513	2.0746
Near largest load(s)	Bus 4	2.0663	2.0812
	Bus 7	2.0642	2.0801
	Bus 49	2.0526	2.0749

6.5. Discussion and Summary

The two optimization problems – cost minimization and loss minimization – have been solved for the two sets of parameters for the storage device. Table 14 summarizes the results for the various scenarios.

Table 14 – Optimal Location for Various Objectives/Scenarios

Objective	Bus #	Optimal Solution
System Cost Minimization	Case 1	Bus 48, Bus 49
	Case 2	Bus 47
System Loss Minimization	Case 1	Bus 47
	Case 2	Bus 47

It can be concluded that locating the storage device near the wind turbines or near the large loads improve system performance by reducing energy cost and energy loss. The actual improvements vary from system to system. For the model system, Bus 47 (near the wind turbines) is the most frequently chosen optimum location for the storage device.

Chapter 7: Selection of Storage Device Capacity

Once a location for the storage device is chosen, the Capacity Analysis module of the Matlab tool can be used to obtain optimal capacity parameters for the device. In terms of capacity, storage devices have two important limits – energy capacity and power capacity. The total charge storage ability of the storage device is known as the energy capacity. Power capacity is the rate at which the device can charge or discharge energy.

The main goals in selecting the size parameters of the storage device are:

1. Load following capability of wind turbines is maximized
2. Utilization of wind energy is maximized
3. System energy loss is minimized
4. System energy cost is minimized

For each of the goals outlined above, individual mixed integer non-linear optimization problems have been proposed to obtain the most suitable sizing parameters of the storage device. The parameters to be determined are the energy storage capacity and the charging/discharging. Once the results for individual goal optimization problems are obtained, a weighted selection process has been proposed to take into account multiple goals with various priority levels.

To compare the improvements resulting from various capacity combinations of the storage device, it is essential to calculate comparable values for the "no-storage" scenario. In this scenario, only nodal structure, loads and wind turbines are used to calculate the standard deviation of substation supplied power, wind turbine capacity factor, system energy loss and system energy cost. These values are presented in Table 15. When calculating percentage improvement for various objectives, these values are used as the base case.

Table 15 – System Performance Without Storage Device

Parameter	Value
Standard Deviation of Substation Supplied Power	2860.5
Capacity Factor of Wind Turbines	0.2414
System Energy Loss	2.087 GWh
System Energy Cost	$25.046 Million

7.1. Test Cases

To facilitate the size determination optimization problems, a discrete set of values have been chosen for the energy storage capacity and charge/discharge ramp rates of the storage device. The range for energy storage capacity is chosen to be between 25% and 300% of available wind generation capacity. The selected interval for discrete values is 25% of the rated wind generation capacity. In the model system, there are 4 wind turbines with rated capacity of 1.5 MW each. Thus, the energy storage capacities selected for evaluation are between 1.5 MWh and 18 MWh with increments of 1.5 MWh.

For each energy storage capacity level, the range for charge/discharge ramp rates is chosen to be between 20% and 100% of the energy storage capacity. The selected interval for the discrete values of the ramp rate is 20% of the energy storage capacity. For example, if the device's energy storage capacity is 3 MWh, the ramp rates to be evaluated are 600 kW/hr, 1.2 MW/hr, 1.8 MW/hr, 2.4 MW/hr and 3 MW/hr. For storage devices with energy capacity higher than the rated wind generation capacity of the system, the charge-discharge rates are limited to 20%, 40%, 60%, 80% and 100% of the wind generation capacity. Charge-discharge rates higher than the wind generation capacity may lead to voltage instability and excessive losses.

The parameters of the storage device used in these optimization problems are provided in Table 16. A total of 12 different energy storage capacities and, for each of them, 5 different ramp rates have been selected for evaluation. The complete set of energy and power capacity values for the model system is provided in Appendix 5.

Table 16 – Storage Device Parameters for Capacity Analysis Cases

Parameter	Value
Location	Bus 47
Energy Capacity [kWh]	Variable
Initial Charge [kWh]	0
Charging Ramp Rate [kW/hr]	Variable
Discharging Ramp Rate [kW/hr]	Variable
Charging Trigger Level	20
Discharging Trigger level	80

7.2. Capacity Selection by Maximizing Load Following Capability

The peak generation of wind turbines is weather dependant while peak power demand is a function of time and day. They generally have very little correlation and do not necessarily coincide with each other. If generation is higher than the demand and no back feed is allowed out of the area, the excess power has to be discarded to maintain system stability. Similarly, if demand is higher than generation, the substation must supply the balance energy to maintain system reliability. For islanded operation, failure to follow the changes in demand can result in system outages.

With a storage device installed in the system, the "excess" energy during high generation periods can be stored for later use. The storage device can act as a pseudo source when wind generation is low. The combination of storage device and wind turbines in the distribution level leads to a lesser dependence on the substation to supply energy for the unmet demand. This load following capability of the wind turbines can be assessed by evaluating the standard deviation of the amount of energy supplied from the substation/source for every hour. The better the load following capability the lower the standard deviation will be. The optimization problem formulation is similar to the previously presented problem for location analysis. The location identifier *b* has been replaced with {*e*, *p*} which indicates the energy and power capacities respectively.

Objective:

$$\min \quad \sqrt{\sum_{h=1}^{H} \left(E_{sub,h,e,p}\right)^2}$$

Data from Power Flow:

$$E_{sub,h,e,p} = \mathrm{Re}\left(V_{sub,h,e,p} \times I^{*}_{sub,h,e,p} \times S_{rated}\right) \quad \text{(i)}$$

$$[V_{sub,h,e,p} \quad I_{sub,h,e,p}] = \mathrm{PowerFlowTool}\ (\ \mathrm{CONFIG_h},\ \ \mathrm{LOAD_{h,e,p}}) \quad \text{(ii)}$$

$$\mathrm{LOAD_{h,e,p}} = E_{demand,h} + E_{storage,h,e,p} - E_{wind,h,e,p} \quad \text{(iii)}$$

Wind Energy:

$$E^{max}_{wind,h} = \mathrm{GE15SLE}\left(v_{wind,h}\right) \quad \text{(iv)}$$

$$E_{wind,h,e,p} \leq E^{max}_{wind,h} \quad \text{(v)}$$

Energy Storage:

$$0 \leq E^{T}_{storage,h,e,p} \leq E^{max}_{storage,e} \quad \text{(vi)}$$

$$E^{T}_{storage,h,e,p} = E^{T}_{storage,h-1,e,p} + E_{storage,h,e,p} \quad \text{(vii)}$$

$$-E_{storage,h,e,p} \leq M y_{CH,h,e,p} \quad \text{(viii)}$$

$$I_{TRI,CH} - I_{sub,h} \leq M(1 - y_{CH,h,e,p}) \quad \text{(ix)}$$

$$E_{storage,h,e,p} \leq M y_{DCH,h,e,p} \quad \text{(x)}$$

$$I_{sub,h} - I_{TRI,DCH} \leq M(1 - y_{DCH,h,e,p}) \quad \text{(xi)}$$

Binary Variables:

$$y_{CH,h,b} \in \{0,1\}$$

$$y_{DCH,h,b} \in \{0,1\}$$

Indexing Ranges:

$$h \in \{1, \ldots, H\}$$

where,

$C_{energy,h}$	cost of energy during hour *h*
CONFIG_{h}	system configuration parameters during hour *h*
e	setting for energy capacity (integer)
$E_{demand,h}$	energy demand during hour *h*
$E_{sub,h,e,p}$	energy from substation during hour *h* for setting {*e*, *p*}
$E_{storage,h,e,p}$	energy consumed by storage during hour *h* for setting {*e*, *p*}
$E^{T}_{storage,h,e,p}$	energy state (present charge during hour *h* for setting {*e*, *p*}
$E^{max}_{storage,e}$	energy capacity of storage device for setting {*e*, *p*}
$E_{wind,h,e,p}$	energy supplied by wind generators during hour *h* for setting {*e*, *p*}
$E^{max}_{wind,h}$	energy generated by wind generators during hour *h*
GE15SLE( )	function to calculate wind generation using GE 1.5 MW SLE turbine power curve
$I_{sub,he,p}$	current supplied from the substation during hour *h* for setting {*e*, *p*}
$I_{TRI,CH}$	current level for charging phase trigger setting

$I_{TRI,DCH}$	current level for discharging phase trigger setting
$\mathrm{LOAD}_{\mathrm{h,e,p}}$	load distribution and variation during hour *h* for setting {*e*, *p*}
p	setting for charge-discharge (power) capacity (integer)
S_{rated}	rated power of the system
$V_{sub,h,e,p}$	voltage of the substation bus during hour *h* for setting {*e*, *p*}
$v_{wind,h}$	velocity (average) of wind during hour *h*
$y_{CH,h,b}$	binary variable for charging trigger condition
$y_{DCH,h,b}$	binary variable for discharging trigger condition

Figure 29 illustrates the percentage improvement in load following capability for various storage device sizing parameters. The percentage improvement is calculated based on the standard deviation value from Table 15. For example, 5% improvement in load following capability indicates that the standard deviation of substation energy supply for that case is 5% lower than the standard deviation in the no–storage scenario. Detailed results are provided in Appendix 5.

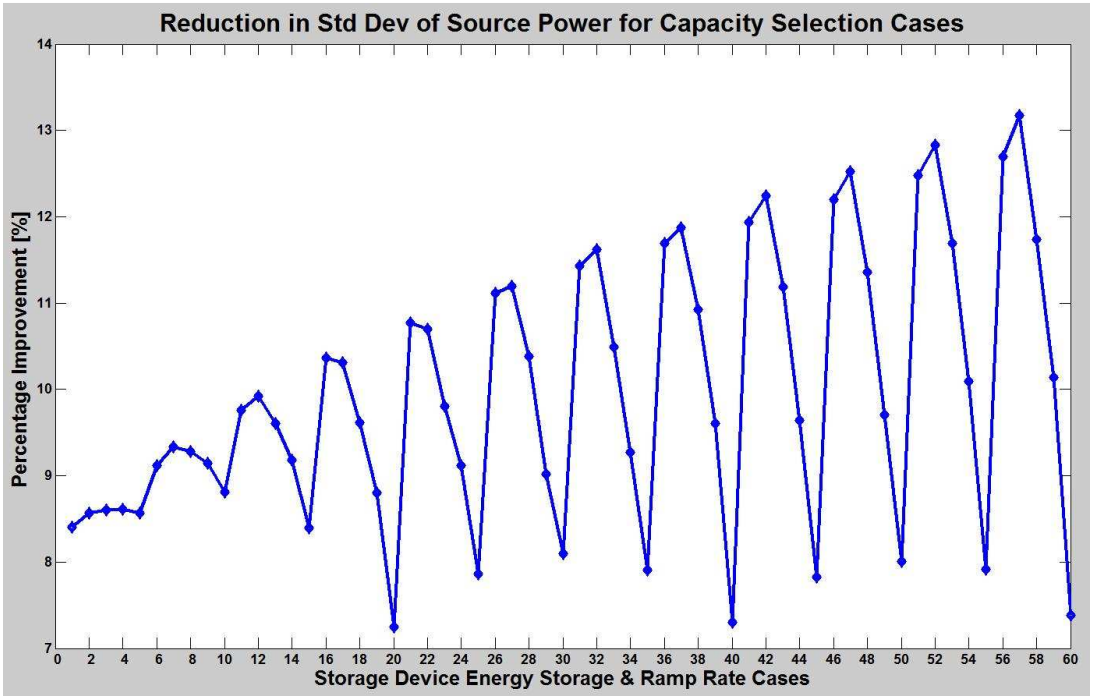

Figure 29 – Improvement in Load Following Capability for Storage Capacity Selection Cases

The improvement in load following capability of the wind turbines vary between 7.25% and 13.17% for various capacity parameters of the storage device. Load following capability increases (i.e. the standard deviation of substation supplied energy decreases) as the energy

storage capacity of the storage device is increased. For low values of charge-discharge ramp rates (power capacities), increasing the ramp rates also increases the load following capability. But this increase reaches a maximum after the 2nd increase in ramp rates and, following that maximum, increasing the charge-discharge rate reduces the load following capability. The best result is obtained when the storage device with largest energy storage capacity and moderate charge-discharge rate is chosen. For the model system, Case 57 provides the optimal result where the energy storage capacity is 18 MWh and the ramp rate is set to 2400 kW/hr.

7.3. Capacity Selection by Maximizing Wind Energy Utilization

By storing excess wind energy for use during peak demand periods, the utilization of wind turbines can be increased. Higher utilization of wind turbines leads to higher capacity factors. The objective function for capacity parameter selection by maximizing wind energy utilization is provided below. The constraints remain same as those in the previous subsection.

Objective: max $\frac{\sum_{h=1}^{H} E_{wind,h,e,p}}{N \times E_{wind}^{Rated}}$

For the model system, capacity factor of the wind turbines is 24.14%. The limiting factor for the capacity factor in this case is the availability of useful wind. Wind is considered to be useful for a wind turbine when its speed is within the rated and cut–off limits of the turbine. Of the 8760 hours evaluated, only 366 hours, i.e. 4.18%, had excess wind energy. Figure 30 shows the percentage changes in capacity factors for storage devices of various capacities. Detailed results are presented in Appendix 5.

Various combinations of energy storage capacity and charge-discharge capacity lead to between 0.03% and 0.41% improvement in capacity factor of the wind turbines. Devices with larger energy storage capacities are able to store greater amount of electrical charge and, thus, lead to higher capacity factors. The relationship between increase in energy storage capacity and increase in capacity factor is of diminishing nature. That is, increasing the energy capacity results in higher increase in capacity factor for smaller values of energy storage capacity than it is for higher values. Increasing the charge-discharge capacity (ramp rate) decreases the capacity factor. The best result is obtained by Case 56 where the energy storage capacity is 18 MWh and ramp rate is 1200 kW/hr.

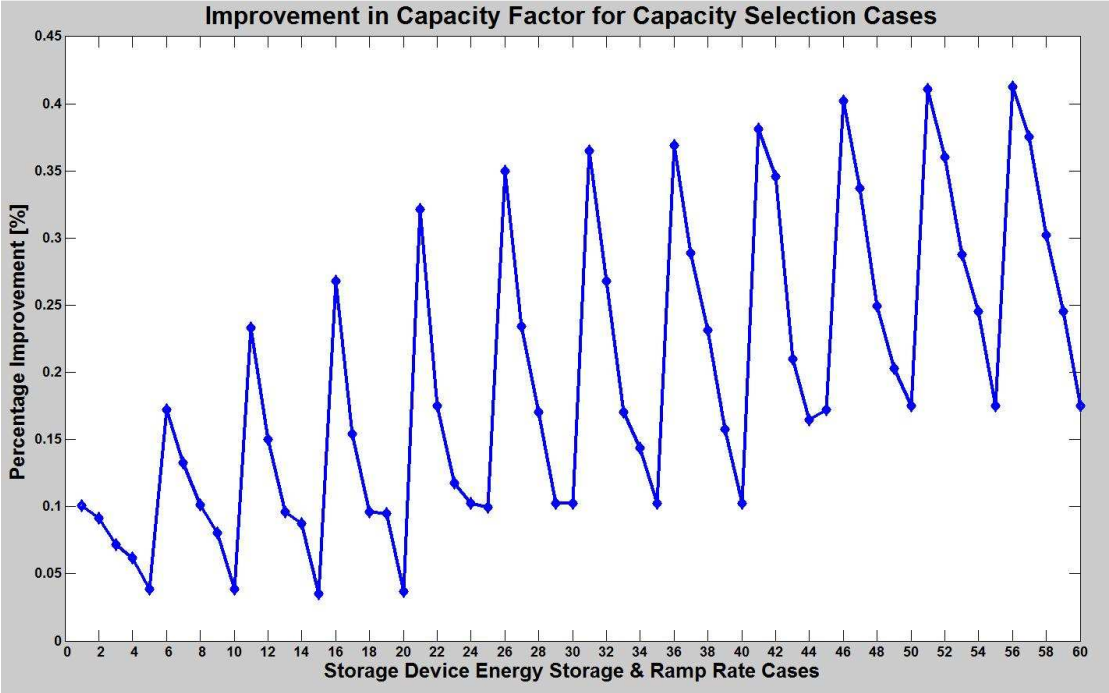

Figure 30 – Improvement in Capacity Factors for Storage Capacity Selection Cases

7.4. Capacity Selection by Minimizing System Energy Losses

Depending on the size and location of the storage device, the charging and discharging operation incurs varying levels of line losses. Here, it is assumed that the storage device is loss–less. Any losses associated with the storage device, such as energy leakage, power electronic conversion losses etc., are not accounted for in the following analysis. Depending on the technology chosen and durations of storage, the device specific losses can increase the overall system energy loss.

System energy loss is defined by the difference between available energy supply and effective demand. Energy can be supplied from the substation/source, wind turbines and storage device (discharging phase). Energy demand is the sum of storage device load (charging phase) and the other loads connected to the system. The objective function to minimize the system losses is shown below. The constraints remain the same as used in previous capacity selection problems except for one additional constraint to calculate the power losses.

$$\min \quad \sum_{h=1}^{H} E_{loss,h,e,p}$$

$$E_{loss,h,e,p} = E_{sub,h,e,p} - \text{LOAD}_{\text{h,e,p}}$$

Figure 31 shows the reduction in system total energy losses for the selected cases of storage device capacity parameters. The percentage improvement in system energy losses are plotted on the y–axis. A positive percentage improvement means a reduction in losses while a negative value for percentage improvement refers to an increase in losses. Again, the detailed values are provided in Appendix 5.

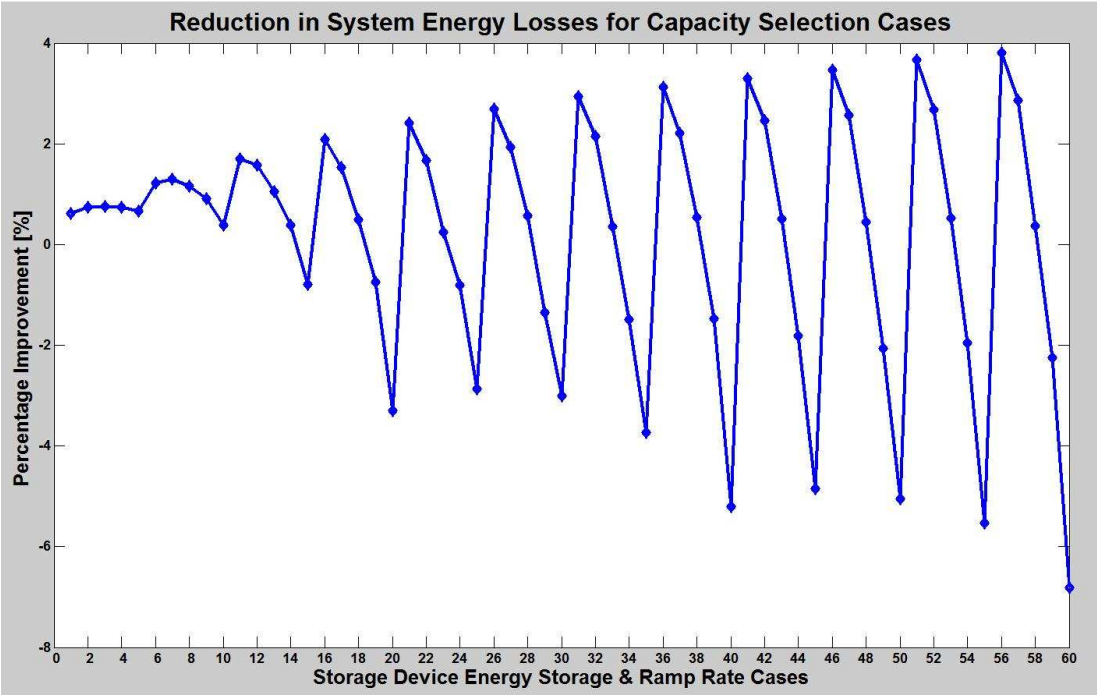

Figure 31 – Improvement in Energy Losses for Storage Capacity Selection Cases

Various combinations of energy storage capacity and charge-discharge (ramp) rates lead to between -6.81% and 3.81% improvement in system losses. Again, negative percentage improvement means increase in losses. As energy storage capacity of the device is increased, the energy loss is reduced (i.e. higher percentage improvements). Increasing the ramp rates of the storage device increase the system losses. For the model system, best result is obtained for Case 56 which specifies 18 MWh energy storage capacity and 1200 kW/hr charge-discharge rate.

7.5. Capacity Selection by Minimizing System Annual Energy Cost

The final objective in selecting the storage device capacity paramters is to minimize the system annual energy cost. Peak demand hours typically correlate with higher energy price periods. Storing lower cost energy during low demand periods and utilizing that energy during higher cost periods can result in reductions in the energy cost. Other cost savings can result from lowered system energy losses as discussed in the previous sub–section. The objective function for this optimization is as follows:

$$\min \quad \sum_{h=1}^{H} E_{sub,h,e,p} * C_{energy,h}$$

Figure 32 illustrates the improvements in system annual energy costs for various parameters of the storage device's size. Here, percentage improvement refers to percentage reduction in cost. Detailed results are provided in Appendix 5.

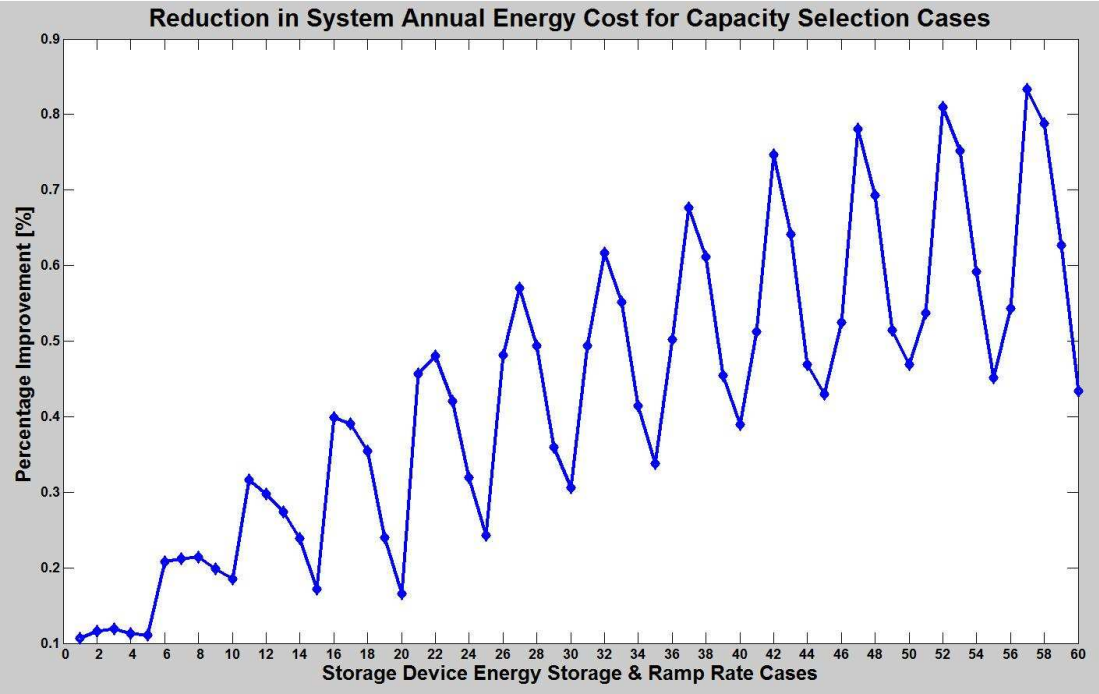

Figure 32 – Improvement in Energy Costs for Storage Capacity Selection Cases

For the model system, the system cost of energy can be reduced by up to 0.83% by optimizing the capacity parameters. Energy capacities of the storage device and percentage improvement (decrease) in energy costs are somewhat linearly related. As the energy storage capacity is increased, the overall cost of energy is decreased. Lower values of charge-discharge rate

provide better cost reduction. In this case, the best results are obtained for Case 57 where the energy storage device is rated at 18 GWh with a ramp rate of 2400 kW/hr.

7.6. Capacity Selection Using Weighted Objectives

In each of the previous four subsections, the storage device capacity parameters are optimized with one specific goal in mind. For maximizing load following capabilities and minimizing system energy costs, Case 57 provides the optimum results. For maximizing wind energy utilization and minimizing system energy losses, Case 56 provides the best results. A weight based selection process is proposed to obtain a single solution the four objectives. The percentage improvement values for various scenarios are multiplied by a weighting factor. The weighting factor is determined based on the priority or importance of the four objectives. The case with the highest weighted improvement is considered the optimal solution for the model system. The weighted percentage improvement for case *C* is calculated using the following formula:

$$i_{w,C} = w_{lf} i_{lf,C} + w_{util} i_{util,C} + w_{loss} i_{loss,C} + w_{cost} i_{cost,C} \quad (6)$$

$$w_{lf} + w_{util} + w_{loss} + w_{cost} = 1 \quad (7)$$

where,

$i_{w,C}$	weighted percentage improvement for Case *C*
$i_{lf,C}$	% improvement (increase) in load following *for* Case *C*
$i_{util,C}$	% improvement (increase) in wind energy utilization for Case *C*
$i_{loss,C}$	% improvement (decrease) in system energy losses for Case *C*
$i_{cost,C}$	% improvement (decrease) in system energy costs for Case *C*
w_{lf}	weight for improvement (increase) in load following
w_{util}	weight for improvement (increase) in wind energy utilization
w_{loss}	weight for improvement (decrease) in system energy losses
w_{cost}	weight for improvement (decrease) in system energy costs

To illustrate this concept, the following weights have been assigned to the four objectives:

Table 17 – Weight Distribution of Objectives for Multi-Objective Capacity Selection

Goal	Weight	Optimum Solution
Load Following	0.25	Case 57
Wind Energy Utilization	0.25	Case 56
Energy Loss Minimization	0.25	Case 56
Energy Cost Minimization	0.25	Case 57

The vector of weights is first normalized such that their sum adds up to 1. Then the normalized weights are used to calculate the weighted percentage improvement for each of the size parameter cases. Figure 33 plots the results for the cases under study.

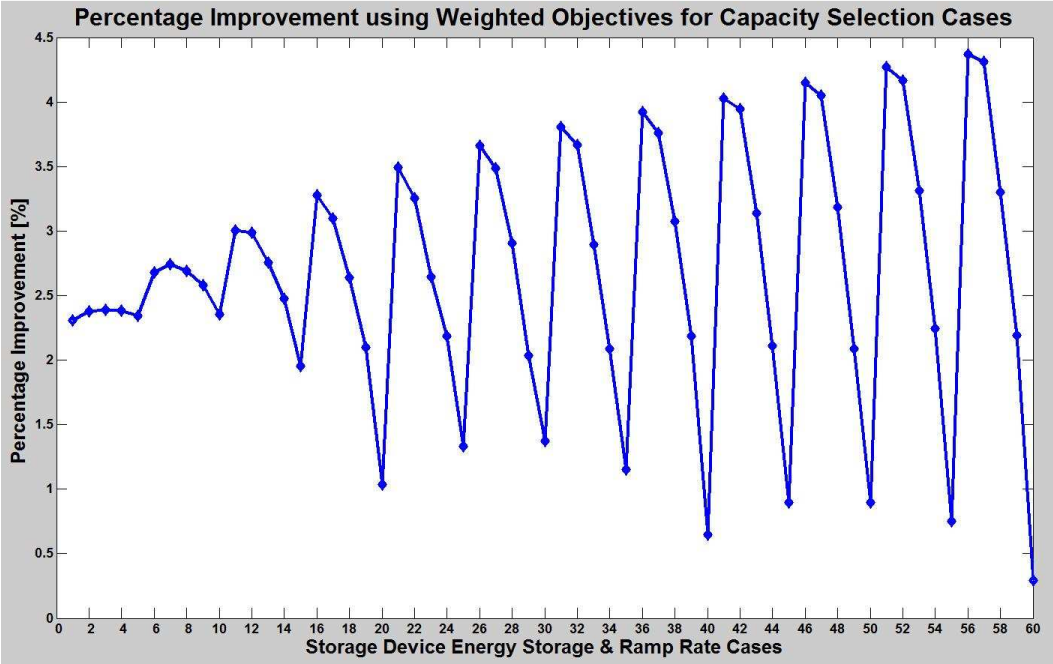

Figure 33 – Improvements in Weighted Objectives for Storage Capacity Selection Cases

As expected, Case 56 and Case 57 provide the most improvements for the model system. Given the weights selected, Case 56 has a slight edge over Case 57. In general, system performance can be improved by increasing the energy storage capacity. Increasing the charge-discharge capacity provides mixed results – improvements are observed at first which

are then followed by significant reductions. As such, lower values of ramp rates are recommended.

7.7. Capacity Selection Using Randomized Objective Weights

To account for various combinations of weight distribution of the four objectives, 10,000 random sets of weights have been generated. For each set of weights, the case that provides the highest improvement is selected. Probability of selection for each case has been provided in Appendix 5. The results plotted in Figure 34 show that, depending on the objective weight distribution, Case 56 and Case 57 represent the most likely storage device capacity parameters.

Figure 34 – Frequency of Capacity Case Selection with Randomized Objective Weights

Chapter 8: Selection of Charge-Discharge Triggering Level

Effective triggering operation allows the storage device to operate the most suitable charging and discharging schedules for the device. Usually the charging operation of a storage device is performed during low demand periods while the discharging operation is performed during high demand periods. It is possible that, for some area, higher wind generation periods coincide with the higher demand periods. As such, the effective load to the substation/source is lower during the period when the loads consume most power. Therefore, the power supplied from the substation or source is a better measure of the effective demand of the area. For the purposes of this project, it is assumed that the storage device has access to the effective energy demand of the study area for a 7–day period (a user selectable variable in the Matlab tool). The storage device parameters store two trigger levels for the charging and discharging operations respectively. Percentile rankings of the stored effective demand data are used to obtain current/load demand values at which the storage device will trigger. For example, if the charging trigger level for a storage device is set to 25, that device starts charging when the current hour's effective demand is lower than 25% of the stored demand values.

Usually the charging trigger level is preferred to be as low as possible. During charging operation, the storage device acts like a load. A low charging trigger level ensures that the extra load created by the storage demand is apparent only during low demand periods. But, if the charging trigger level is too low, the device will be unable to store enough energy to supply during periods when wind generation cannot meet the energy demand. Similarly, the discharge trigger level is preferred to be as high as possible. During discharge operation, the storage device acts like a source. Thus, a high trigger level ensures that the storage device supplies energy when the difference between wind generation and energy demand is at maximum. But, if the discharging trigger is set too high, the device will not be able to operate long enough to discharge all the stored energy.

The main objectives in determining the effective trigger levels for charging and discharging operations of a storage device are similar to the goals outlined in the previous section for energy storage capacity and charge-discharge capacity selection. The objectives are provided below:

1. Load following capability of wind turbines is maximized
2. Utilization of wind energy is maximized
3. System energy loss is minimized

4. System energy cost is minimized

Each of the above objectives is individually optimized to obtain the suitable triggering levels for the storage device. The results for each objective optimization are then combined based on a set of objective weights. This facilitates an approach to select the most appropriate triggering setting by focussing on one or more objectives. A more general solution is then obtained using randomly generated weight values.

8.1. Test Cases

To facilitate the triggering level optimization problems, a discrete set of values have been chosen for charging and discharging trigger values. The two ranges must be disjoint. That is, the charging trigger level cannot be higher than the discharging trigger level. The range for charging trigger level is chosen to be between 5 and 40 with increments of 5. The range for discharging trigger level is chosen to be between 60 and 95 with increments of 5. Thus a total of 64 different cases – combinations of 8 charging levels and 8 discharging levels – are evaluated to obtain the most feasible trigger settings for charging and discharging operations. Cases 1 through 8 are for charging trigger level 5 with discharging trigger level varying between 60 and 95 with increments of 5. Similarly, cases 9 through 16 are for charging trigger level 10, cases 17 through 24 are for charging trigger level 15 and so on. Appendix 6 shows a table with all the cases and the associated charging and discharging levels. Storage device parameters for the charge-discharge trigger level selection analysis are provided in Table 18.

Table 18 – Storage Device Parameters for Charge-Discharge Trigger Analysis Cases

Parameter	Value
Location	Bus 47
Energy Capacity [MWh]	18
Initial Charge [MWh]	0
Charging Ramp Rate [kW/hr]	1200
Discharging Ramp Rate [kW/hr]	1200
Charging Trigger Level	Variable
Discharging Trigger level	Variable

8.2. Trigger Setting Selection by Maximizing Load Following Capability

By charging the storage device to when excess energy is available and discharging it when energy demand is higher than the wind generation, trigger level settings play a major role in ensuring that the load following capability of wind turbines is maximized. When the generation-demand difference is positive, i.e. generation is higher than demand, the storage device should start charging itself to effectively increase the demand and reduce the difference. Similarly, if the generation-demand difference is negative, the storage device should start discharging energy to lower the difference as much as possible.

Similar to the storage device energy capacity and ramp rate selection process, a wind turbine's ability to follow load is measured using the standard deviation of the power supplied by the substation or source. Figure 35 shows the percentage reduction in standard deviation of substation power for various triggering settings. The base for the percentage calculation is obtained from Table 15 which lists performance values for the scenario where no storage device is attached to the system.

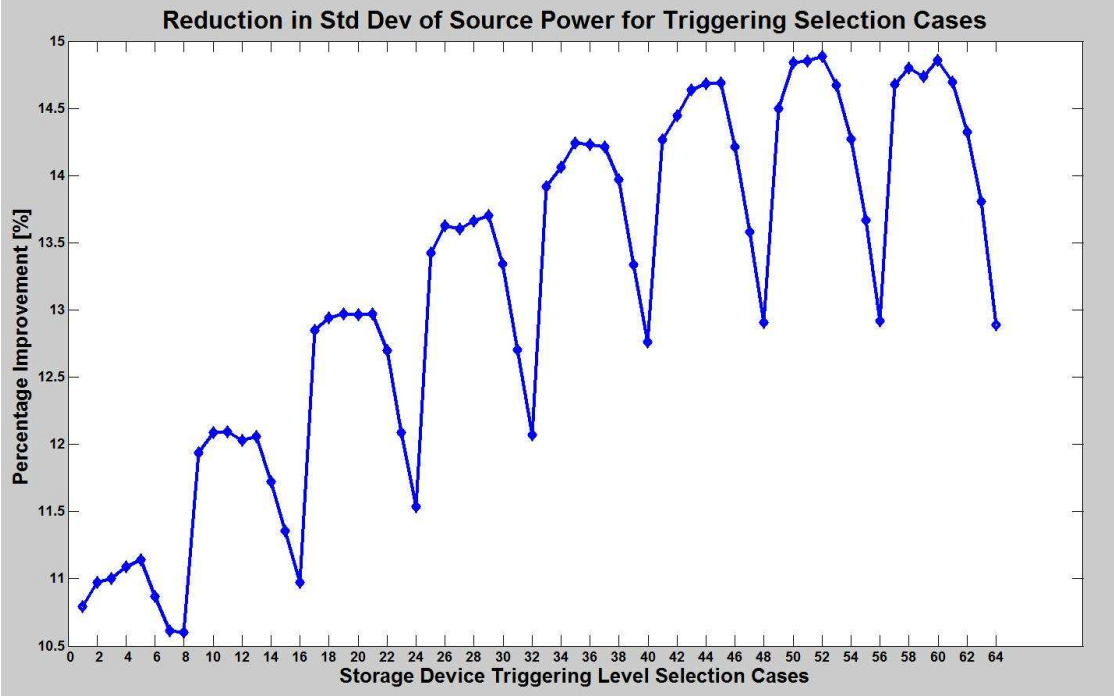

Figure 35 – Improvement in Load Following Capability for Triggering Parameter Cases

The standard deviation of energy supplied from the substation/source can be reduced by between 10.6% and 14.89% depending on the two trigger settings. Detailed results for various cases are provided in Appendix 6. Reduction in standard deviation is greater when the charging

trigger level is increased. Increasing the discharging trigger level results in mixed results. Low to moderate discharging trigger levels provide the highest percentage improvement (reduction) in the standard deviation. For the model system, best results are obtained for Case 52 which indicates charge trigger level of 35 and discharge trigger level of 75. The next best result is obtained for Case 60 providing 14.86% improvement. The trigger levels for Case 60 are 40 and 75 respectively for charging and discharging operations.

8.3. Trigger Setting Selection by Maximizing Wind Energy Utilization

Charging and discharging trigger settings should help maximize the use of energy generated by the wind turbines. At low charging trigger level, the storage device becomes charged quickly – leaving little or no capacity left to store excess wind energy, if/when available. On the other hand, a high charging trigger level comes with the risk that the storage device may not have enough stored energy to supply the demand when necessary. Similarly, optimal discharge trigger level discharges energy before it excess energy is available. Complex charging-discharging mechanisms featuring next-hour wind speed projection and load demand approximation can help achieve the best utilization of wind energy. For the purposes of this project, the charging-discharging mechanism is solely based on trigger levels and stored 7-day source energy supply values. Capacity factors of the wind generators has been used as the measure of wind energy utilization.

Figure 36 illustrates the percentage increase in capacity factor of the wind generators for various cases of charge-discharge trigger levels. A higher value indicates higher usage of wind energy compared to the scenario without a storage device (Table 15). Capacity factor increases for each of the cases are provided in Appendix 6.

Wind energy is best utilized when charging and discharging trigger levels are set at low values. As either value is increased, the capacity factor improvement is decreased. The reduction in capacity factor improvement is more profound for increases in the discharging trigger level. For the 64 cases under study, the capacity factor improvement varies between about 0.06% and 1.89%. The best results are obtained for Case 1 where both trigger values are set to their lower bounds: charging trigger level of 5 and discharging trigger level of 60.

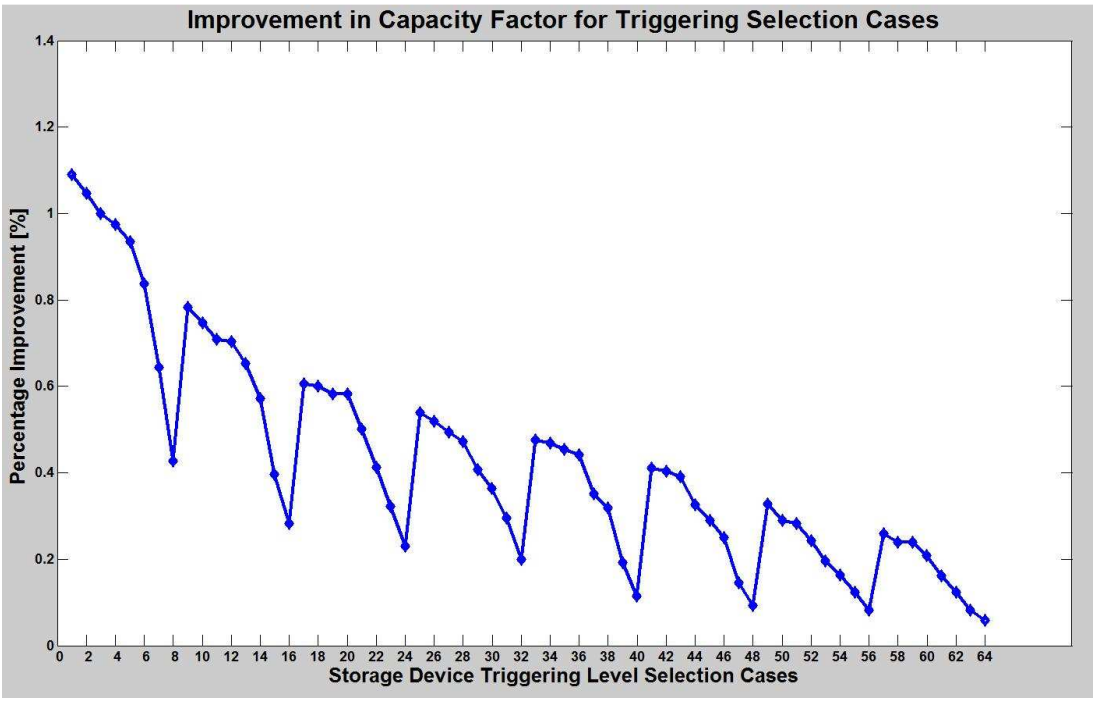

Figure 36 – Improvement in Capacity Factor for Triggering Parameter Cases

8.4. Trigger Setting Selection by Minimizing System Energy Losses

Timing of charge and discharge operations plays a major role in the overall power flow within the system. The system losses are a direct function of the flow of power between the buses. Efficient operation of the storage devices can optimize the flow of power and thus reduce the overall energy loss. Here, it is assumed that the storage device is loss–less. Any losses associated with the storage device, such as energy leakage, power electronic conversion loss etc., are not accounted for in the following analysis. Figure 37 shows the system total energy losses for the various cases. Percentage improvement in system energy losses are plotted on the y–axis. A positive percentage improvement means a reduction in losses while a negative value for percentage improvement refers to an increase in losses.

Various triggering selection cases provide between 2.41% to 4.33% improvement in system losses. Moderate values of both charging and discharging triggering levels provide the most reductions in energy losses. Case 37 with charging trigger level of 25 and discharging trigger level of 80 provide the best results for the model system. Case 29 provide the next best result with 4.32% improvement in losses. The charging and discharging trigger levels for this case are 20 and 80 respectively.

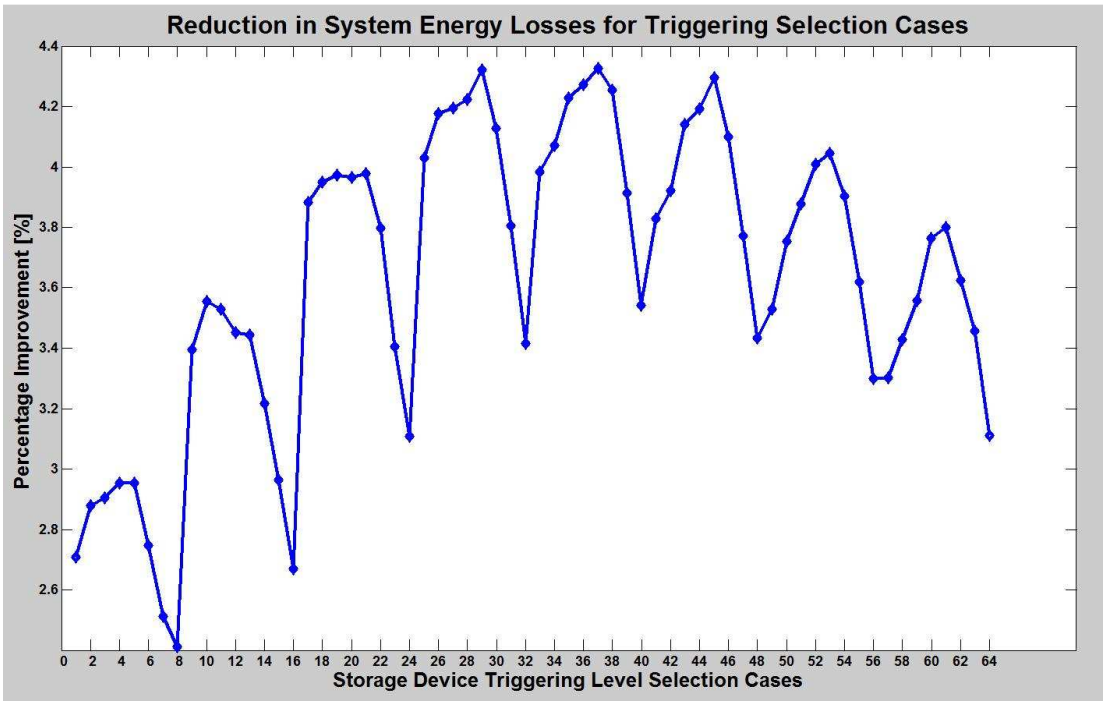

Figure 37 – Improvement in Energy Losses for Triggering Parameter Cases

8.5. Trigger Setting Selection by Minimizing System Annual Energy Cost

Charge and discharge trigger settings allow the storage device to store energy during low cost periods and use that energy when prices are higher. In this project, the triggering is controlled via recorded load data from previous 7 days. In most cases, marginal energy price is very hard to predict. The optimum trigger settings will allow the cheapest energy to be stored for use during highest possible price periods. Other cost savings can result from lowered system energy losses as discussed in the previous sub-section.

Figure 38 illustrates the improvements in system annual energy costs for various trigger level combinations. Here, percentage improvement refers to percentage reduction of energy cost in comparison to the scenario without a storage device. Appendix 6 contains the detailed results. Energy cost is reduced as charging trigger levels are higher. Mixed results are obtained for increasing the discharge trigger level. The percentage reduction in energy cost varies between 0.36% and 1.36%. High charging trigger level and moderate discharging trigger level provides the best results. For the model system, Case 59 provides the maximum reduction in system energy costs. The case has charging trigger level of 40 and discharging trigger level of 70. The next best result is obtained from Case 52 with 35 and 75 as the two trigger levels.

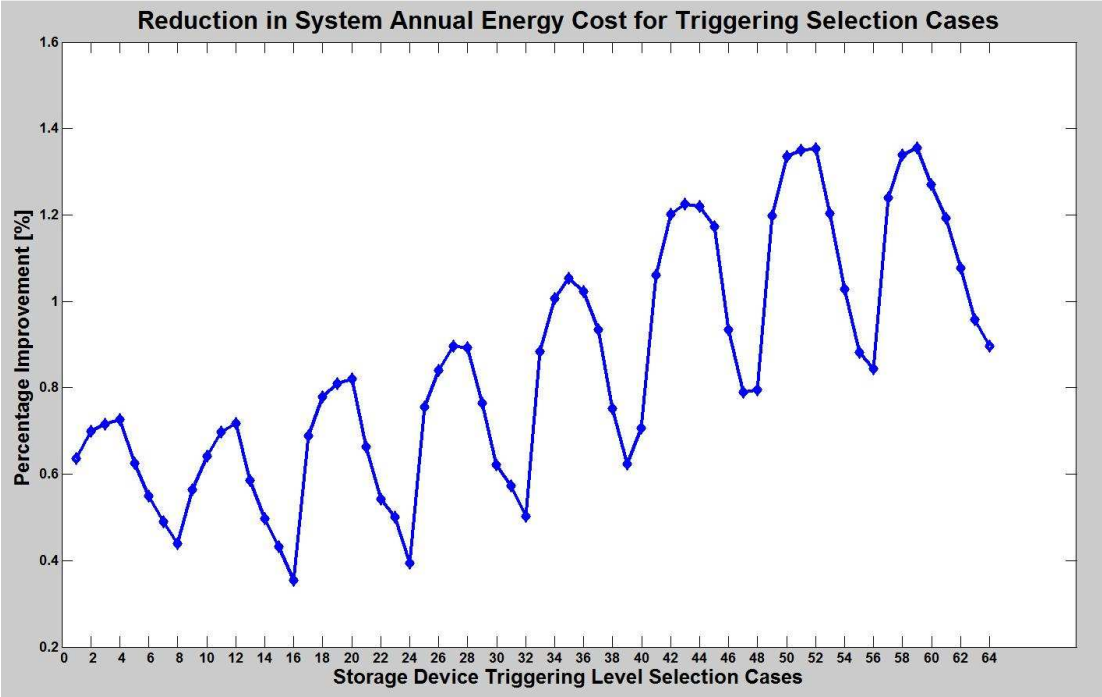

Figure 38 – Improvement in Energy Costs for Triggering Parameter Cases

8.6. Trigger Setting Selection Using Weighted Objectives

The four objectives used to obtain the optimal trigger setting provided four different results. To obtain a single solution that takes into account all four objectives, a single objective is formed by assigning various weights to each of the four objectives. The case that provides the highest weighted percentage improvement is the optimum solution. This weight based system is similar to the one used for obtaining energy storage capacity and ramp rate of the storage device. The weighted percentage improvement for case *C* is calculated using the following formula:

$$i_{w,C} = w_{lf} i_{lf,C} + w_{util} i_{util,C} + w_{loss} i_{loss,C} + w_{cost} i_{cost,C} \quad (8)$$

$$w_{lf} + w_{util} + w_{loss} + w_{cost} = 1 \quad (9)$$

where,

$i_{w,C}$	weighted percentage improvement for Case *C*
$i_{lf,C}$	% improvement (increase) in load following *for* Case *C*
$i_{util,C}$	% improvement (increase) in wind energy utilization for Case *C*
$i_{loss,C}$	% improvement (decrease) in system energy losses for Case *C*

$i_{cost,C}$	% improvement (decrease) in system energy costs for Case *C*
w_{lf}	weight for improvement (increase) in load following
w_{util}	weight for improvement (increase) in wind energy utilization
w_{loss}	weight for improvement (decrease) in system energy losses
w_{cost}	weight for improvement (decrease) in system energy costs

To illustrate this concept, the following weights have been assigned to the four objectives:

Table 19 – Weight Distribution of Objectives for Multi-Objective Trigger Setting Selection

Goal	Weight	Optimum Solution
Load Following	0.25	Case 52
Wind Energy Utilization	0.25	Case 1
Energy Loss Minimization	0.25	Case 37
Energy Cost Minimization	0.25	Case 59

The vector of weights is first normalized such that the sum of the weights adds up to 1. Then the normalized weights are used to calculate the weighted percentage improvement for each of the size parameter cases. Figure 39 plots the results for the cases under study.

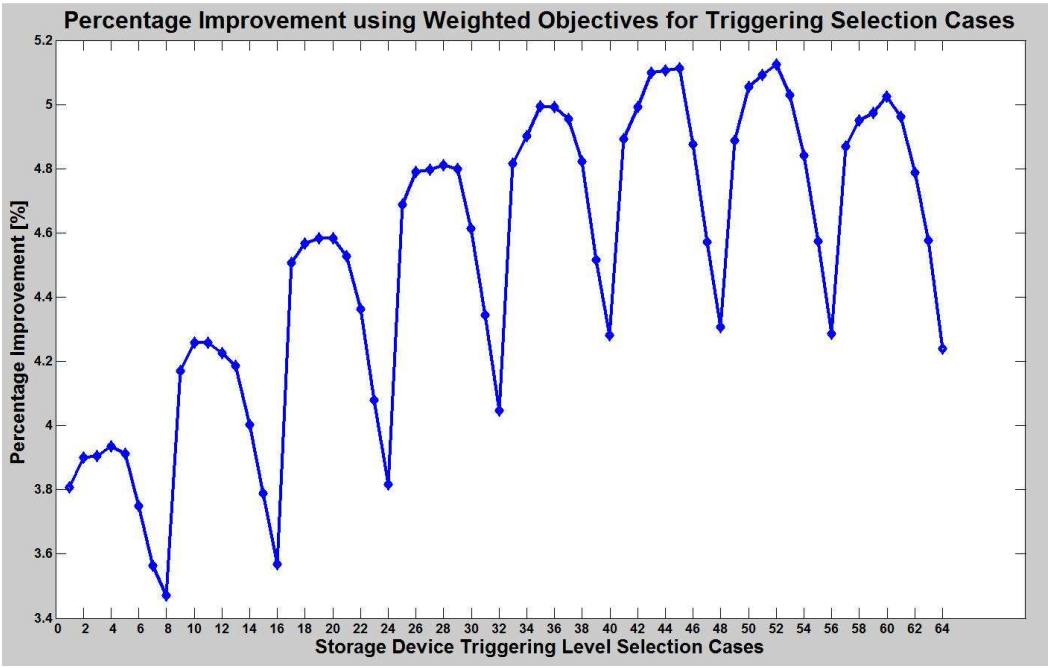

Figure 39 – Improvements in Weighted Objectives for Triggering Level Selection Cases

The weighted evaluation process provides between 3.47% and 5.12% improvement across the various objectives. The highest percentage improvement is obtained for Case 52. Thus, for the given weights, Case 52 contains the most optimum triggering parameters. Detailed results are provided in Appendix 6.

8.7. Trigger Setting Selection Using Randomized Objective Weights

To account for various combinations of weight distribution of the four objectives, 10,000 random sets of weights have been generated. For each set of weights, the case that provides the highest improvement is selected. Figure 40 shows the frequency of selection for the cases under consideration. Case 52 is the most frequently selected solution to the triggering level determination problem. The next best results are obtained using Case 45.

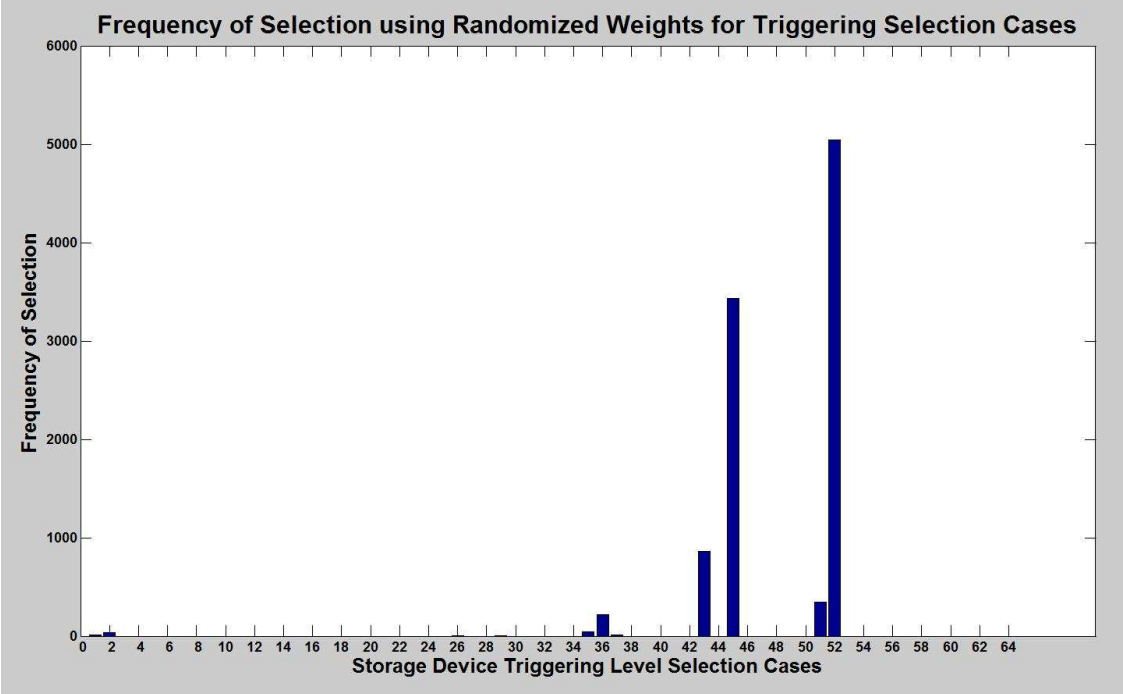

Figure 40 – Frequency of Triggering Case Selection with Randomized Objective Weights

.

Chapter 9: Impact of Storage Device Parameters on Bus Voltages

The charging and discharging operations of a storage device adds extra load and supply, respectively, to the system. The storage device acts like a load by consuming power during charging phase. Similarly, the device acts like a source by supplying energy in to the system during discharging phase. Depending on the charge-discharge ramp rates, buses close to the storage device may experience a voltage dip during the charging operation and a voltage swell during the discharging operation. For each hour, the bus bar voltages are different due to varying demand-supply conditions.

In the previous sections of this report, optimal location, capacity and triggering settings for the storage device have been obtained. These parameters are used to investigate the impact of the storage device on the bus voltages. Table 20 summarizes the parameters of the storage device.

Table 20 – Storage Device Parameters for Bus Voltage Variation Analysis

Parameter	Value
Location	Bus 47
Energy Capacity [MWh]	18
Initial Charge [MWh]	0
Charging Ramp Rate [kW/hr]	1200
Discharging Ramp Rate [kW/hr]	1200
Charging Trigger Level	35
Discharging Trigger level	75

Figure 41 shows a plot illustrating the upper and lower bounds of bus bar voltages across the system. The triangles represent the median voltage value of the bus bar. It should be noted that the upper and lower bounds are specific to the bus bar and do not necessarily occur simultaneously (in the same hour). As expected, the largest voltage swells and dips are observed near Bus 47, the location of the storage device.

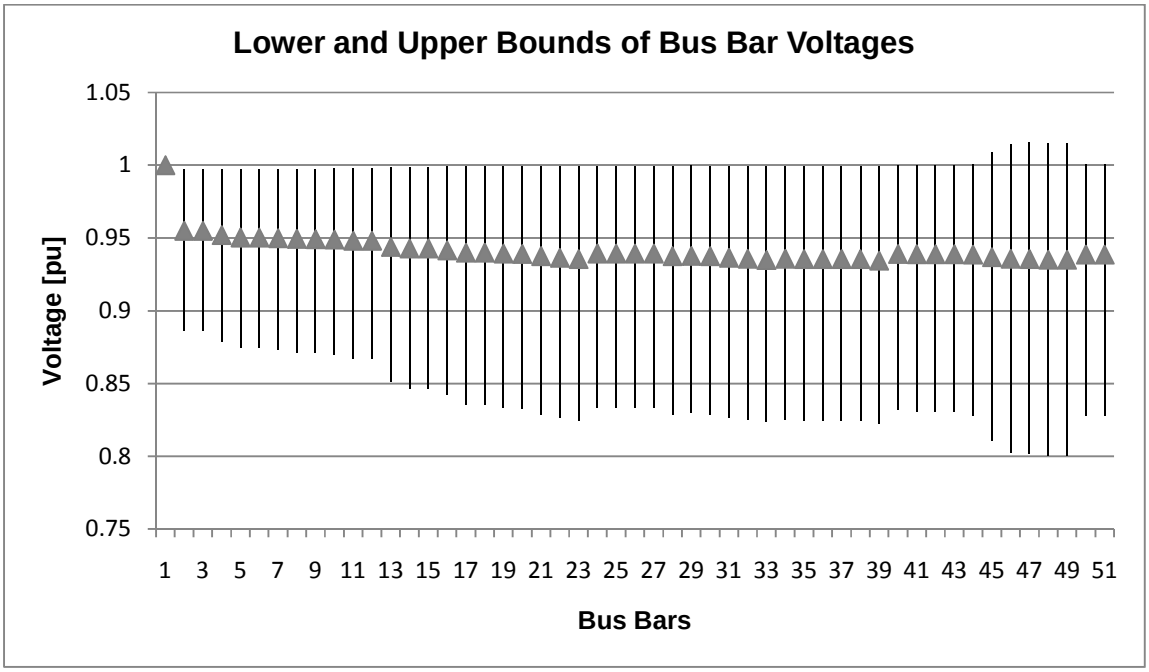

Figure 41 – Bus Bar Voltage Variations: Upper Bound, Lower Bound and Median Values

The voltage variations shown in Figure 41 represent the extreme scenario where all the loads in the system are at their peaks simultaneously. This scenario is the result of the assumption that all loads keep their respective ratios constant as system demand levels changes. The steep voltage drops near the end of the distribution line can be improved by introducing load diversity. For example, if the load at Bus 49 peaks between 8am and 6pm, the maximum voltage drop in the system is limited to less than 0.15 pu. The voltage variations after introducing load diversity is shown in Figure 42.

Other possible methods of mitigating large voltage drops include installation of voltage regulators and relocation of loads. The Matlab tool used in this analysis does not take into account effects of a voltage regulator. Use of a voltage regulator will most certainly improve the voltage profile of the system. The voltage profile shown below can used as a starting point in identifying potential locations of the regulator.

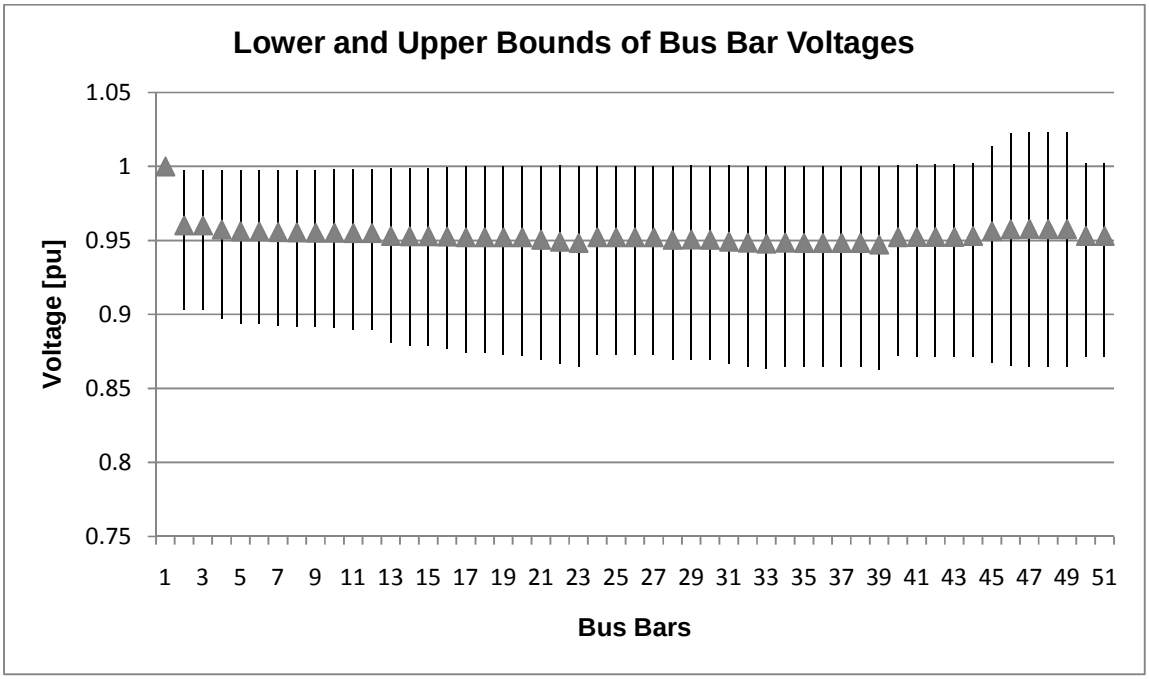

Figure 42 – Bus Bar Voltage Variations after Load Diversity

Chapter 10: System Performance Ranges for Variations of Input

So far, the analysis in this report has been performed based on data sets for the calendar year 2006. Wind speed, energy prices and load demand values will certainly vary from one year to the other. To analyse the impact of such variations, a Monte Carlo simulation based approach is proposed. Random noise of up to one standard deviation around the mean is added to the three data sets. This controlled fluctuation around the original data set allows the values to vary in a pseudo random manner while preserving location-specific characteristics. These input parameters are then used as input to the Matlab tool to calculate output parameters such as substation/source energy supply, wind energy generation, system energy losses, system energy cost and number of cycles of the storage device. A total of 1000 iterations have performed and the output parameters for the iterations are saved for later analysis.

Figure 43 shows the variations in the substation/source supplied energy. The values vary between 42.12 GWh and 44.55 GWh. The probability distribution is divided into two sections with the highest probabilities observed in the range between 44.2 GWh and 44.8 GWh.

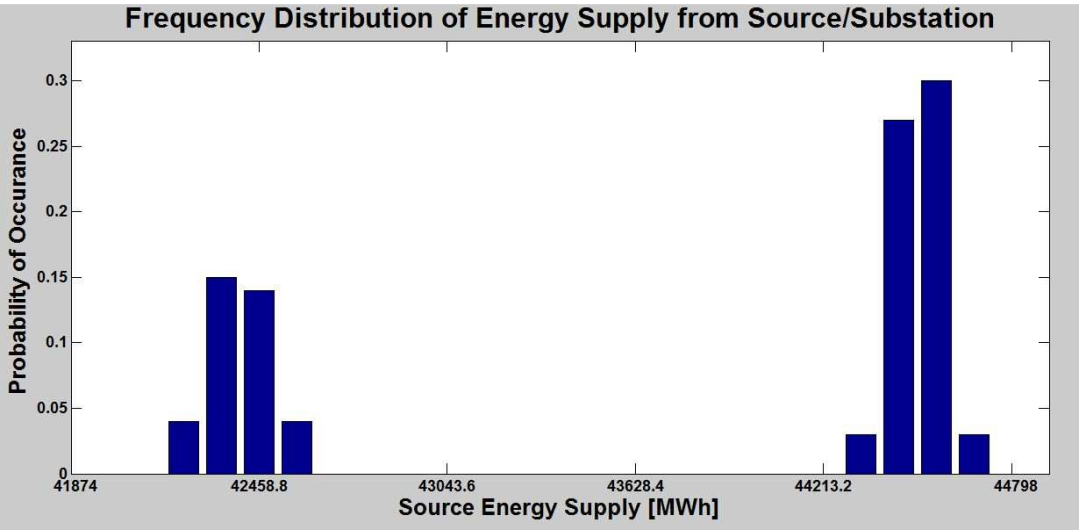

Figure 43 – Probability Distribution of Energy Supply from Source/Substation

Figure 44 shows the variation in power generated by the wind turbines in the model system. The probability distribution of the wind power generation values is similar to that of a normal distribution. Wind generation values for the year range between 12.62 GWh and 12.87 GWh. The highest probability of 0.15 is observed for generation value around 12.75 GWh.

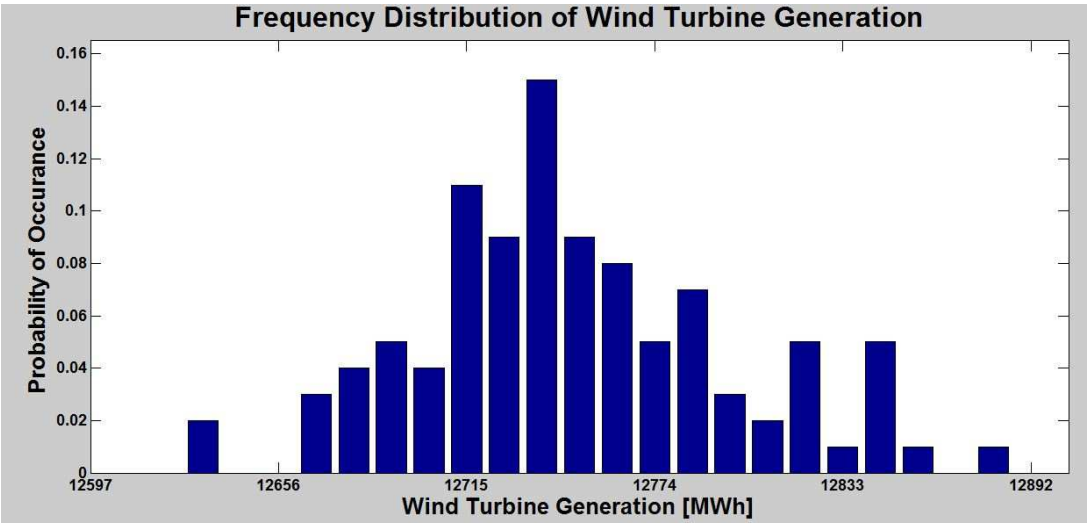

Figure 44 – Probability Distribution of Wind Turbine Generation

Figure 45 shows the probability distribution of system annual energy losses. This distribution is also divided into two sections. Line losses range between 1.91 GWh and 2.03 GWh. The highest probability of 0.29 is around 2.012 GWh.

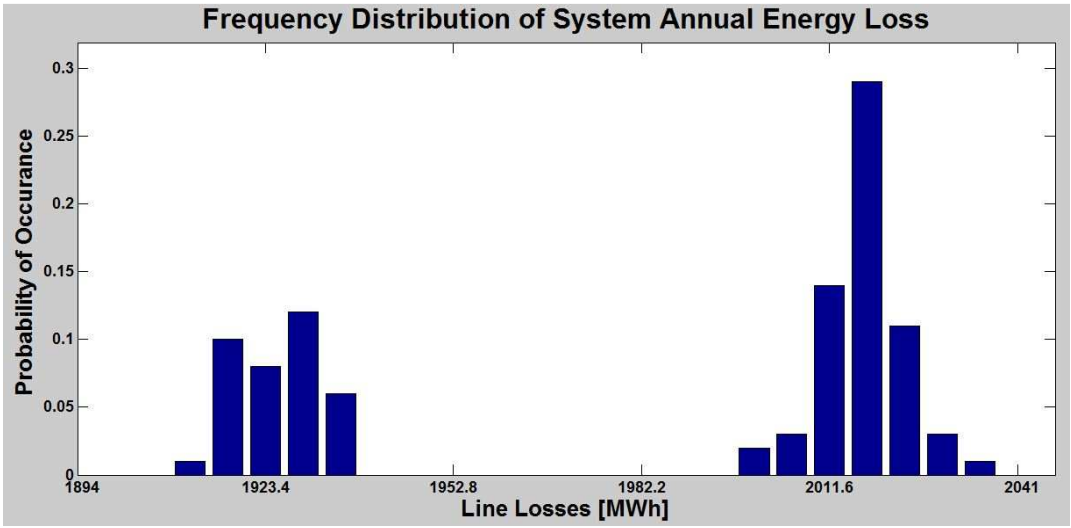

Figure 45 – Probability Distribution of System Annual Energy Loss

Figure 46 shows the probability distribution for system annual energy cost. This distribution shows the higher variation compared to the previous three plots. The system energy costs range between $23.87 million and $24.54 million for the year. The highest probability of 0.34 is observed in the range between $24.28 million and $24.35 million. Figure 47 shows the probability distribution for the number of charge-discharge cycles performed by the storage device.

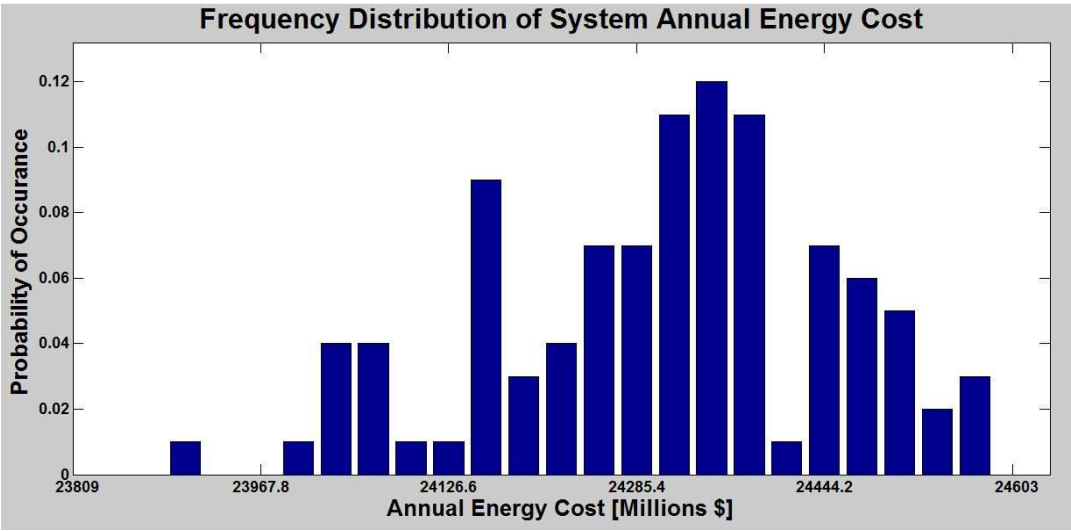

Figure 46 – Probability Distribution of System Annual Energy Cost

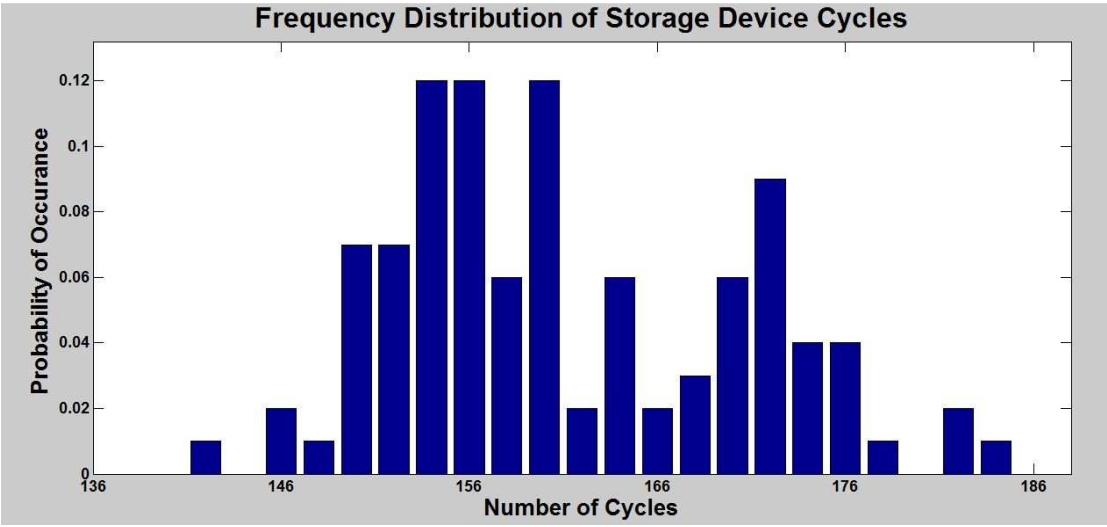

Figure 47 – Probability Distribution of Storage Device Cycles

Table 21 outlines the maximum, minimum, mean and standard deviation values for the five output parameters. As seen from the table, the output parameters vary within very narrow

ranges. Except for storage device cycle count, the other four parameters have very low standard deviations.

Table 21 – System Performance Ranges for Variations of Input

Parameter	Maximum	Minimum	Mean	Standard Deviation
Substation/Source Energy [GWh]	44.55	42.12	43.6	1.13
Wind Generation [GWh]	12.87	12.62	12.74	0.05
Energy Loss [GWh]	2.03	1.91	1.98	0.04
Energy Cost [$M]	24.54	23.87	24.27	0.14
Cycle of Storage	354	281	314.28	16.71

Chapter 11: Summary and Directions for Future Work

This project has evaluated the steady state system performance for installation of storage devices to complement wind based power generators. Strategies and algorithms have been proposed and implemented to obtain various parameters of the storage device. Storage device location is obtained using a non-linear optimization problem. The energy capacity and charge-discharge capabilities of the device have been determined by evaluating a weighted multi-objective non-linear optimization technique. Similar approach has been used to obtain the optimal control strategy (charge-discharge triggering levels) of the storage device. The impact on the existing power system voltages have been evaluated to avoid any drastic drop in system performance. Finally, pseudo random variation of input data has been used to obtain possible variations of the expected results following the installation of the storage device.

Future avenues of research in this topic may focus on two areas of interest: dynamic system responses and use of specific storage device models. This project focuses on steady state values and, as such, does not evaluate the impact on system dynamic performance due to the interaction between the storage device and rest of the power system. Also, a simple and generic storage device model has been used for this project. Future work may restrict the storage device capabilities to match a specific storage technology and lead to technology specific analysis.

References

[1] T. Ackermann, “Historical Development and Current Status of Wind Power” in *Wind Power in Power Systems*, 1st Ed. Sussex, UK: Wiley, 2005, pp. 11-13

[2] E.K. Brock and K. Strunz, “Hybrid plant of renewable stochastic source and multilevel storage for emission–free deterministic power generation”, Symp. 2003 Quality and Security of Electric Power Delivery Systems, pp. 214-218

[3] “Wind Power Integration: Energy Storage for Firming and Shaping”, Final Report, EPRI, Mar. 2005

[4] Canadian Wind Energy Association (CanWEA), “Canadian Wind Farms”, 2009, Available: http://www.canwea.ca/farms/index_e.php

[5] Danish Wind Industry Association (DWIA), “Wind Energy”, 2008, Available: http://www.windpower.org/tour/wres/enerwind.htm

[6] A.D. Hansen, “Generators and Power Electronics for Wind Turbines” in *Wind Power in Power Systems*, T. Ackermann ed., 1st Ed. Sussex, UK: Wiley, 2005, pp. 11-13

[7] General Electric Power, “1.5 MW Wind Turbine”, 2009, pp. 5, Available: http://www.gepower.com/prod_serv/products/wind_turbines/en/15mw/index.htm

[8] K. Strunz and X. Yu, “Combined Long–term and Short–term Access Storage for Sustainable Energy System”, IEEE Power Engineering Society General Meeting, Jun. 2004, vol. 2, pp. 1946–1951

[9] Aerostar Inc., “Adjusting Published Wind Speed for a Lower Height”, 2007, Available: http://www.aerostarwind.com/ windspeeddata.html

[10] A.N. Celik, “A Statistical Analysis of Wind Power Density Based on the Weibull and Rayleigh Models at the Southern Region of Turkey”, Renewable Energy, Apr. 2004, vol. 29, issue. 4, pp. 593 – 604

[11] J.A. Carta and P. Ramirez, “Influence of the Data Sampling Interval in the Estimation of the Parameters of the Weibull Wind Speed Probability Density Distribution: A Case Study”, Energy Conversion and Management, Sep. 2005, vol. 46, issues 15-16, pp. 2419-2438

[12] T.W. Lambert and J.V. Seguro, “Modern Estimation of the Parameters of the Weibull Wind Speed Distribution for Wind Energy Analysis”, Journal of Wind Engineering and Industrial Aerodynamics, Mar. 2000, vol. 85, issue 1, pp. 75-84

[13] T.O. Halawani, *et. al.*, “Weibull Parameters for Wind Speed Distribution in Saudi Arabia”, Solar Energy, Dec. 1994, vol. 53, issue 6, pp. 473-479

[14] D. Weisser, “A Wind Energy Analysis of Grenada: an Estimation Using the ‘Weibull’ Density Function”, Renewable Energy, Sep. 2003, vol. 28, issue 11, pp. 1803-1812

[15] J.C. Lam and I.Y.F. Lun, “A Study of Weibull Parameters Using Long-term Wind Observations”, Renewable Energy, Jun. 2000, vol. 20, issue 2, pp. 145-153

[16] T. Ackermann, “Distributed Resources in a Re-regulated Market”, Ph.D. dissertation, Royal Institute of Technology, Department of Electrical Engineering, Stockholm, Sweden, May 2004

[17] Independent Electricity System Operator, “Wind Power in Ontario”, 2009, Available: http://www.ieso.ca/imoweb/marketdata/windpower.asp

[18] Ontario Power Authority, “Generation Development: Wind Power”, 2009, Available: http://www.powerauthority.on.ca/Page.asp?PageID=924&SiteNodeID=234

[19] A. Ter-Gazarian, “Energy Conversion: From Primary Sources to Consumers” in *Energy Storage for Power Systems*, 1st Ed., London, UK: Peter Peregrinus, 1994, pp. 5-7

[20] C. Abbey and G. Joos, “Coordination of Distributed Storage with Wind Energy in a Rural Distribution System”, Ann. Meeting IEEE Industry Application, Sep. 2007, vol. 2007, pp. pp. 1087-1092

[21] J. Desteese, *et. al.*, “On the use of energy storage technologies for regulation services in electric power systems with significant penetration of wind energy”, 5th Int. Conf. European Electricity Market, May 2008, pp. 1-6

[22] EIA, Energy Information Administration, Oct. 2007, Available: http://www.eia.doe.gov/

[23] J. Enslin, and G. Thijssen, “Cost Comparison for a 20 MW Flywheel–based Frequency Regulation Power Plant”, Beacon Power Corporation, Sep. 2007

[24] G. Balzer, *et. al.*, “Wind Energy Storages – Possibilities”, Proc. IEEE Lausanne POWERTECH, 2007, pp. 615-620

[25] M. Kamibayashi and K. Tanaka, "Recent Sodium Sulphur Battery Applications", IEEE/PES Transmission and Distribution Conf. and Expo., Nov. 2001, vol. 2, pp. 1169 – 1173

[26] R. B. Schainker, “Executive Overview: Energy Storage Options for a Sustainable Energy Future”, IEEE Power Engineering Society General Meeting, Jun. 2004, pp. 2309-2314

[27] M. Lazarewicz and J. Arseneaux, "Status of Pilot Projects Using Flywheels for Frequency Regulation," IEEE Power engineering society general meeting, Jun. 2006, pp. 3

[28] VRB Power Systems Inc. "The VRB Energy Storage System (VRB–ESSTM): The Multiple Benefits of Integrating the VRB–ESS with Wind Energy—Case Studies in MWH Applications", 2007, Available: http://www.vrbpower.com/publications/casestudies.html.

[29] K. Sato and A. Shibata, "Development of Vanadium Redox Flow Battery for Electricity Storage", Power Engineering Journal, Jun. 1999, vol. 13, issue 3, pp. 130-135

[30] VRB Power Systems Inc. "A Comparison with Lead Acid Batteries", 2007, Available: http://www.vrbpower.com/publications/casestudies.html.

[31] L. Barote, *et. al.*, “Stand-alone Wind System with Vanadium Redox Battery Energy Storage”, Int. Conf. Optimization of Electrical and Electronic Equipment, May 2008, pp. 407-412

[32] E. Kadoma and Y. Kurashima, "Development of a Compact Sodium Sulphur Battery", Power Engineering Journal, Jun 1999, vol. 13, issue 3, pp. 136-141

[33] B. Norris *et. al.*, "NAS Battery Demonstration at American Electric Power – A Study for the DOE Energy Storage Program," Sandia National Laboratories, Mar. 2007.

[34] B. Jonshagen and P. Lex, "The Zinc/Bromine Battery System for Utility and Remote Area Applications", Power Engineering Journal, Jun. 1999, vol. 13, issue 3, pp. 142-148

[35] I. Lex and J. Mathews, “Recent Developments in Zinc–Bromine Battery Technology at Johnson Controls”, Proc. 35th Int. Power Sources Symposium, Jun 1992, pp. 88-92

[36] W.V. Hassenzahl and S.M. Schoenung, “Long– vs. Short– Term Energy Storage Technologies Analysis: A Life–cycle Cost Study,” Sandia Natl. Lab., Albuquerque, NM, Sandia Rep. SAND2003–2783, 2003.

[37] W.T. Jewell and P. Poonpun, "Analysis of the Cost per Kilowatt Hour to Store Electricity", IEEE Transaction on Energy Conversion, Jun. 2008, vol. 23, issue 2, pp. 529-534

[38] Energy Information Administration, “Average Retail Price of Electricity to Ultimate Customers by End–Use Sector”, Electric Power Annual with data for 2005, Oct. 2006, Available: http://www.eig.gov/cneaf/electricity/epa/epat7p4.html

[39] M. Bhatnagar, *et. al.*, “UW Power System Simulator”, University of Waterloo, Waterloo, Canada, Feb. 2007

[40] Elangovan, *et. al*., “A New Approach for Power Flow Analysis of Balanced Radial Distribution Systems”, Electric Power Components and Systems, Apr. 2000, vol. 28, issue 4, pp. 325-340

[41] J. Liu, M.M.A. Salama, and R.R. Mansour, “An Efficient Power Flow Algorithm for Distribution Systems with Polynomial Load”, Int. Journal of Electrical Engineering Education, UK, Oct. 2002, vol. 39, issue. 4, pp. 371-386

[42] Y.M. Atwa and E.F. El-Saadany, “Reliability Evaluation for Distribution System with Renewable Distributed Generation During Islanded Mode of Operation”, IEEE Transactions on Power Systems, May 2009, vol. 24, issue 2, pp. 572-581

[43] National Climate Data and Information Archive, “Weather Data Online”, Available: http://climate.weatheroffice.ec.gc.ca/climateData/canada_e.html

[44] Independent Electricity System Operator, “Market Data: IESO Public Reports”, 2009, Available: http://www.ieso.ca/imoweb/marketdata/marketData.asp

Appendix 1: Input Data for Matlab Tool Validation

```
global SYS_RatedVoltage;
global SYS_RatedPower;
SYS_RatedVoltage = 16e3; %V
SYS_RatedPower = 100e6; %VA

global STATION_DATA;
STATION_DATA = [
    9000    16e3
];
%   kVA     Voltage

global FEEDER_MODEL;
FEEDER_MODEL = [
    -1          1            0                    0+0i
     1          2         5700       1.6911e-004+4.1821e-004i
     2          3         1010       1.6911e-004+4.1821e-004i
     2          4          400       1.6911e-004+4.1821e-004i
     4          5          380       1.6911e-004+4.1821e-004i
     5          6          130       1.6911e-004+4.1821e-004i
     5          7          170       1.6911e-004+4.1821e-004i
     7          8          260       1.6911e-004+4.1821e-004i
     8          9          140       1.6911e-004+4.1821e-004i
     8         10          380       1.6911e-004+4.1821e-004i
    10         11          560       1.6911e-004+4.1821e-004i
    11         12          300       1.6911e-004+4.1821e-004i

];
%   Node0   Node1      Distance [m]        ohm/m
```

Appendix 2: Model System Parameters (Line Model)

Equipment/Line	From Bus	To Bus	Length [m]	Impedance [Ω/m]
Generator	-1	1	0	0+0i
Line 1	1	2	5900	1.6911e-004+4.1821e-004i
Line 2	2	3	1010	1.6911e-004+4.1821e-004i
Line 3	2	4	400	1.6911e-004+4.1821e-004i
Line 4	4	5	380	1.6911e-004+4.1821e-004i
Line 5	5	6	130	1.6911e-004+4.1821e-004i
Line 6	5	7	170	1.6911e-004+4.1821e-004i
Line 7	7	8	260	1.6911e-004+4.1821e-004i
Line 8	8	9	140	1.6911e-004+4.1821e-004i
Line 9	8	10	380	1.6911e-004+4.1821e-004i
Line 10	10	11	560	1.6911e-004+4.1821e-004i
Line 11	11	12	300	1.6911e-004+4.1821e-004i
Line 12	11	13	3300	1.6911e-004+4.1821e-004i
Line 13	13	14	1030	1.6911e-004+4.1821e-004i
Regulating Station	14	15	0	0+0i
Line 14	15	16	1080	1.6911e-004+4.1821e-004i
Line 15	16	17	1640	1.6911e-004+4.1821e-004i
Recloser	17	18	0	0+0i
Line 16	18	19	470	1.6911e-004+4.1821e-004i
Fuse	19	24	0	0+0i
Line 17	24	25	470	3.4812e-004+4.6848e-004i
Transformer	25	26	0	0+0i
Line 18	26	27	960	1.3919e-003+4.7881e-004i

Line 19	19	20	190	3.4812e-004+4.6848e-004i
Line 20	20	21	1940	3.4812e-004+4.6848e-004i
Fuse	21	28	0	0+0i
Line 21	28	30	1360	3.4812e-004+4.6848e-004i
Line 22	28	29	2450	3.4812e-004+4.6848e-004i
Line 23	21	22	1630	3.4812e-004+4.6848e-004i
Fuse	22	31	0	0+0i
Line 24	31	32	1200	5.5228e-004+4.8524e-004i
Line 25	32	34	820	5.5228e-004+4.8524e-004i
Line 26	32	33	1550	5.5228e-004+4.8524e-004i
Line 27	22	23	2120	3.4812e-004+4.6848e-004i
Line 28	23	35	730	5.5228e-004+4.8524e-004i
Fuse	35	36	0	0+0i
Line 29	36	37	750	5.5228e-004+4.8524e-004i
Line 30	37	38	1070	5.5228e-004+4.8524e-004i
Line 31	23	39	2540	3.4812e-004+4.6848e-004i
Line 32	20	40	360	2.7652e-004+4.5858e-004i
Line 33	40	41	260	2.7652e-004+4.5858e-004i
Fuse	41	42	0	0+0i
Line 34	42	43	3580	5.5228e-004+4.8524e-004i
Line 35	41	44	770	2.7652e-004+4.5858e-004i
Fuse	44	50	0	0+0i
Line 36	50	51	2080	3.4812e-004+4.6848e-004i
Line 37	44	45	4510	2.7652e-004+4.5858e-004i
Line 38	45	46	3240	1.6911e-004+4.1821e-004i
Line 39	46	47	400	1.6911e-004+4.1821e-004i

Line 40	47	48	400	1.6911e-004+4.1821e-004i
Transformer	48	49	0	0+0i

Appendix 3: Model System Parameters (Load Diversity)

Load #	Phase	Location/Bus	Real Power [kW]	Reactive Power [kVAr]
M1	3Ø	4	2193.67	721.02
M2	3Ø	4	0.00	0.00
M3	3Ø	4	0.00	0.00
M4	3Ø	6	72.00	40.80
M5	3Ø	6	274.00	155.28
M6	3Ø	7	1099.00	361.22
M7	3Ø	9	256.00	225.77
M8	3Ø	12	6.33	0.00
M9	3Ø	13	0.00	0.00
M10	3Ø	13	50.00	16.43
M11	3Ø	13	170.00	55.88
M12	3Ø	13	0.00	0.00
M13	1Ø - B	27	0.00	0.00
M14	1Ø - B	29	0.00	0.00
M15	1Ø - A	33	160.00	52.59
M16	1Ø - C	38	0.00	0.00
M17	3Ø	39	50.00	16.43
M18	3Ø	39	130.00	42.73
M19	3Ø	39	0.00	0.00
M20	3Ø	39	0.00	0.00
M21	1Ø - C	43	0.00	0.00
M22	3Ø	45	0.00	0.00
M23	3Ø	45	60.00	19.72

M24	3Ø	49	749.00	246.18
M25	1Ø - B	51	0.00	0.00
M26	3Ø	20	10.00	3.29
Total	3Ø Only		5120.00	1904.75

Appendix 4: Location Analysis Results

Node	Energy Cost [M $]		Energy Loss [GWh]	
	Case 1	Case 2	Case 1	Case 2
No Storage	25.048		2.0864	
1	24.900	24.989	2.0888	2.0874
2	24.871	24.988	2.0691	2.0817
3	24.869	24.986	2.0686	2.0816
4	24.871	24.985	2.0658	2.0806
5	24.877	24.985	2.0647	2.0802
6	24.876	24.985	2.0645	2.0802
7	24.876	24.985	2.0642	2.0801
8	24.873	24.985	2.0641	2.0801
9	24.877	24.985	2.0645	2.0802
10	24.868	24.986	2.0641	2.0800
11	24.866	24.986	2.0636	2.0798
12	24.866	24.986	2.0636	2.0797
13	24.863	24.988	2.0606	2.0790
14	24.855	24.987	2.0590	2.0785
15	24.859	24.985	2.0588	2.0785
16	24.859	24.986	2.0584	2.0782
17	24.861	24.984	2.0575	2.0776
18	24.860	24.983	2.0572	2.0775
19	24.862	24.983	2.0568	2.0774
20	24.866	24.983	2.0561	2.0772
21	24.859	24.986	2.0645	2.0801

22	24.860	24.988	2.0716	2.0828
23	24.873	24.989	2.0804	2.0858
24	24.863	24.983	2.0566	2.0773
25	24.864	24.984	2.0585	2.0780
26	24.864	24.984	2.0587	2.0780
27	24.869	24.988	2.0760	2.0838
28	24.859	24.986	2.0644	2.0801
29	24.867	24.987	2.0752	2.0841
30	24.862	24.988	2.0715	2.0824
31	24.864	24.990	2.0717	2.0827
32	24.868	24.989	2.0797	2.0855
33	24.877	24.986	2.0913	2.0891
34	24.878	24.989	2.0862	2.0878
35	24.872	24.989	2.0864	2.0877
36	24.873	24.989	2.0867	2.0877
37	24.877	24.986	2.0920	2.0895
38	24.879	24.988	2.1008	2.0922
39	24.880	24.986	2.0937	2.0899
40	24.871	24.983	2.0550	2.0769
41	24.871	24.983	2.0548	2.0767
42	24.872	24.983	2.0554	2.0770
43	24.881	24.986	2.0812	2.0853
44	24.870	24.983	2.0549	2.0767
45	24.865	24.979	2.0514	2.0749
46	24.847	24.980	2.0518	2.0746
47	24.846	24.978	2.0513	2.0746

48	24.844	24.979	2.0525	2.0748
49	24.844	24.979	2.0526	2.0749
50	24.872	24.983	2.0547	2.0765
51	24.878	24.983	2.0643	2.0796

Appendix 5: Capacity Analysis Results

Case	Energy Capacity [MWh]	Power Capacity [kW/hr]	Percentage Improvements				Probability of Selection for Randomized Weights
			Maximize Load Following	Maximize Capacity Factor	Minimize Energy Loss	Minimize Energy Cost	
1	1.5	300	8.406	0.101	0.619	0.107	0
2	1.5	600	8.563	0.092	0.740	0.116	0
3	1.5	900	8.603	0.072	0.761	0.119	0
4	1.5	1200	8.614	0.062	0.746	0.113	0
5	1.5	1500	8.571	0.038	0.660	0.111	0
6	3.0	600	9.116	0.172	1.222	0.208	0
7	3.0	1200	9.333	0.133	1.303	0.212	0
8	3.0	1800	9.282	0.101	1.160	0.214	0
9	3.0	2400	9.142	0.081	0.909	0.199	0
10	3.0	3000	8.810	0.038	0.390	0.186	0
11	4.5	900	9.764	0.233	1.701	0.316	0
12	4.5	1800	9.919	0.150	1.582	0.297	0
13	4.5	2700	9.604	0.096	1.057	0.274	0
14	4.5	3600	9.185	0.087	0.392	0.238	0
15	4.5	4500	8.396	0.035	-0.790	0.172	0
16	6.0	1200	10.363	0.268	2.084	0.399	0
17	6.0	2400	10.309	0.154	1.538	0.390	0
18	6.0	3600	9.613	0.096	0.495	0.354	0
19	6.0	4800	8.802	0.095	-0.751	0.240	0
20	6.0	6000	7.250	0.037	-3.299	0.165	0
21	7.5	1200	10.774	0.321	2.416	0.457	0

22	7.5	2400	10.702	0.175	1.666	0.480	0
23	7.5	3600	9.803	0.118	0.241	0.421	0
24	7.5	4800	9.119	0.103	-0.804	0.319	0
25	7.5	6000	7.859	0.100	-2.874	0.243	0
26	9.0	1200	11.118	0.350	2.685	0.482	0
27	9.0	2400	11.199	0.234	1.936	0.570	0
28	9.0	3600	10.382	0.170	0.570	0.494	0
29	9.0	4800	9.015	0.103	-1.343	0.359	0
30	9.0	6000	8.093	0.103	-3.009	0.306	0
31	10.5	1200	11.432	0.365	2.935	0.494	0
32	10.5	2400	11.624	0.268	2.151	0.616	0
33	10.5	3600	10.496	0.171	0.358	0.551	0
34	10.5	4800	9.273	0.144	-1.488	0.414	0
35	10.5	6000	7.908	0.103	-3.734	0.338	0
36	12.0	1200	11.691	0.369	3.120	0.502	0
37	12.0	2400	11.877	0.289	2.206	0.676	0
38	12.0	3600	10.921	0.231	0.535	0.611	0
39	12.0	4800	9.602	0.158	-1.469	0.454	0
40	12.0	6000	7.302	0.103	-5.208	0.390	0
41	13.5	1200	11.933	0.381	3.289	0.513	0
42	13.5	2400	12.244	0.346	2.455	0.747	0
43	13.5	3600	11.186	0.210	0.509	0.642	0
44	13.5	4800	9.639	0.164	-1.821	0.469	0
45	13.5	6000	7.825	0.172	-4.842	0.430	0
46	15.0	1200	12.195	0.402	3.470	0.525	0
47	15.0	2400	12.520	0.337	2.561	0.780	0

48	15.0	3600	11.360	0.250	0.446	0.693	0
49	15.0	4800	9.706	0.203	-2.069	0.514	0
50	15.0	6000	8.006	0.175	-5.052	0.469	0
51	16.5	1200	12.477	0.411	3.661	0.537	0
52	16.5	2400	12.831	0.360	2.673	0.810	0
53	16.5	3600	11.690	0.288	0.529	0.751	0
54	16.5	4800	10.096	0.245	-1.961	0.592	0
55	16.5	6000	7.918	0.175	-5.532	0.452	0
56	18.0	1200	12.699	0.413	3.812	0.543	0.622
57	18.0	2400	13.172	0.375	2.869	0.833	0.378
58	18.0	3600	11.735	0.302	0.368	0.788	0
59	18.0	4800	10.137	0.245	-2.248	0.628	0
60	18.0	6000	7.384	0.175	-6.809	0.434	0

Appendix 6: Trigger Analysis Results

Case	Charging Trigger Level	Dis-charging Trigger Level	Percentage Improvements				Probability of Selection for Randomized Weights
			Maximize Load Following	Maximize Capacity Factor	Minimize Energy Loss	Minimize Energy Cost	
1	5	60	10.793	1.089	2.710	0.636	0.001
2	5	65	10.976	1.048	2.878	0.700	0.003
3	5	70	11.003	1.000	2.905	0.715	0
4	5	75	11.089	0.974	2.953	0.726	0
5	5	80	11.139	0.934	2.955	0.625	0
6	5	85	10.868	0.838	2.747	0.550	0
7	5	90	10.610	0.644	2.511	0.490	0
8	5	95	10.604	0.428	2.411	0.439	0
9	10	60	11.939	0.783	3.394	0.564	0
10	10	65	12.090	0.747	3.555	0.642	0
11	10	70	12.096	0.708	3.529	0.697	0
12	10	75	12.032	0.704	3.453	0.717	0
13	10	80	12.061	0.653	3.443	0.586	0
14	10	85	11.723	0.572	3.218	0.497	0
15	10	90	11.359	0.396	2.965	0.432	0
16	10	95	10.971	0.283	2.669	0.355	0
17	15	60	12.849	0.606	3.882	0.688	0
18	15	65	12.942	0.601	3.949	0.779	0
19	15	70	12.972	0.582	3.973	0.811	0
20	15	75	12.964	0.582	3.964	0.820	0
21	15	80	12.970	0.502	3.977	0.663	0

22	15	85	12.696	0.413	3.798	0.542	0
23	15	90	12.089	0.322	3.406	0.500	0
24	15	95	11.534	0.230	3.108	0.394	0
25	20	60	13.426	0.539	4.029	0.756	0
26	20	65	13.626	0.520	4.178	0.841	0.003
27	20	70	13.602	0.494	4.196	0.897	0
28	20	75	13.660	0.472	4.223	0.892	0
29	20	80	13.700	0.408	4.322	0.764	0.003
30	20	85	13.343	0.363	4.128	0.622	0
31	20	90	12.704	0.295	3.804	0.573	0
32	20	95	12.073	0.200	3.415	0.502	0
33	25	60	13.918	0.477	3.982	0.883	0
34	25	65	14.062	0.470	4.071	1.007	0
35	25	70	14.241	0.455	4.230	1.053	0.003
36	25	75	14.233	0.442	4.272	1.023	0.022
37	25	80	14.211	0.352	4.328	0.934	0.001
38	25	85	13.967	0.319	4.256	0.752	0
39	25	90	13.334	0.192	3.915	0.624	0
40	25	95	12.762	0.115	3.541	0.706	0
41	30	60	14.266	0.411	3.829	1.061	0
42	30	65	14.443	0.404	3.922	1.201	0
43	30	70	14.639	0.390	4.141	1.225	0.087
44	30	75	14.683	0.325	4.192	1.219	0
45	30	80	14.692	0.291	4.295	1.174	0.339
46	30	85	14.215	0.251	4.101	0.935	0
47	30	90	13.579	0.146	3.772	0.790	0

48	30	95	12.907	0.092	3.434	0.795	0
49	35	60	14.498	0.329	3.529	1.198	0
50	35	65	14.840	0.291	3.752	1.335	0
51	35	70	14.855	0.284	3.878	1.351	0.035
52	35	75	14.889	0.242	4.010	1.354	0.509
53	35	80	14.674	0.197	4.044	1.203	0
54	35	85	14.273	0.163	3.903	1.029	0
55	35	90	13.669	0.124	3.618	0.882	0
56	35	95	12.917	0.083	3.300	0.845	0
57	40	60	14.676	0.259	3.303	1.239	0
58	40	65	14.800	0.239	3.428	1.338	0
59	40	70	14.738	0.239	3.558	1.356	0
60	40	75	14.860	0.208	3.763	1.270	0
61	40	80	14.694	0.161	3.801	1.193	0
62	40	85	14.325	0.124	3.625	1.076	0
63	40	90	13.806	0.082	3.456	0.958	0
64	40	95	12.888	0.059	3.111	0.896	0